EPRI
Electric Power
Research Institute

Keywords:
Intergranular Corrosion
Sodium Hydroxide
Silicates
Stress Corrosion
Electrochemical Corrosion

EPRI NP-3040
Project S183-2
Final Report
May 1983

EPRI-NP--3040

DE83 902666

Neutralization of Tubesheet Crevice Corrosion

Prepared by
Westinghouse Electric Corporation
Pittsburgh, Pennsylvania

MASTER

DISTRIBUTION OF THIS DOCUMENT IS UNLIMITED

DISCLAIMER

This report was prepared as an account of work sponsored by an agency of the United States Government. Neither the United States Government nor any agency thereof, nor any of their employees, makes any warranty, express or implied, or assumes any legal liability or responsibility for the accuracy, completeness, or usefulness of any information, apparatus, product, or process disclosed, or represents that its use would not infringe privately owned rights. Reference herein to any specific commercial product, process, or service by trade name, trademark, manufacturer, or otherwise does not necessarily constitute or imply its endorsement, recommendation, or favoring by the United States Government or any agency thereof. The views and opinions of authors expressed herein do not necessarily state or reflect those of the United States Government or any agency thereof.

DISCLAIMER

Portions of this document may be illegible in electronic image products. Images are produced from the best available original document.

Neutralization of Tubesheet Crevice Corrosion

NP-3040
Research Project S183-2

Final Report, May 1983

Prepared by

WESTINGHOUSE ELECTRIC CORPORATION
Research & Development Center
1310 Beulah Road
Pittsburgh, Pennsylvania 15235

Principal Investigators
W. M. Conner
R. G. Aspden
R. Hermer
N. Pessall

Prepared for

Steam Generator Owners Group

and

Electric Power Research Institute
3412 Hillview Avenue
Palo Alto, California 94304

EPRI Project Manager
A. R. McIlree

Nuclear Power Division

DISTRIBUTION OF THIS DOCUMENT IS UNLIMITED

ORDERING INFORMATION

Requests for copies of this report should be directed to Research Reports Center (RRC), Box 50490, Palo Alto, CA 94303, (415) 965-4081. There is no charge for reports requested by EPRI member utilities and affiliates, U.S. utility associations, U.S. government agencies (federal, state, and local), media, and foreign organizations with which EPRI has an information exchange agreement. On request, RRC will send a catalog of EPRI reports.

Copyright © 1993 Electric Power Research Institute, Inc. All rights reserved.

NOTICE

This report was prepared by the organization(s) named below as an account of work sponsored by the Electric Power Research Institute, Inc. (EPRI) and the Steam Generator Owners Group. Neither EPRI, members of EPRI, the Steam Generator Owners Group, the organization(s) named below, nor any person acting on behalf of any of them: (a) makes any warranty, express or implied, with respect to the use of any information, apparatus, method, or process disclosed in this report or that such use may not infringe privately owned rights; or (b) assumes any liabilities with respect to the use of, or for damages resulting from the use of, any information, apparatus, method, or process disclosed in this report.

Prepared by
Westinghouse Electric Corporation
Pittsburgh, Pennsylvania

EPRI PERSPECTIVE

PROJECT DESCRIPTION

Steam generator tubing, which had experienced extensive intergranular attack (IGA) and stress corrosion cracking (SCC) in the region of the tube-to-tubesheet crevice, was removed from the Ginna and Point Beach nuclear power plants. Analyses of corrosion deposits on this tubing have identified myriad chemical species. Excess sodium, which could form caustic NaOH, has been suspect since the secondary-side IGA-SCC phenomenon was first observed. The influence of the many other species on either accelerating or retarding the attack needed to be determined. This project (RPS183-2) uses screening type tests and evaluates numerous chemical compounds.

PROJECT OBJECTIVES

The objectives of this project are (1) to determine the sensitivity of Alloy 600 to IGA when various chemical contaminants are added to the corrosion environment either alone or in combination and (2) to preliminarily evaluate proposed neutralizers.

PROJECT RESULTS

The project concluded that:

- Fifty percent NaOH at 650°F produced about 1 mil of general IGA in 60 to 90 days.
- Cr_2O_3 added to 50% NaOH at 650°F produced an 8- to 9-fold increase in the rate of IGA.
- $NaNO_3$ additions acted to inhibit the rate of IGA and SCC.
- Silicates were found to enhance the initiation and propagation of IGA.

- Stress corrosion cracking was greatly accelerated when silicate with zinc and copper oxides were added.
- Anodic polarization promoted SCC and did not promote IGA.

This report will be of interest to plant chemists and materials personnel.

A. R. McIlree, Project Manager
Steam Generator Project Office
Nuclear Power Division

ABSTRACT

Alloy 600 intergranular attack (IGA) representative of that observed in operating plants has been produced in isothermal capsule tests. Uniform IGA occurred to a depth of 6-8 mil in 90 days at 650°F in a test environment consisting of 40 wt % NaOH + 10 wt % KOH + 12 wt % Cr_2O_3. Lesser amounts of IGA (1-2 mil) were produced in the same environment without Cr_2O_3 in 90 days. In 40 wt % NaOH + 10 wt % KOH, sodium nitrate prevented all stress corrosion cracking (SCC) and IGA in stressed C-ring and isothermal capsule tests. Other additives to this environment such as SiO_2, CuO + ZnO, SiO_2 + CuO + ZnO decreased IGA but increased the susceptibility of mill annealed Alloy 600 to SCC.

Neither IGA nor SCC was produced in a single tube model boiler heat transfer test operated on all-volatile chemistry plus hydrazine with continuous inleakage of simulated Lake Ontario water. Attempts to reduce the propensity for SCC and to stimulate IGA by reducing the amount of oxidant in the sludge was apparently responsible for the absence of both SCC and IGA.

CONTENTS

CONTENTS (Continued)

ILLUSTRATIONS

ILLUSTRATIONS (continued)

TABLES

TABLES (continued)

ILLUSTRATIONS (continued)

SUMMARY

Intergranular attack (IGA) of mill annealed Alloy 600 has been observed in the tubesheet crevice region of several operating steam generators. The purpose of this test program was to produce IGA in the laboratory and to test inhibitors that can be applied to steam generators experiencing this phenomenon. The test facilities used to study IGA are the Single Tube Model Boiler Test Facility at Westinghouse Forest Hills and the Electrochemical, Mini-Autoclave, and Isothermal Capsule Facilities at the Westinghouse Research and Development Center. Screening tests were conducted in these latter facilities to determine the effect of stress level and contaminants on the intergranular attack of Alloy 600.

The reference environment used for the electrochemical (and other screening) tests was 40 wt % NaOH + 10 wt % KOH at 650°F. In this environment, unpolarized C-rings, stressed at $\geq$ the yield stress, which were exposed for 30 days contained IGA to a maximum depth of 0.04 to 0.06 mm (1.5 to 2.5 mils). Testing of C-rings and tubing sections at potentials in the active range at the active peak, and in the active to passive transition region showed that short duration ($\leq$ 3 day) exposures with anodic polarization were ineffective in increasing IGA in any test environment. However, these electrochemical tests revealed that the application of high tensile stresses and anodic polarization resulted in severe localized intergranular cracking in highly stressed regions in some environments. Results of an electrochemical test in the reference environment + 12% SiO_2 showed that a combination of chemical environment and stress (> yield stress) can increase IGA by a factor of two.

Screening tests conducted with C-rings stressed at 0, 25 and 75% of the yield stress were conducted in miniautoclaves with the reference conditions for 84 and 112 days. In the reference environment, 40 wt % NaOH + 10 wt % KOH, the depth of IGA (0.01-0.03 mm) was the same regardless of stress level or exposure time. However, the depth of SCC was greater for specimens stressed at 75% of the yield stress than at 25% of the yield stress. Also, for the more highly stressed specimens, the depth of SCC increased with increasing exposure time. Addition of

12 wt % SiO_2 or 7 wt % CuO + 3 wt % ZnO to the reference environment resulted in a slight decrease in IGA and an increase in SCC when specimens with the same stress levels were compared. Combining 12 wt % SiO_2 with 7 wt % CuO + 3 wt % ZnO caused a reduction in the depth of observed IGA and a significant increase in the rate of SCC. Through-wall or nearly through wall cracking was produced on specimens stressed to 75% of the yield stress during the first month (672 hours) of exposure. The effect of adding 12 wt % sodium nitrate to the reference environment was the same as observed in the electrochemical tests. No IGA or SCC was observed but general corrosion of the Alloy 600 surface occurred.

Isothermal capsule tests to evaluate the effect of additives were comprised of three groups. The first group (Test 1) contained the reference environment, the second group (Tests 2-8) contained selective additives without caustic addition, and the third group (Tests 10-22) contained the reference environment plus additives. In the reference environment, 1 to 2 mil (0.025 - 0.050 mm) of uniform IGA was produced in the ~ 90 days of exposure achieved before the capsule began to leak. For Tests 2 through 8 some IGA was produced even without 50% caustic additions. The magnitude of the IGA was, generally, 1/5 to 1/10 that produced in the reference caustic environment. Environments containing SO_4^{2-} showed minor intergranular involvement to a depth of 0.2 to 0.4 mil (0.005 to 0.010 mm). Shallow intergranular penetrations of only 0.2 mil (0.005 mm) resulted from exposure to the 12% NaF environment. No attack was found in capsules containing 12% SiO_2 and 12% $NaNO_3$. The maximum amount of IGA found in a capsule without caustic additions was produced by exposure to 12% Na_2CO_3. The 0.2 to 0.8 mil(0.005 to 0.020 mm) of IGA produced by 12% Na_2CO_3 in the ~40 days of exposure occurred prior to a leak developing in the capsule.

Of the additives to the reference caustic environment tested in isothermal capsules, several did not affect the amount of observed IGA. Sodium, calcium, and magnesium sulfates, aluminum, sodium chloride, sodium phosphate and sodium fluoride additions to the reference environment did not promote IGA. Silica additions to caustic appear to have reduced the incidence of IGA slightly. Because the caustic and silica environment was difficult to contain, only very limited results were obtained with this environment in capsules. Both capsules containing this environment leaked during the first three weeks of exposure. These observations on silica additives, however, are consistent with the C-ring and electrochemistry results with the same test environment. Sodium nitrate

additions to the reference environment inhibited IGA but enhanced general corrosion. No IGA was observed on specimens in which copper and zinc oxides were the additives. Both capsules which contained this environment leaked through cracks in welds in less than 161 days. Two additives were observed to increase the amount of IGA produced when specimens were exposed to the reference environment. In the reference environment + 12 wt % Na_2CO_3, IGA occurred to a depth of 2.8 to 3.6 mil (0.07 to 0.09 mm) which is twice the amount of IGA produced in the reference environment alone. The effect produced by Cr_2O_3 addition was even more pronounced. Uniform IGA to a depth of 7.6 mil (0.19 mm) was produced after 92 to 98 days exposure to the reference environment plus 12% Cr_2O_3. Because of the uniformity of the IGA produced, and the rapidity with which it was generated, Cr_2O_3 additions to caustic should be considered as the reference environment for additional testing (capsule, C-ring, or electrochemical) to evaluate potential chemical inhibitors.

Many of the isothermal capsules exposed to the 40% NaOH + 10% KOH solutions during the capsule proof tests, and a limited number of capsules in the test series to evaluate the effect of additives, contained A508 low alloy steel slugs. After exposure of these capsules, prior to destructive examination, it was observed that the capsules were bulged in the region of the tube where the A508 slug was located. The fact that tube deformation can be produced in a caustic environment suggests that the minor denting indicated at the top of the tubesheet in some operating plants by eddy current data may have been produced by the same alkaline environment thought to produce the IGA and SCC observed deeper within the tubesheet crevice.

A single tube model boiler test was conducted to form an in situ deposit that simulates the composition of the tubesheet crevice deposits and to determine if the deposits can cause IGA. This test was operated on all-volatile chemistry plus hydrazine with continuous additions of simulated Lake Ontario water which contained Na, Mg, and Ca carbonates. The test produced only very limited grain boundary attack and no SCC. The absence of cupric oxide which precludes the formation of a highly oxidizing environment, and frequent thermal cycling which flushed alkalinity from the crevice prohibited concentration of caustic to levels sufficient to produce extensive attack.

The results of this test program lead to the recommendation that further screening tests be conducted in 40 wt % + 10 wt % KOH + 12 wt % Cr_2O_3 which has been demonstrated to cause extensive IGA. The effect of remedial actions also can be evaluated in this environment. In parallel with this effort single tube model boiler testing is also recommended to establish a reference IGA test environment in which to evaluate remedial actions.

Section 1

INTRODUCTION

BACKGROUND

Evaluation of Ni-Cr-Fe Alloy 600 tubes removed from several operating steam generators have shown evidence of a general intergranular corrosion attack (IGA). This corrosion, which occurs on the outer surface of the tube in the tubesheet crevice region, has been observed to penetrate part way through the tube wall. Occasional cracks extending from the zone of IGA toward the inside diameter (i.d.) of the tube have also been observed. In some cases, the cracks have extended through the wall to result in primary to secondary side leakage.

Destructive examination of tubes, removed from affected steam generators has provided some information concerning the composition of the contaminants that are present on the tubes and in the sample of deposits from the tube sheet hole after tube removal.

Although published laboratory data on the conditions leading to stress corrosion cracking (SCC) of mill annealed Alloy 600 have shown the effects of stress level, temperature, and various contaminants such as lead oxide, sodium and/or potassium hydroxide, etc., a similar data base does not exist for conditions which may lead to IGA. It is necessary therefore, to include screening tests in the experimental approach to the eventual resolution of this corrosion issue.

APPROACH

The individual tasks are linked in the following manner to obtain recommendations for field application of a tubesheet crevice neutralizer or other corrective action.

Background data sources such as laboratory work and plant experience, especially the work conducted in EPRI Project S138, were evaluated to suggest the most

plausible mechanisms for the formation of deep crevice deposits. A specific test description for Task 200 including crevice depth, composition of sludge, sludge depth, etc., was recommended from this review and proposed to the EPRI project manager for concurrence.

Task 200 tested the postulated mechanism for formation of crevice deposits in a single tube model boiler (STMB) heat transfer test. The crevice deposit formed from this testing was characterized and compared to deposits from operating plants.

Task 300 utilized electrochemical tests, mini-autoclaves for C-ring testing and stressed capsules in a variety of media suggested by the review of background data.

Task 400 utilized input from the background data and ongoing work in Tasks 200 and 300 to recommend candidate neutralizers. The neutralizers judged most likely to succeed are recommended for confirmatory testing under prototypical conditions in a model boiler. The result of such testing would form the basis for recommendations of a specific neutralizer for field use.

OBJECTIVES

The objectives of this project are to produce IGA in the laboratory with conditions consistent with the results of field studies. With knowledge of these conditions, limited evaluation of possible inhibitors and/or other corrective actions that can be applied in the field will be conducted. Specifically, the objectives of each task are given below.

Task 200: Mechanism Selection and Demonstration

The objective of this task was to form a deposit in-situ that simulates the composition of tubesheet crevice deposits and determine if these deposits can cause IGA of Alloy 600 in the tubesheet crevice.

Task 300: Screening Tests

The objective of this task was to determine the sensitivity of Alloy 600 to intergranular attack (IGA) when various chemical contaminants are added to the corrosion environment, either singly or in combination. The choice of

contaminants was based on evaluation of plant data and previous laboratory testing of the corrosion resistance of Alloy 600. A second objective was to preliminarily evaluate proposed neutralizers.

Task 400: Neutralizer or Inhibitor Selection and Evaluation

The objective of this task was to evaluate and select candidate tubesheet crevice corrosion neutralizers, and to define a test program to test the neutralizer(s) judged most likely to succeed.

Section 2

CONCLUSIONS

1. No SCC and only a very limited amount of grain boundry attack was produced in the Task 200 single tube model boiler (STMB) test. Two test conditions are thought to have produced these results. First, the absence of cupric oxide from the sludge formulation precluded formation of the oxidizing environment and kept the electrochemical potential out of the cracking regime. Secondly, frequent thermal cycling flushed alkalinity from the crevice (as evidenced by hideout-return data) and prohibited concentration of caustic to levels sufficient to produce IGA.

2. Short duration, 1-2 day, anodic polarization exposures at potential values at the middle of the active range, at the active peak, or at the active to passive transition are ineffective in promoting IGA in strongly alkaline solutions (50 wt % caustic). The resultant IGA was no greater in depth than was observed on identical specimens at open circuit potential in the same chemical environment. Anodic polarization did promote SCC in many of the environments which were tested.

3. Subtask 302-A C-ring data and Subtask 302-B isothermal capsule data indicate that IGA produced in the reference test environment (40 wt % NaOH + 10 wt % KOH at 650^{o}F) proceeds at a very slow rate (1 to 2 mils in 90 to 180 days). Capsule data show that addition of Cr_2O_3 to the reference environment accelerates IGA. With this additive to the caustic environment, very uniform IGA to a depth of 6-8 mils is produced in only 90 days. By producing a relatively large amount of IGA in a short period of time, the caustic + Cr_2O_3 environment is an excellent candidate reference environment for laboratory evaluation of chemical additives as potential IGA inhibitors.

4. Results obtained from electrochemical tests (Subtask 301) show that a combination of chemical environment and stress (> the yield stress) can

increase IGA by as much as a factor of two. Results of C-ring and capsule tests in the same environments (Subtasks 302-A and 302-B) show that at stress levels below the yield stress, increasing the applied stress to 75% of the yield stress has no effect on the resulting amount of IGA.

5. In 50% caustic environments (Subtasks 301, 302-A and 302-B), SCC was accelerated by increases in stress both below and above the yield stress. The magnitude of the resulting SCC associated with stress increases was much greater than the corresponding IGA produced on the same specimens. In the environments which were tested, the net effect of increased stress was to propagate through wall cracks before a significant (2 to 3 mil deep) matrix of uniform IGA could be generated.

6. In all devices in which it was tested, sodium nitrate additions to the reference caustic environment were found to inhibit both SCC and IGA. Although eliminating the occurrence of these localized forms of corrosion, nitrate additions promoted general surface corrosion.

7. Other additives to the reference environment, such as SiO_2, CuO + ZnO, and SiO_2 + CuO + ZnO, decrease IGA and increase the SCC susceptibility of mill-annealed Alloy 600.

8. Under simulated tubesheet conditions of temperature (600 and 650^{o}F), materials (A508 slug within a mill-annealed Alloy 600 tube), and the chemical environment of ~50 wt % caustic, accelerated non-protective corrosion of the low alloy steel has been observed. This corrosion, in turn, produced tube deformation as evidenced by capsule bulging. These results indicate that the tube deformation, detected by eddy current measurements, at the top of the tubesheet in some operating plants may have been produced by the same caustic environment thought to produce IGA and SCC deeper within the tubesheet crevices of those same plants.

Section 3

APPARATUS AND PROCEDURE

MODEL BOILER TEST (TASK 200)

Materials

The single tube model boiler (STMB) test configuration used in Task 200 is shown in Figure 3-1. It consisted of a 3/4 in. OD (0.043" wall thickness) mill annealed Inconel 600 tube (heat 1183 - see Table 3-1 for chemical and physical description) with a tubesheet and a support plate simulant. The tubesheet simulant was constructed of 4130 carbon steel, a material similar to the SA 508 carbon steel used for tubesheets in some steam generators. The tubing was mechanically rolled approximately one inch into the bottom of the tubesheet simulant leaving a 2-3/4 in. long by 0.008 in. radial crevice between the collar and the tubing. The top of the tubesheet was counterbored 1/4 in. to form a sludge cup. A porous Alloy 600 frit was used to retain sludge in the cup. The support plate simulant was constructed of SA 285 carbon steel and formed a 3/4 in. by 0.0125" radial crevice. Frits covered the top and bottom of the support to retain prepacked sludge.

Operating Conditions

The STMB test facility has been previously described in detail (1). It is sufficient to note that the primary system consists of a high pressure (2200 psi), high temperature (620^{o}F) stainless steel loop. Water from the primary loop flows down a bayonet tube located within the Alloy 600 tube (which has an Alloy 600 plug welded into the bottom end) and then exits the boiler by flowing back up the annulus beween the bayonet tube and test device. Steam is produced by heat transferred from the primary side to the 15 inches of secondary water covering the tube. The tube, secondary water, and steam are contained in a 4 in. schedule 160 carbon steel pipe with a Graylock closure. The steam flows out of the closure through a condenser in the closed cycle natural circulation loop, which comprises the secondary system (Figure 3-2), and re-enters at the bottom of the boiler as subcooled water to repeat the cycle.

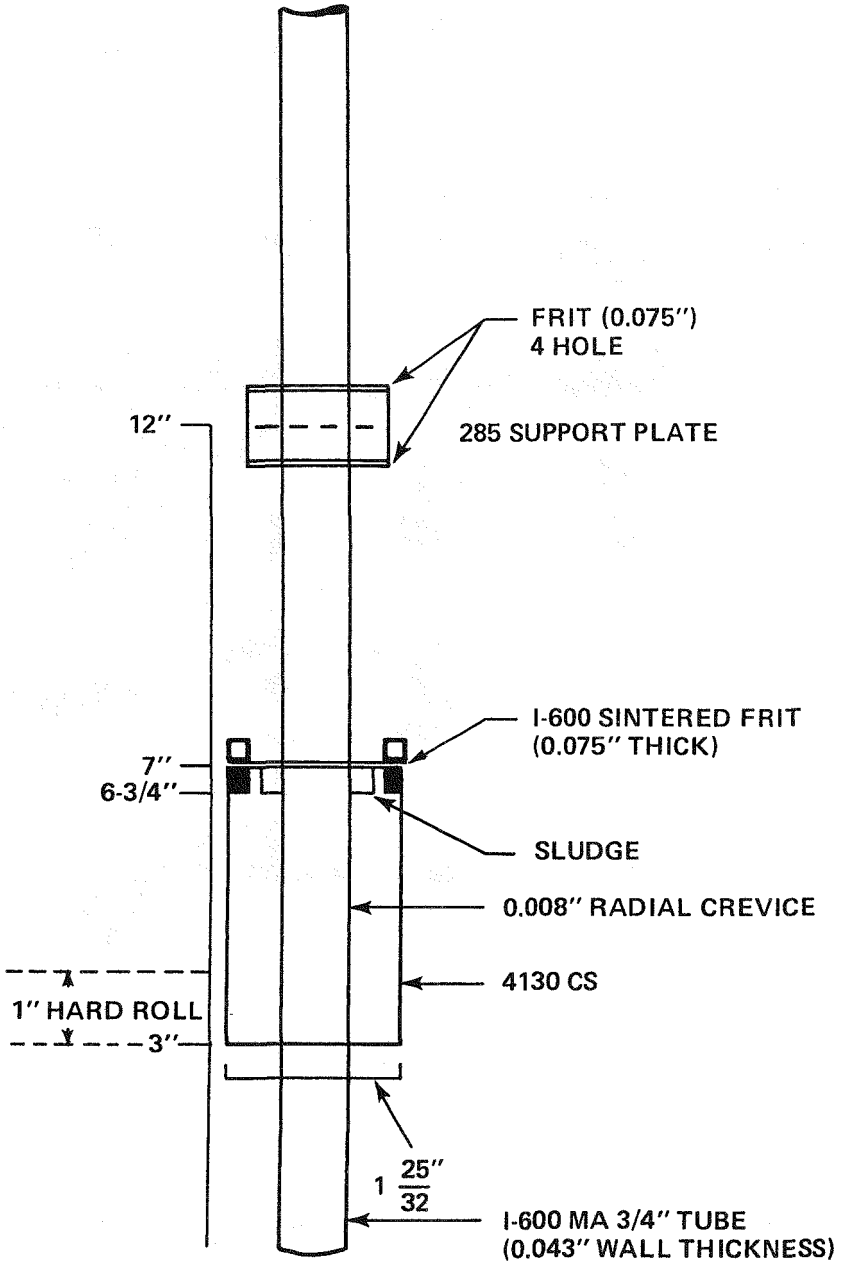

Figure 3-1. Schematic of Task 200 Model Boiler Test Configuration

Table 3-1

CHEMICAL AND PHYSICAL PROPERTIES OF ALLOY 600 HEAT NX 1183

Chemical Analysis Element	Weight Percentage
Ni	73.58
Cr	16.31
Fe	9.39
C	0.024
Mn	0.29
S	0.002
Si	0.18
Cu	0.23
Al	0.11
Ti	0.20
Mg	0.005
Co	0.04
P	0.009
B	0.004
Pb	<0.001

Mechanical Properties

Yield Strength 55,050 psi

Ultimate Tensile Strength 100,000 psi

Percent Elongation 35.6 Percent

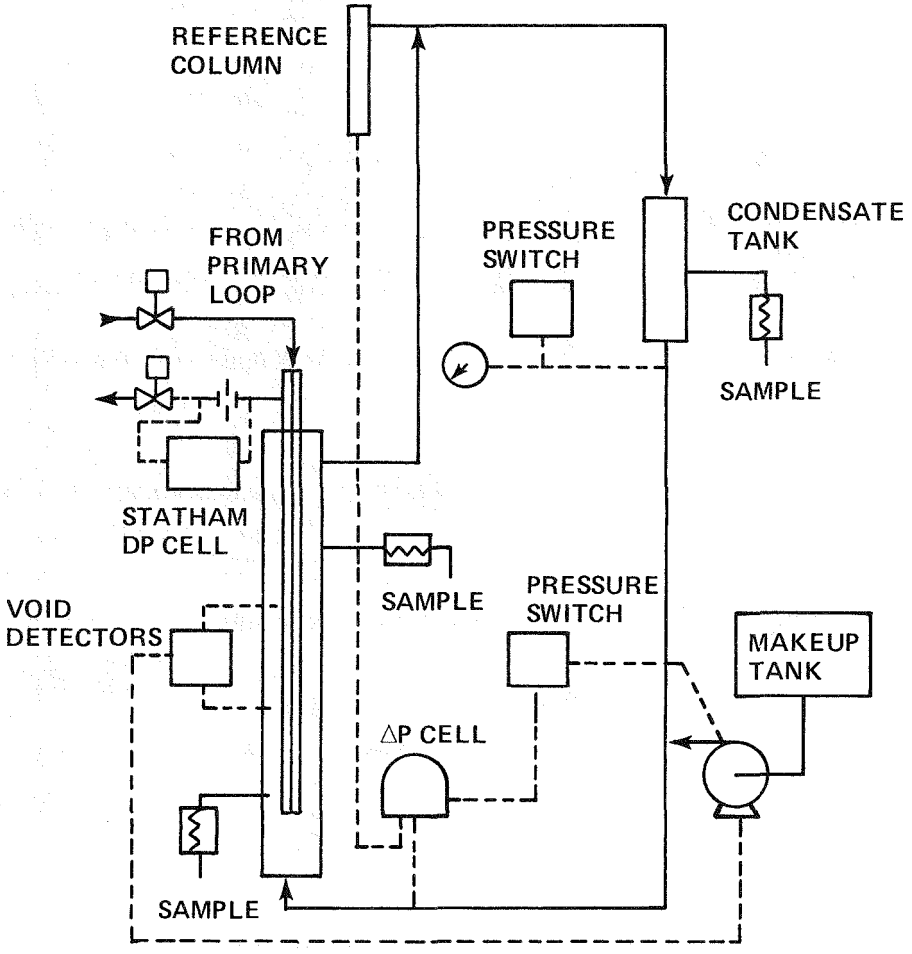

Figure 3-2. Schematic of Model Boiler Test System

Thermal and hydraulic specifications for this test are shown in Table 3-2. Actual operating conditions are given in Section 4. Thermal cycling was conducted twice per week during the first month of testing and once every 2 weeks for the remainder of the test. A typical thermal cycle (shown in Figure 3-3) was conducted by decreasing the temperature at a rate of 50°F/hour, holding at a bulk water temperature of 200°F for 1 hour, then increasing the temperature to normal operating temperature. The purpose of thermal cycling was to simulate plant operating cycles and to allow more ingress of solution to the crevice region to promote deposit formation.

Chemistry

The chemistry conditions for this test were chosen to simulate condenser inleakage of Lake Ontario water into a steam generator operating on all-volatile chemistry in an attempt to evaluate the propensity for caustic concentration and crevice deposit formation from such an occurence. The boiler chemistry conditions were a result of feeding 50 ppb N_2H_4, 2.2 ppm NH_4OH, and simulated Lake Ontario water from the makeup tank at a rate of a 12 liters/day (see Table 3-3 for simulated Lake Ontario water ingredients and Table 3-4 for its analysis). Continuous steam bleed was conducted 24 hr/day at a rate of 8 mL/min. and continuous blowdown at a rate of 1 mL/min was conducted 8 hr./day which resulted in a total volume loss of 12 liters/day. Volume losses due to sampling were replaced by pumping solution from the makeup tank to the boiler. Nonvolatile components in the boiler were concentrated to the maximum achievable, which is calculated by multiplying the makeup tank concentration times the ratio of steam bleed to blowdown. Typically the concentration factor is 20 for 10 liters per day steam bleed and 0.5 liters per day blowdown. The boiler water chemistry analysis results are given in Section 4.

Pretest Sludge Additions

Prior to testing, 0.40 gram of Mapico-Fe_3O_4 (particle size 0.2-0.5 micrometer) and 0.40 gram of Meramec-Fe_3O_4 (particle size 20-50 micrometers) were prepacked in the support plate crevice. Also, 1.46 grams of simulated Lake Ontario sludge with the formulation given in Tables 3-5 and 3-6 was packed in the sludge cup of the tubesheet simulant.

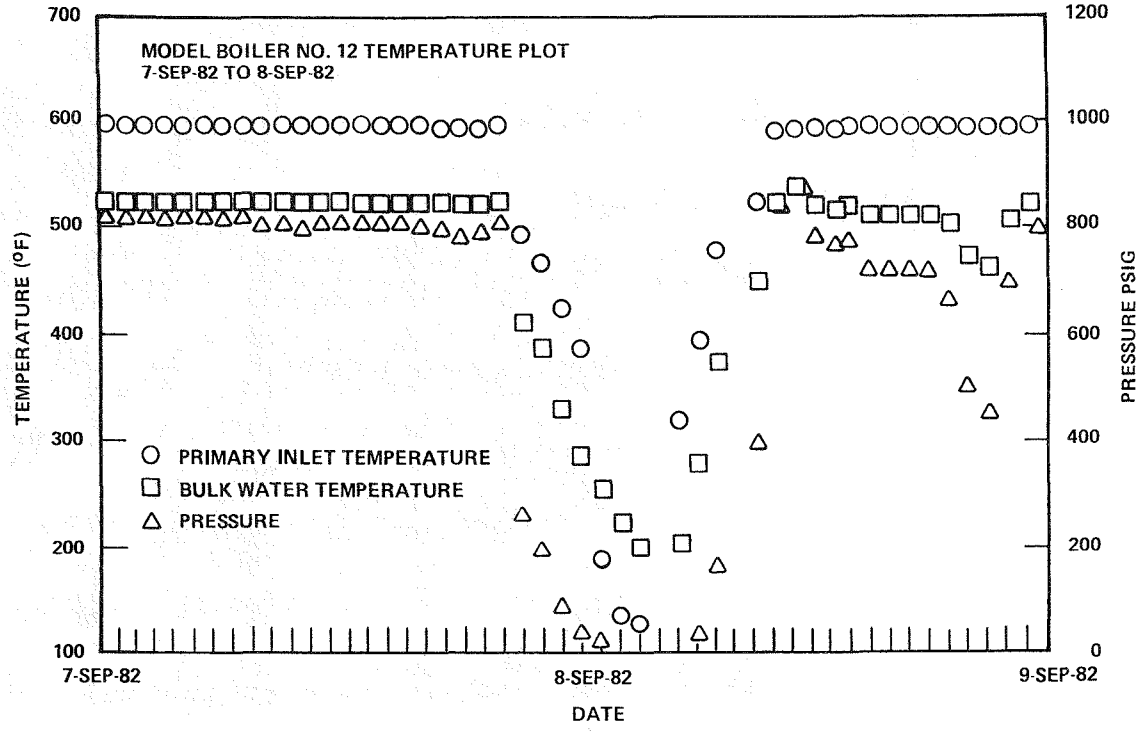

Figure 3-3. A typical thermal transient performed on Boiler No. 12 to allow ingress of solution into the crevice region

Table 3-2

S183-2 TASK 200 STMB OPERATING SPECIFICATIONS

Primary loop temperature	$620^{o}F \pm 3^{o}F$
Primary loop pressure	2200 psi
Primary boiler inlet temperature	$610^{o}F \pm 5^{o}F$ (Variable to $620^{o}F$)
Primary boiler outlet temperature	$595^{o}F \pm 5^{o}F$ (Variable to $600^{o}F$)
Secondary temperature (800 psi)	$520^{o}F$ (Variable)
Heat flux range	10K to 90K Btu/hr-ft^2
Steam bleed	8 mL/min - continuous
Blowdown	1 mL/min - 8 hrs/day

Table 3-3

SIMULATED LAKE ONTARIO WATER INGREDIENTS
(5X CONCENTRATE)

Quantity Added to 10 Liters Water

6.86 gm CaO
3.84 gm $Mg(OH)_2$
4.26 gm Na_2CO_3
0.76 gm KCl

0.99 mL conc. HCl (38 percent)
0.85 mL conc. H_2SO_4 (98 percent)
0.16 mL conc. HNO_3 (68 percent)
0.03 mL conc. H_3PO_4 (85 percent)

After dissolving, carbon dioxide was bubbled through the solution to saturate it, then after standing a few hours, solid precipitates were filtered off. The filtrate was added to the makeup tank as 100 mL per 100 liters of water. Final dilution of lakewater in boiler is 200 fold.

Table 3-4

ANALYSIS OF SIMULATED LAKE ONTARIO WATER 5X (FILTRATE)

Analysis for:	Results
pH	8.23
Conductivity	1300 $\mu S/cm^2$
Na	142.5 ppm
Ca	11.2 ppm
Mg	145.9 ppm
Cu	2.1 ppm
Fluoride (F^-)	0.8 ppm
Phosphate (PO_4^{-3})	0.12 ppm
Nitrate (NO_3^-)	25.8 ppm
Sulfate (SO_4^{-2})	162.94 ppm
Carbonate (CO_3^{-2})	1650 ppm

Table 3-5

ANALYSIS OF SIMULATED LAKE ONTARIO WATER PRECIPITATE

Emission Spectrographic, Atomic Absorption, Organic Carbon Results

Element	Weight Percent
Al	0.42
Ca	36.6
Cr	0.0079
Cu	0.0027
Fe	0.068
K	0.01
Mg	0.24
Mn	0.025
Na	0.08
Ni	0.12
P	0.28
Si	0.42
Ti	0.0073
Carbon	13.5
Total	51.78 Percent

X-ray Diffraction detected only $CaCO_3$.

Remainder is mostly oxygen since oxygen makes up 48 w/o of $CaCO_3$. By leaching out slightly soluble compounds from the precipitate it was found by ion chromatography that the solid also contained 19 ppm fluoride, 210 ppm chloride, 198 ppm phosphate, 47 ppm nitrate, 343 ppm sulfate.

Table 3-6

COMPOSITION OF SLUDGE PACKED INTO TUBESHEET CREVICE (PRETEST)

Compound	Quantity (gram)	Weight Percentage
Simulated Lake Ontario Water Precipitate	0.365	25.0
Fe_3O_4	0.782	53.6
Cu	0.273	18.7
Cu_2O	0.022	1.5
NiO	0.011	0.7
Cr_2O_3	0.005	0.3
Total	1.458	

ELECTROCHEMICAL TESTS (SUBTASK 301)

Apparatus. The apparatus (shown in Figure 3-4) employed a two liter nickel-201 autoclave which was equipped with five symmetrically located openings in the autoclave head. The openings accommodated insulated leads (0.125" dia. nickel rods) which contacted a nickel sheet electrode (1" x 1") that was used as a reference, three test specimens in the form of Alloy 600 (specifications in Table 3-7) C-rings, and a flat coupon of Alloy 600 that was used as a counter electrode. A nickel 201 thermowell was also centrally located in the autoclave head.

Specimens. C-rings and stressed tube sections were utilized in these tests. C-rings were stressed at two levels; some were stressed to the yield point and others were plastically deformed by stressing beyond the yield point. The plastically deformed, closed C-ring specimens were prepared by stressing the C-rings until the legs of the specimens touched. Stressed tube specimens were prepared by inserting a 0.5 in. long carbon steel internal expansion plug into the tube and expanding it until ~0.5% strain was produced.

Procedure. In each test, sufficient water was added to the nominal test installation to provide the necessary steam pressure at the test temperature, and the initial quantity of test electrolyte adjusted so that at the test temperature each C-ring apex was immersed 0.25", exposing 0.744 sq. in. (4.8 cm^2). A cover gas of nitrogen at a room temperature overpressure of 200 psi was used in all tests to maintain a stable immersion level. Prior to application of the overpressure, the solutions were deaerated by repeated pressurizations of the autoclave at room temperature to 500 psig with high purity nitrogen gas (a minimum of five pressurizations was used). Each pressurization was followed by slow release of the gas until the pressure returned to one atmosphere.

In addition to the C-ring specimens on the insulated rods, other specimens were placed on the bottom of the autoclave to provide data under unpolarized conditions. After each test exposure, the specimens were examined using light microscopy. All specimens were subsequently sectioned through the middle and prepared for metallographic study in order to determine the maximum depth and mode of attack.

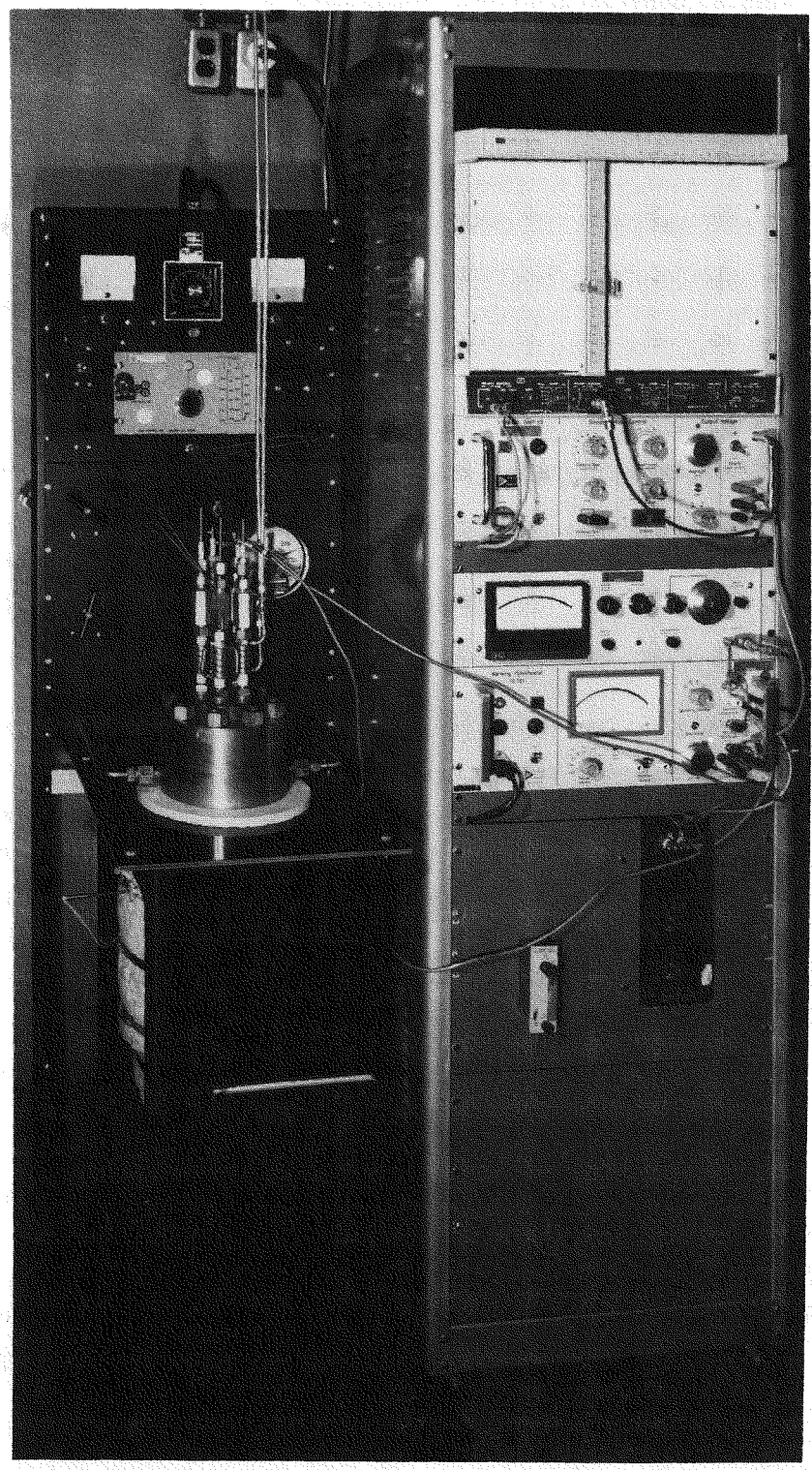

Figure 3-4. Electrochemical Test Facility

C-RING TESTING (SUBTASK 302A)

Specimens. The C-rings were fabricated from mill annealed (non-thermally treated), 7/8 in. O.D. x 0.050 in. wall, Alloy 600 tube (type WESTRO 600 T). The tubing specifications are the same as those for the Electrochemistry Test C-rings (see Table 3-7). The C-rings were formed by removing a 60^{o} segment from a 3/8 in. wide ring section. Two 5/32 in. O.D. holes (diametrically opposed and symmetrical to the 60^{o} cutout) were drilled in each C-ring to accommodate the 6-32 Alloy 600 screw and nut used to apply the stress. The C-rings were stressed to either 25 percent or 75 percent by tightening the screw and nut to produce a C-ring deflection that is related to the stress by the equation,

$$\sigma = \frac{4dEtZ}{\pi D^2}$$

d = deflection (along screw)
E = Young's modulus
t = tube wall thickness
D = tube OD - t
Z = correction factor (2) = 0.96

Mini-Autoclaves. A mini-autoclave, shown in Figure 3-5, is a small pressure vessel which contained the C-ring specimens and caustic test solution. All wetted parts were Nickel 200. The body was a 1-3/4" o.d. rod, 9-3/4" long, with a 1.0" hole bored 8-3/4" deep. A Type 304 stainless steel threaded collar was fastened to the top of the body to permit bolting of the nickel head.

Main Pressure Vessel. The main pressure vessel contained one or four mini-autoclaves and sufficient water to cover them. The main vessel was a standard Autoclave Engineers Type 316 stainless steel bolted closure pressure vessel, either two or four liters in size, depending on whether one or four mini-autoclaves were contained.

Procedure. Nine C-rings were put into each mini-autoclave; four stressed at 25 percent of the room temperature yield strength (ys.) four at 75 percent ys, and one unstressed. The six cap screws were torqued to about 16 ft-lb, and the mini-autoclave was leak checked. The chemicals required to make up the test solution were put into a glove box, together with the mini-autoclave. The glove box was evacuated and back filled with inert gas three times. Degassed and deionized

Table 3-7

SPECIFICATIONS FOR ALLOY 600 TUBE

Heat Number: NX 9955

Mechanical Properties:

TS	103 KSI
YS	56 KSI
Elong.	40%
Hardness	88 R_b

Chemistry:

C	0.026
Mn	0.23
Fe	9.69
S	0.001
Si	0.12
Cu	0.30
Ni	74.07
Cr	15.56
Al	0.06
Ti	0.15
Co	0.03
P	0.011
B	0.004

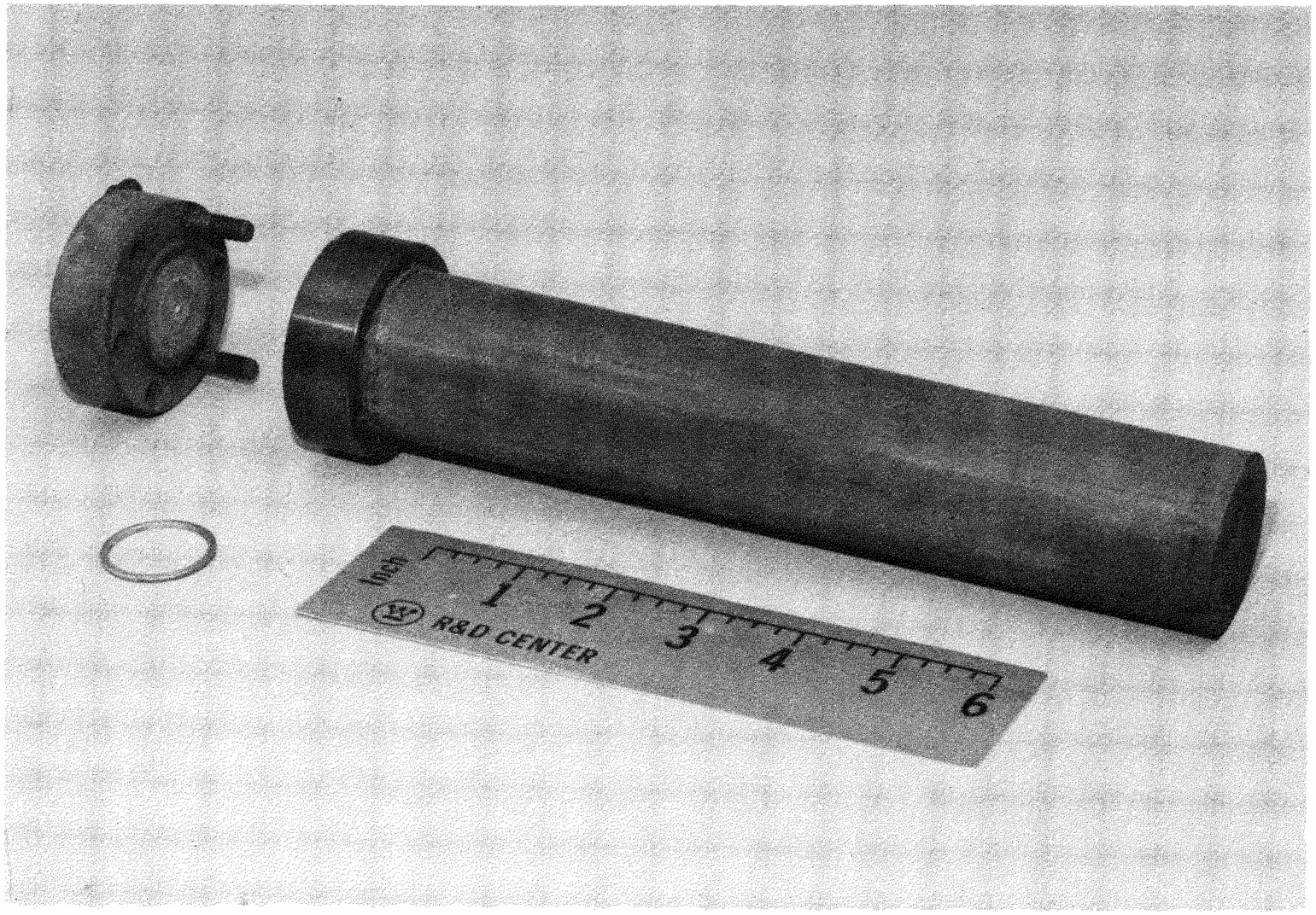

Figure 3-5. Mini-autoclave

water was supplied to the glove box to make up the test solution. The test solution was syringed into the mini-autoclave through a port in the top of the head. The port, an AE 1/4" cone fitting, was sealed while in the glove box.

The mini-autoclave(s) was set into the main pressure vessel (autoclave). Sufficient pure water was added to cover the mini-autoclave(s) at the test temperature. The autoclave was sealed, pressure checked, and deaerated by steaming at 220-250^{o}F. A few hours after attaining the test temperature (650^{o}F), the water bath was sampled to detect any leakage of alkali from the mini-autoclaves. This leak check was repeated, depending on the length of the exposure.

Specimen Evaluation. After each exposure, the specimens were rinsed in pure water, dried, and weighed. After the first exposure period (4 weeks or 672 hours), the specimens were examined at 30 x for IGA, SCC, etc. and returned to test. After the second exposure period (8 weeks or 1344 hours), for a cumulative time of 12 weeks or 2016 hours, the specimens were again examined at 30 x. Four of the nine C-rings (two at each stress level) were removed for microexamination and the remaining five C-rings in each mini-autoclave were returned to test. After the third, and last, exposure period (4 weeks or 672 hours, for a total of 16 weeks or 2088 hours) the remaining five C-rings were examined at 30 x and then microexamined.

The microexamination procedure was to section, mount, polish, and etch the specimens. The etchant was either electrolytic phosphoric or bromine-methanol. The specimens were microscopically examined at 100 to 500 X, before and after etching, and then photographed at 100 to 1000 X after etching.

CAPSULE TESTING (Subtask 302B)

Specimens

A capsule is a test specimen which acts as a self-contained pressure vessel. A cross-sectional view of the capsule is shown in Figure 3-6. The capsule consists of a length of Alloy 600 steam generator tubing with Alloy 600 end plugs welded on the top and bottom. The end plugs are leak checked. The plug welds and adjacent HAZ are stress relief annealed by induction heating at 1300-1400^{o}F for 25 seconds. The tubing specifications are the same as those used in the Electrochemistry and C-ring testing (see Table 3-7). An Alloy 600 Swagelok fitting is welded into the top plug to provide solution access. Some of the capsules had a cylindrical piece of SA-508 tack-welded to the bottom Alloy 600 end plug.

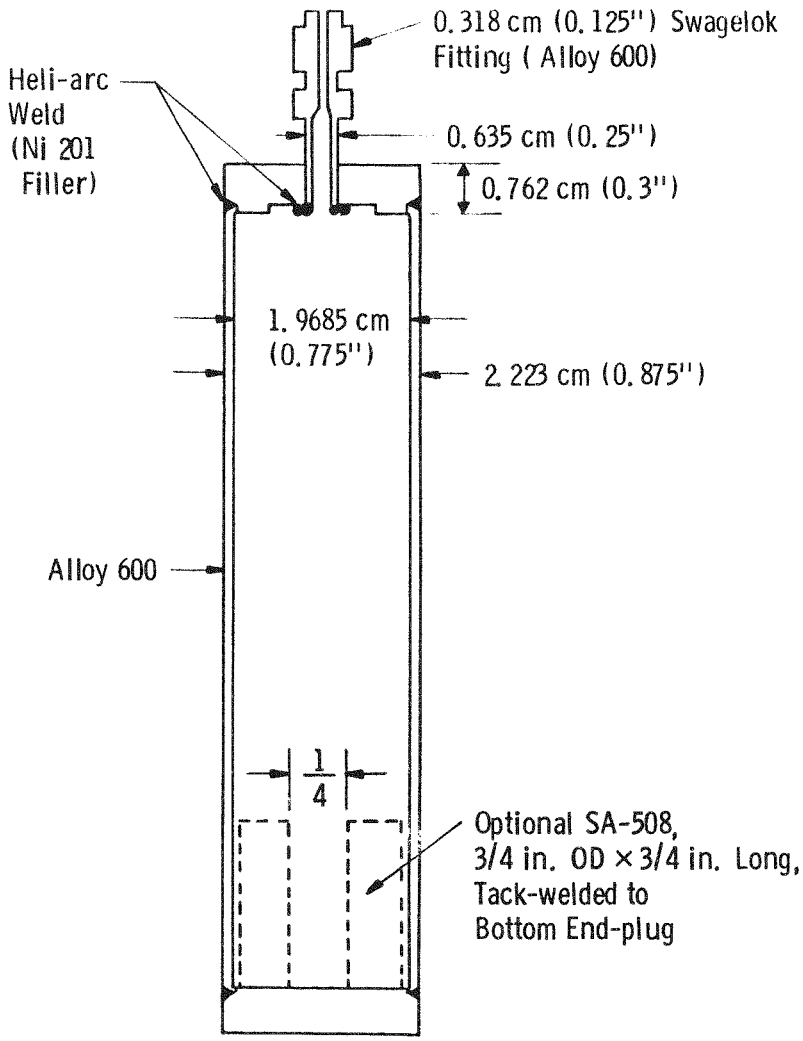

Figure 3-6. Test capsule used for studying IGA and SCC in caustic environments

The above capsule geometry was selected as a result of capsule proof tests designed to evaluate results from two types of capsule geometry. The other type of capsule had a 1-inch long, 29-mil deep flat machined into the external surface of the Alloy 600 capsule. The flat was near the center of the capsule and spanned the liquid-vapor interface.

Capsule Furnace. The capsule furnace is a device for heating 22 capsules. The capsules are placed in safety cans within the furnace (isothermal aluminum block with band heaters and insulation). Figure 3-7 shows a view of several of the furnaces and their control equipment used in capsule experiments. Thermocouples (TYPE J) placed at random inside the block provide input for a G.E. Model BHG multipoint recorder. One of the thermocouples acts as the input to the over temperature control (LFE model 232) for shutdown of band heater power. The temperature of the blocks was maintained at $650^{o}F \pm 4^{o}F$.

Procedure. The capsules were filled with test solution as follows: (1) solid additions to the reference caustic solution were placed in the capsule, (2) the capsules were placed in a glove box, evacuated, and purged with argon three times, (3) the reference caustic solution was prepared in the glove box, (4) 15 mL of the prepared caustic solution was syringed into the capsule and (5) the Swagelok fitting was tightened with the capsule still in the glove box.

The target duration for exposure in the furnaces was 180 days for Subtask 302B capsules. The capsules were removed weekly, cooled, and examined for evidence of through-wall penetration or leakage at the swagelok fitting. Capsule integrity was confirmed by weight measurement. Capsules which did not maintain intergrity were removed from testing for possible further evaluation.

Specimen Evaluation. All capsules which had received their targeted exposure time were sectioned for microexamination . Additionally, some of the capsules removed from test during the weekly examinations were selected for microexamination.

Each of the above capsules was sectioned at three areas; top, center, and bottom. The top and bottom sections were made at 45^{o} to the tube axis. The resulting section contained as one specimen, the weld area, the heat affected zone (HAZ) adjacent to the weld, and unaffected regions further up the tube. The central section was obtained by making two transverse cuts 1.0 in. apart to obtain

Figure 3-7. Isothermal Capsule Test Furnaces

the portion of the tube encompassing the liquid-vapor interface. This 1.0-in long piece of tube was then split longitudinally.

The sections were mounted, polished and etched. The etchant was either electrolytic phosphoric or bromine-methanol. The specimens were microscopically examined at 100 to 500 x, before and after etching, and then photographed at 100 to 1000 X after etching.

REFERENCES

1. Final Report on S112-1, "Laboratory Studies Related to Steam Generator Tube Denting".

2. ASTM G 38-73, "Standard Recommended Practices for Making and Using the C-Ring Stress-Corrosion Cracking Test Specimen".

Section 4

RESULTS AND DISCUSSION

Experimental work was performed under both Task 200, Single Tube Model Boilers, and Task 300, Screening Tests. High temperature electrochemistry tests, Subtask 301, C-rings exposed in nickel mini-autoclaves, Subtask 302-A, and isothermal capsule tests, Subtask 302-B, were performed as a part of Task 300. The results of these Tasks/Subtasks are presented and discussed in this section.

MODEL BOILER TEST (TASK 200)

The Task 200 model boiler test began hot operations on July 31, 1982, in a 4 in. boiler vessel (boiler #12). The Alloy 600 tube used in the test, designated #302, had a support ring and tube sheet simulator as shown in Figure 3-1. Tube #302 was tested for 64 days at the thermal and hydraulic conditions plotted in Figure 4-1 (primary inlet and outlet temperature) and Figure 4-2 (secondary pressure and bulk water temperature). The pressure and temperature excursions in these plots were due to thermal cycling performed twice per week during the first month of testing and once every two weeks for the remainder of the test. These plots show that the test was conducted at the operating conditions initially specified in Table 4-2.

On October 6, 1982, tube #302 was removed from boiler #12 and eddy current tested at 130 kHz, 200 kHz, 400 kHz, and 550 kHz with a double coil self comparison probe. No crack indications were detected. The inner diameter of the tube was then measured in the support ring and tubesheet sludge cup/crevice region and no denting was found. Tube #302 was photographed and sent to metallography for sectioning. After sectioning, sludge samples were taken, and half of the tube was mounted for metallography while the other half was used for sludge analysis and scanning electron microscope (SEM)/energy dispersive x-ray analysis (EDAX). The results of metallography, sludge analysis, SEM/EDAX, and water chemistry analysis are presented below.

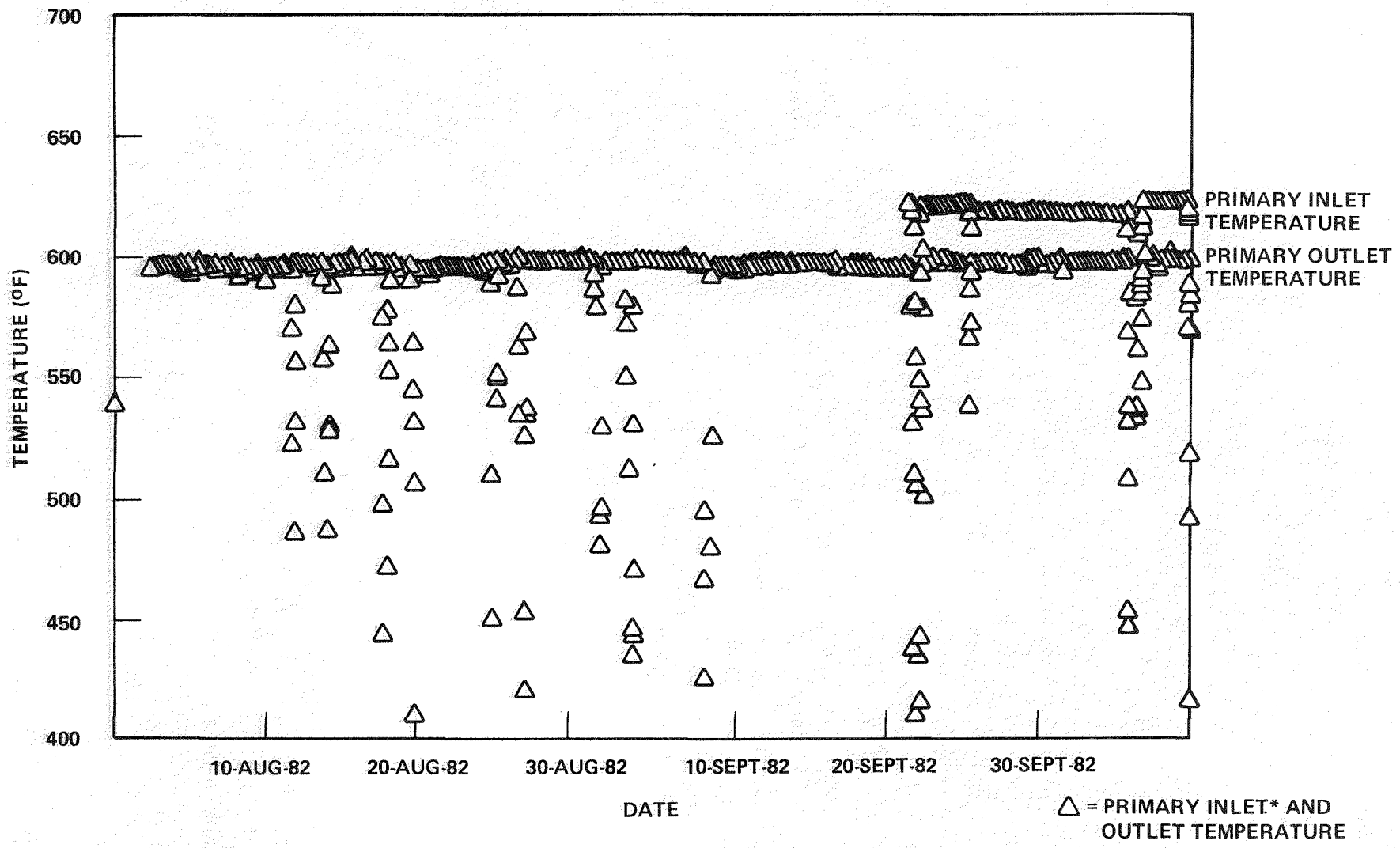

Figure 4-1. Temperatures Lower Than 590°F are a Result of Scheduled Thermal Transients
Model Boiler No. 12 Primary Inlet and Outlet Temperature Plot 31-Jul-82 to 9-Oct-82

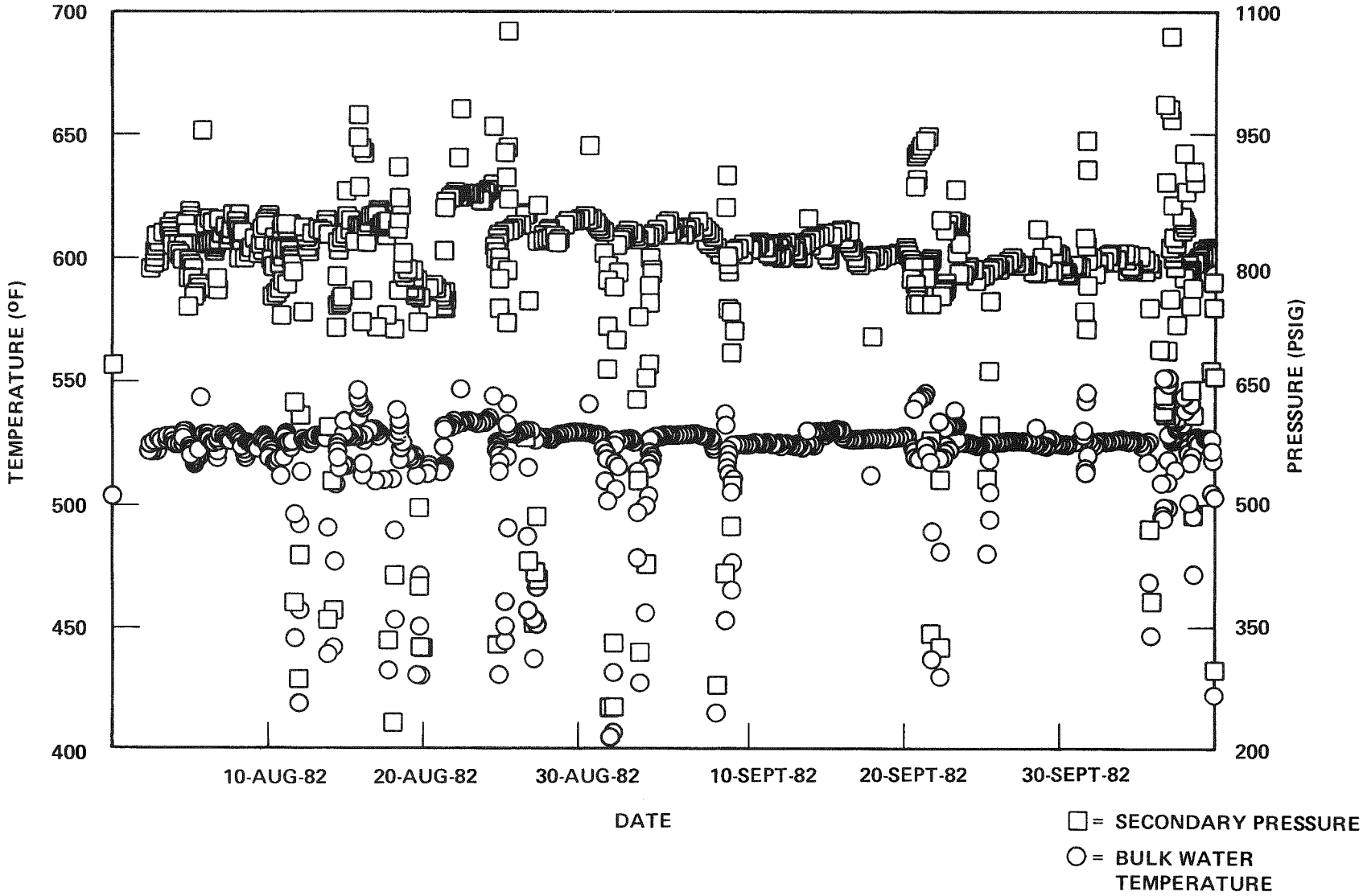

Figure 4-2. Model Boiler No. 12 Secondary Side Pressure and Temperature Plot 31-Jul-82 to 9-Oct-82

Water Chemistry Analysis

Task 200 model boiler chemistry analysis results are plotted in Figures 4-3 and 4-4. These chemistry conditions are a result of feeding simulated Lake Ontario water, having the composition shown in Table 3-4 (diluted 200 fold) with 50 ppb N_2H_4 and 2.2 ppm NH_4OH added, from the makeup tank at a rate of 12 liters/day. Table 4-1 shows that the average secondary water pH was 8.35 with an average conductivity of 14.98 $\mu S/cm^2$. The average chloride level was 0.60 ppm. Sodium was added to the boiler from the makeup tank at a concentration of 0.10-0.14 ppm, while calcium and magnesium were added at a concentration of 0.027-0.190 ppm and 0.13-0.15 ppm, respectively. Table 4-2 shows the mass balance for sodium, magnesium, and calcium. During the test, 45% of the sodium, 96% of the Mg, and 87% of the Ca input accumulated in the boiler. Since these cations were probably added in the carbonate form, an approximate boiler water carbonate concentration can be calculated. Assuming that these three cations were present as carbonates, 0.49-0.83 ppm carbonate was continuously introduced from the makeup tank. Actual analysis of the makeup tank during the final week of testing gave a carbonate concentration of 1.7-2.0 ppm while no carbonate was found in the blowdown sample. From this data it can be concluded that the carbonate concentration during testing was in the range 0.5-2.0 ppm.

Table 4-3 demonstrates the effect thermal cycling had on boiler water chemistry. In all cases, hideout return occurred during down power cycles. Conductivity increased significantly during every transient. In most cases pH increased 0.1-0.7 pH units. Thermal cycling may have flushed alkaline species from the crevice.

Metallography

Tube #302 was cut 1/4 in. above and below the support ring and tubesheet simulator. The support ring was then cut at midplane and the bottom half mounted for metallography while the top half was used for sludge analysis. The tube section in the tubesheet simulator was longitudinally cut at 0^o, 150^o, and 180^o (Figure 4-5). The 0^o-150^o section was used for metallography, the 150^o-180^o section for SEM/EDAX, and the 180^o-360^o section for sludge sampling.

The 0^o-150^o section was mounted and the 0^o face polished. Photographs at various locations in the sludge cup, at the top of the crevice, the midplane of simulator, and the roll transition region were taken at 100X, 200X, and 500X on the 0^o face

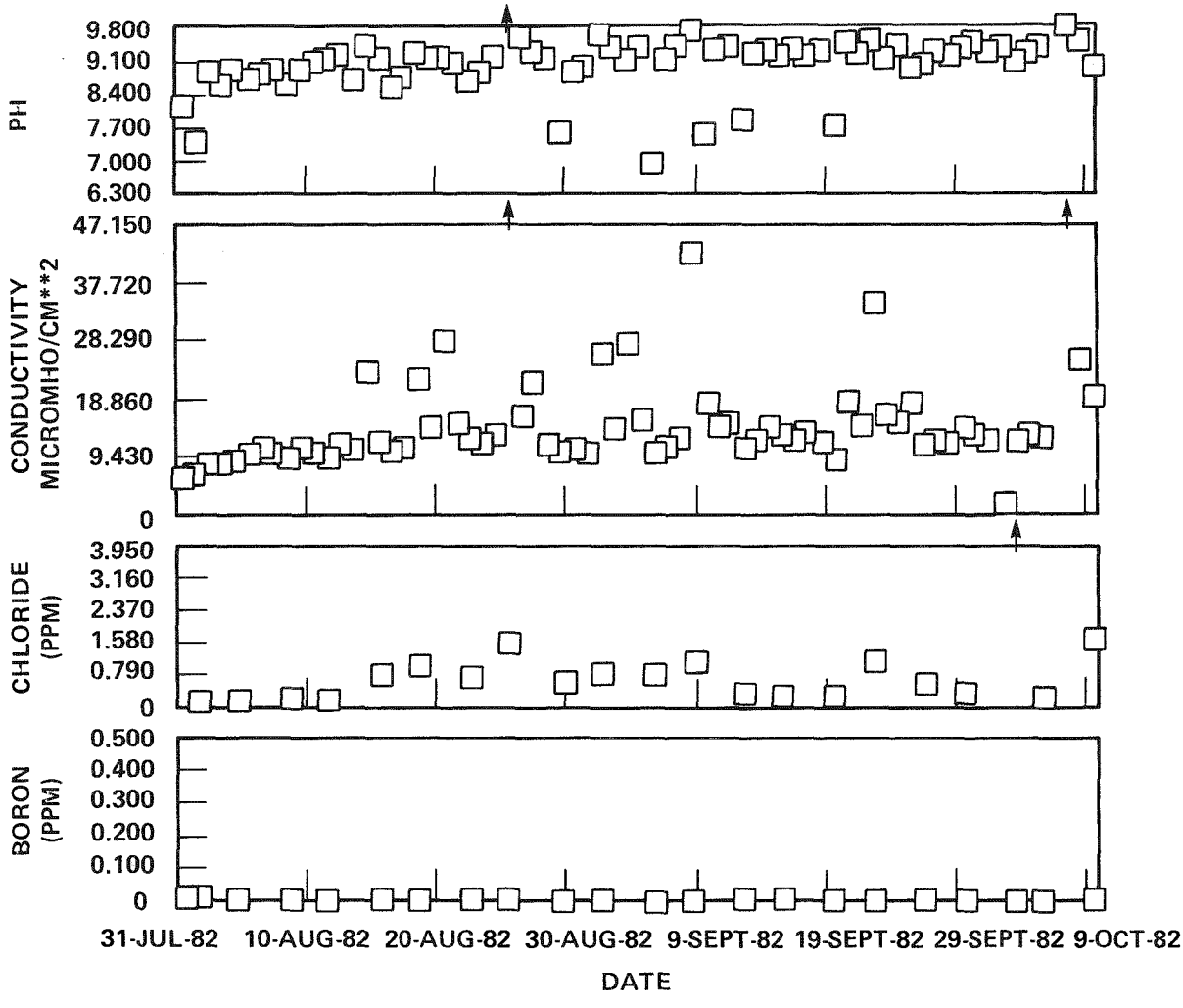

Figure 4-3. Chemistry Plot Boiler No. 12 31-Jul-82 to 9-Oct-82

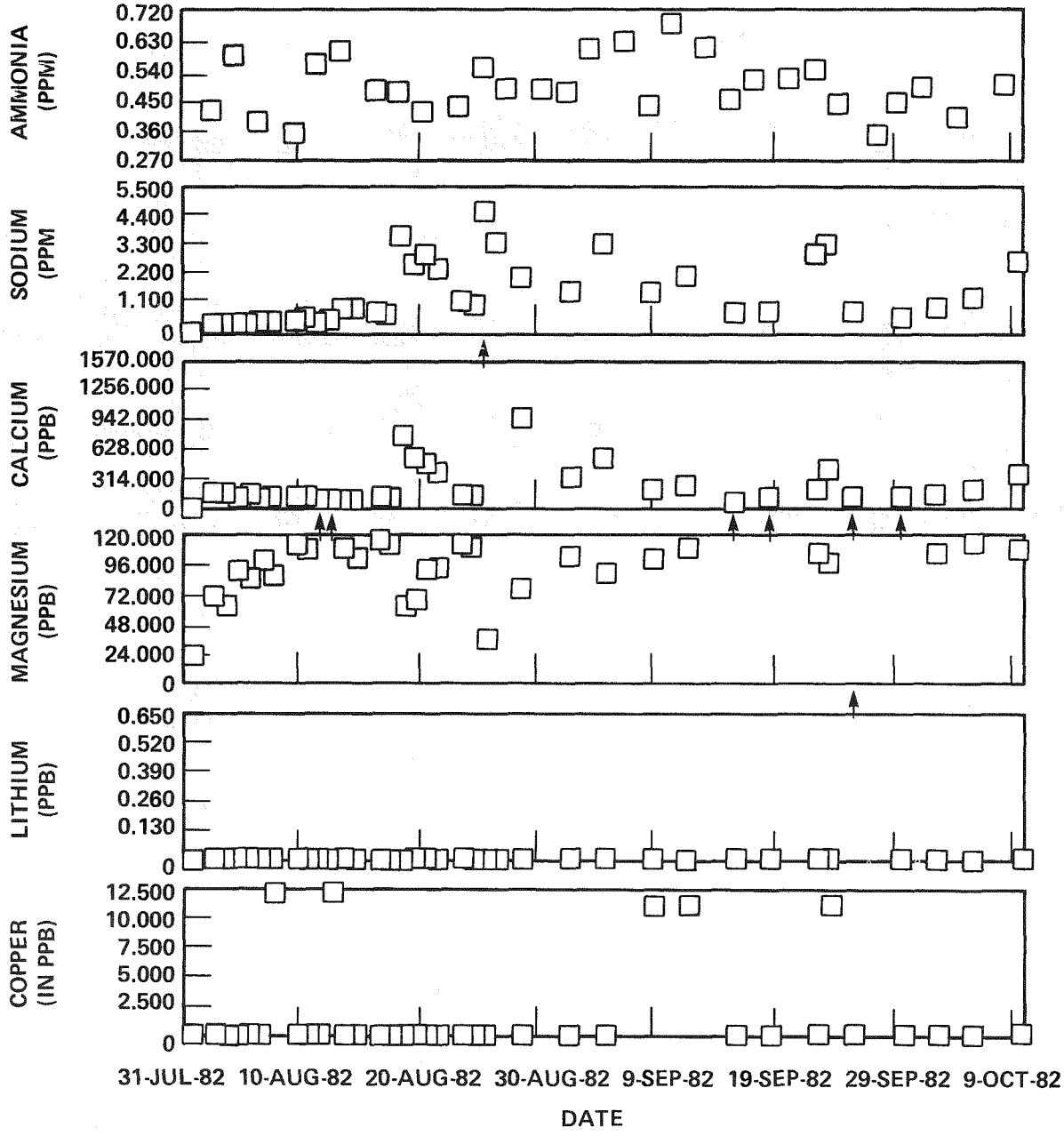

Figure 4-4. Chemistry Plot Boiler No. 12 31-Jul-82 to 9-Oct-82

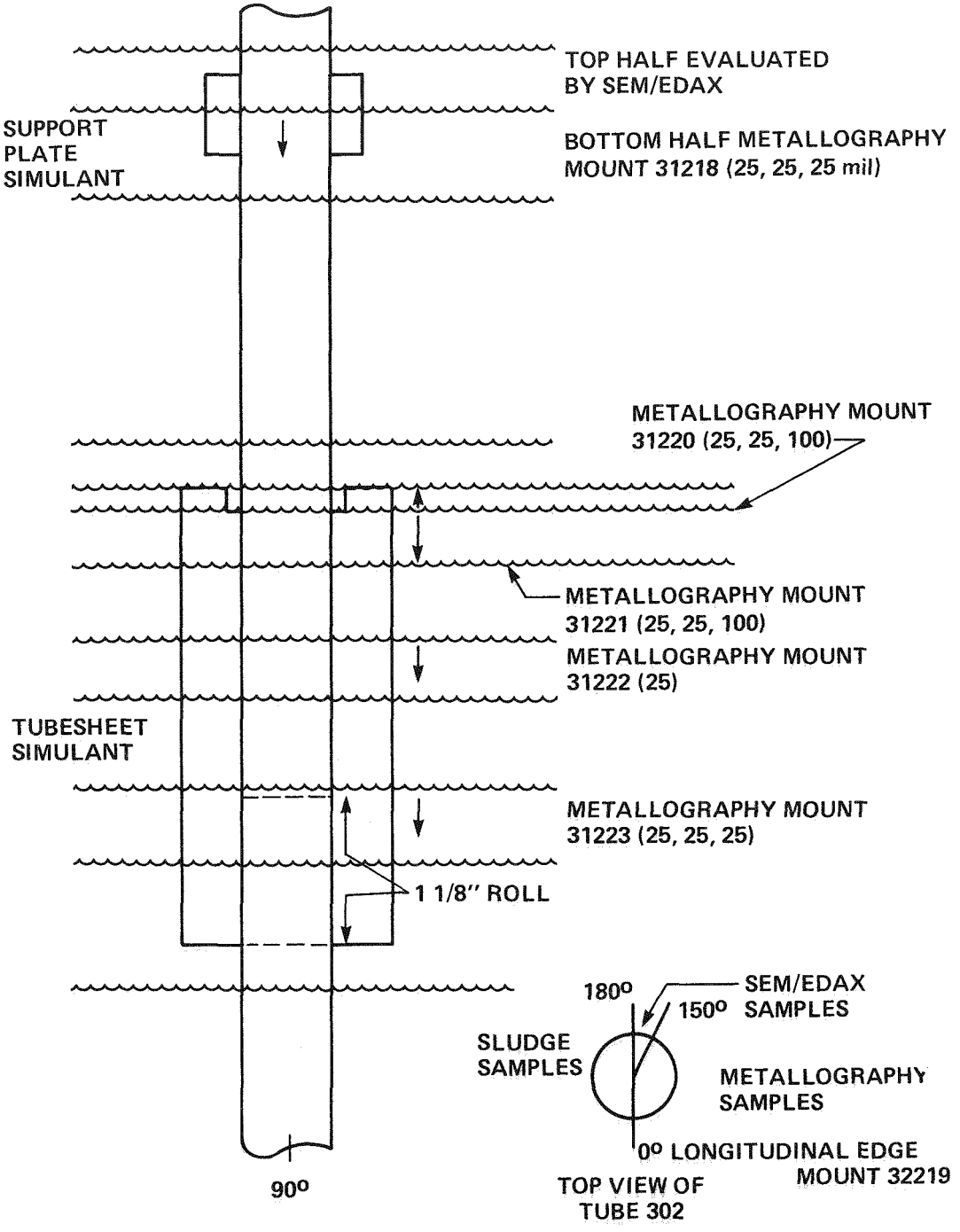

Figure 4-5. Tube 302 Sectioning for Metallography, Sludge Sampling, and SEM/EDAX (Arrow Denotes Direction of Grinding, and Face Examined, Numbers in Parenthesis are the Depth of Grinds after Initial Cut)

Table 4-1

SUMMARY OF TASK 200 MODEL BOILER CHEMISTRY CONDITIONS (BLOWDOWN)

Species	Mean	Maximum	Minimum
pH	8.35	9.83	6.90
Conductivity ($\mu S/cm^2$)	14.98	50.0	6.15
Chloride (ppm)	0.60	1.59	0.13
Ammonia (ppm)	0.49	0.68	0.34
Sodium (ppm)	1.37	4.54	0.00
Calcium (ppm)	0.230	0.945	0.010
Magnesium (ppm)	0.099	0.136	0.021

Table 4-2

SODIUM, MAGNESIUM, AND CALCIUM MASS BALANCE DATA
AT END OF TEST (IN GRAMS)

Species	Boiler Input	Accumulated Amount	Ratio Accumulated/Input
Na	0.116	0.052	0.448
Mg	0.269	0.259	0.964
Ca	0.200	0.173	0.866

Table 4-3

EFFECT OF THERMAL CYCLES ON CONDUCTIVITY

	Conductivity $\mu S/cm^2$		pH	
Thermal Cycle	Before	After	Before	After
8-11-82	9.73	11.83	9.15	9.26
8-13-82	10.71	23.00	8.75	9.45
8-17-82	10.38	21.70	8.80	9.35
8-19-82	14.00	27.80	9.24	9.23
8-24-82	12.50	50.00	9.25	9.83
8-26-82	15.60	21.40	9.60	9.35
8-31-82	9.85	26.40	8.95	9.62
9-2-82	13.50	27.40	9.42	9.18
9-7-82	11.70	41.90	9.39	9.72
9-21-82	14.10	33.80	9.25	9.48
10-5-82	12.30	47.60	9.33	9.72

in the as-polished and 10% oxalic acid etched condition. Representative photographs of these areas are shown in Figures 4-6 to 4-11. No stress corrosion cracking (SCC) or intergranular attack (IGA) was observed. Transverse cuts of this mount were then made at the bottom of the sludge cup, in the middle of the tubesheet simulator, and at the beginning of the roll transition region. The number and depths of grinds on each mount is detailed in Figure 4-5. After the initial cut and after each grind the mounts were examined in the as-polished and etched condition. Representative photographs were taken at 100X, 200X, and 500X on each polished and etched face. None of the mounts revealed any SCC/IGA with the exception of Mount 31220. After grinding 50 mils away from the bottom of the sludge cup (toward the top) a few grains at the tube surface were observed to have grain boundry attack (Figure 4-12). This observation was made at 0^{o} in the as-polished condition. When the sample was etched with 10% oxalic acid, grain boundary attack could not be seen. The sample was lightly polished, 1-2 mils two times in an attempt to find more attack, but none was found. Figure 4-12 represents the only grain boundry damange found in this test.

Representative photographs of the support ring tube outer diameter surface are shown in Figure 4-13. No SCC/IGA was found in this area after three 25 mil grinds down from the midplane. Mounts were examined at 500X after each grind, in the as-polished and 10% oxalic acid etched condition.

Sludge Analysis

Sludge was scraped from the 180^{o}-360^{o} tubesheet section and the support ring at the locations shown in Figure 4-14. These samples were analyzed by emission spectroscopy (ES), atomic absorption (AA), x-ray diffraction (XRD), ion chromatography (IC), and for total carbon. The results of these analyses are presented in Tables 4-4, 4-5, and 4-6. On an adjacent tubesheet section (150^{o}-180^{o}) sludge was analyzed using SEM/EDAX. The SEM photographs and EDAX analysis results (Figure 4-15) are given in Appendix A for both the tubesheet and support ring locations. A summary of major sludge component concentrations is given as a function of tube location in Figure 4-16. A description of the tubesheet tube deposits follows.

A thin black layer of sludge covered a copper colored metallic layer on the tube area 3/8 in. above the sludge cup top. This area was shown to be rich in Fe and Cu by EDAX (Figures A-1 and A-2). Below this area, extending from 1/8 in. above

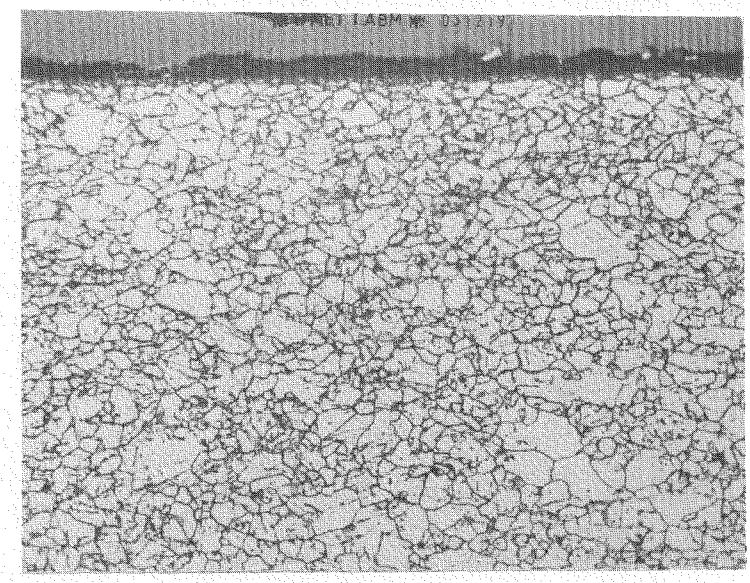

(A) 10% Oxalic Acid Etch

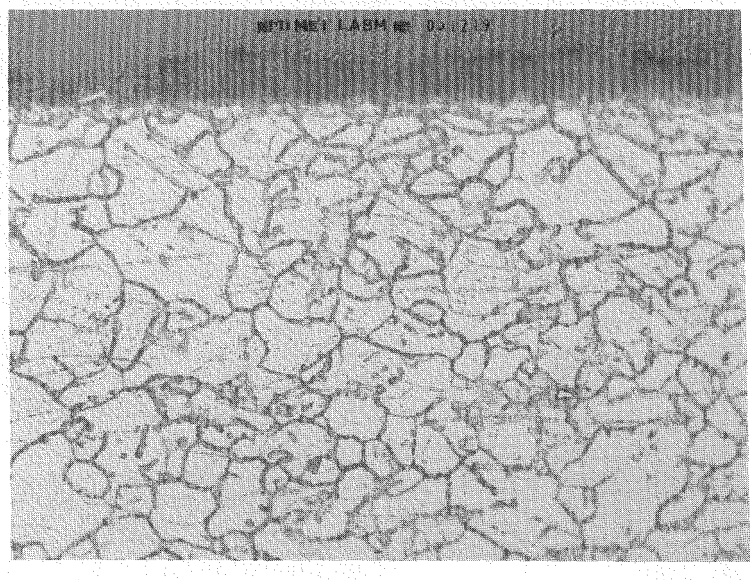

(B) 10% Oxalic Acid Etch

Figure 4-6. (A) 200X* Photograph of tube area at 0° 1/4 in. above tubesheet simulator sludge cup. (B) 500X* Photograph of same area.

*Please note that the illustration(s) on this page has been reduced 10% in printing.

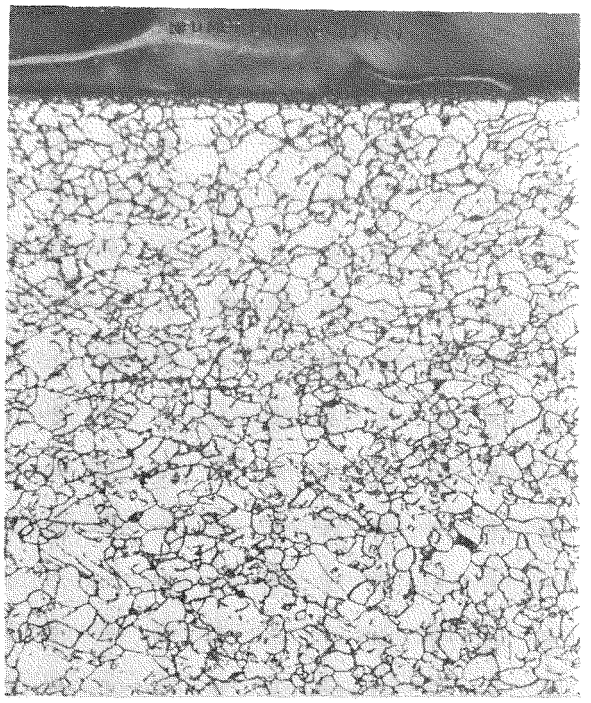

(A) 10% Oxalic Acid Etch

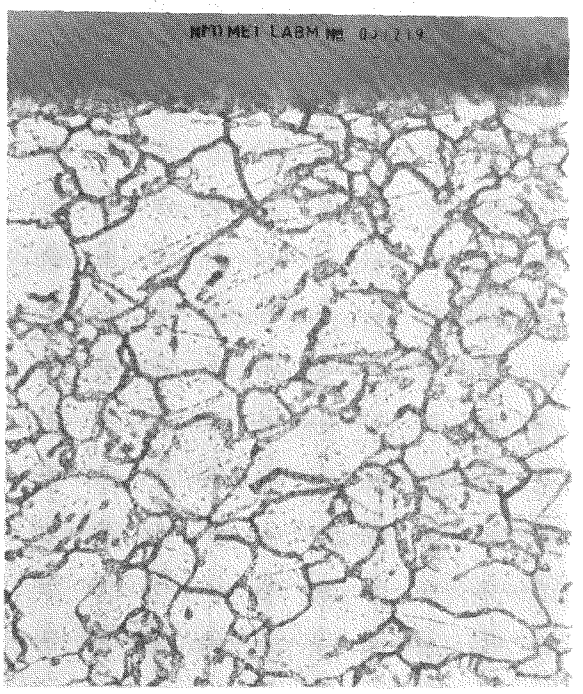

(B) 10% Oxalic Acid Etch

Figure 4-7. (A) 200X* Photograph of tube area at 0° in the middle of tubesheet simulator sludge cup. (B) 500X* Photograph of same area.

*Please note that the illustration(s) on this page has been reduced 10% in printing.

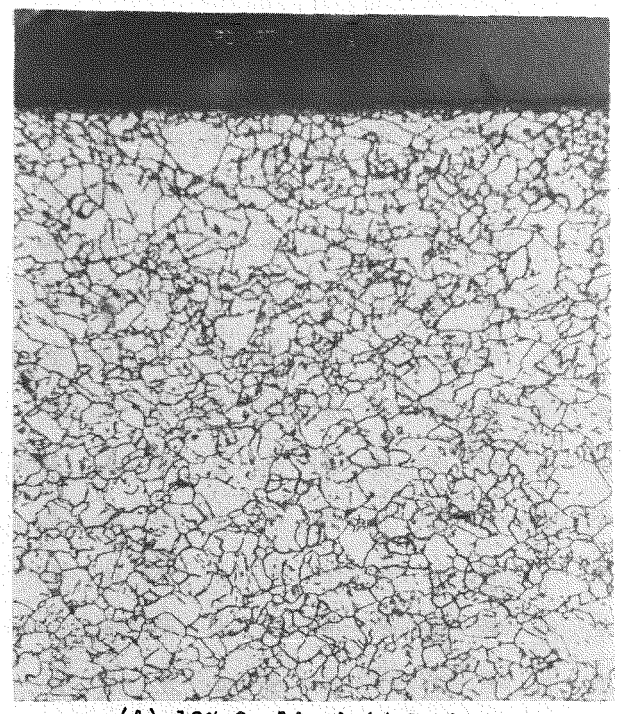

(A) 10% Oxalic Acid Etch

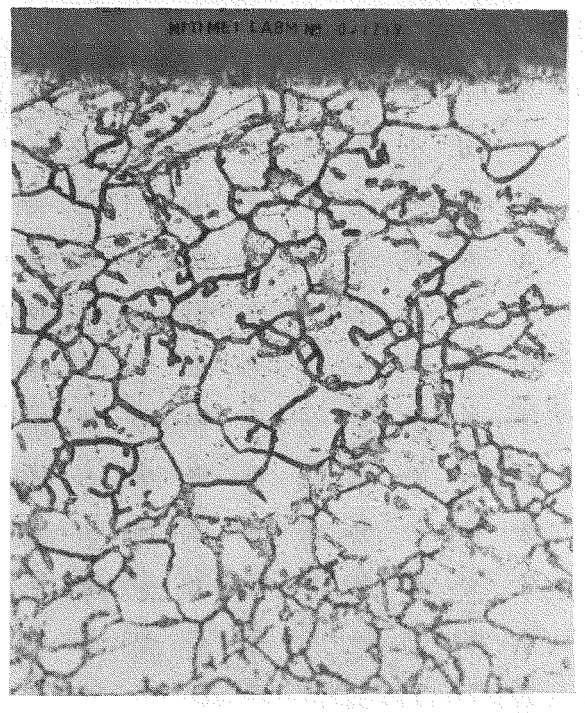

(B) 10% Oxalic Acid Etch

Figure 4-8. (A) 200X* Photograph of tube area at 0° at bottom of tubesheet simulator sludge cup. (B) 500X* Photograph of same area.

*Please note that the illustration(s) on this page has been reduced 10% in printing.

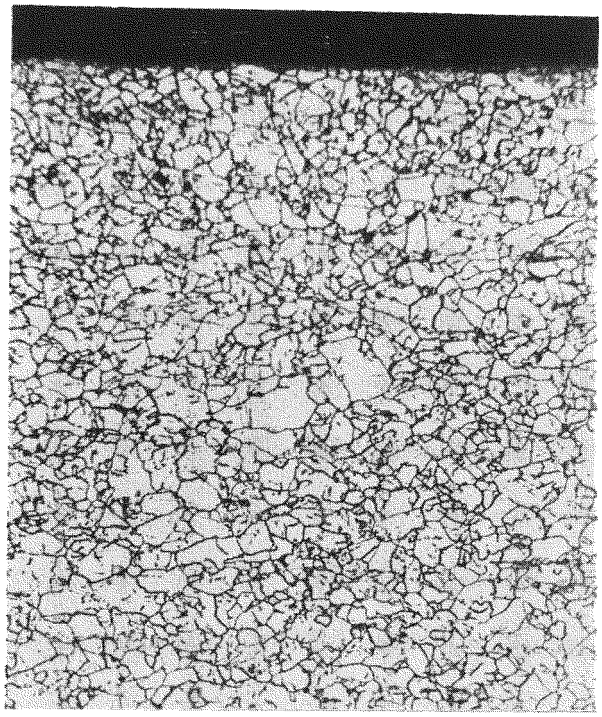

(A) 10% Oxalic Acid Etch

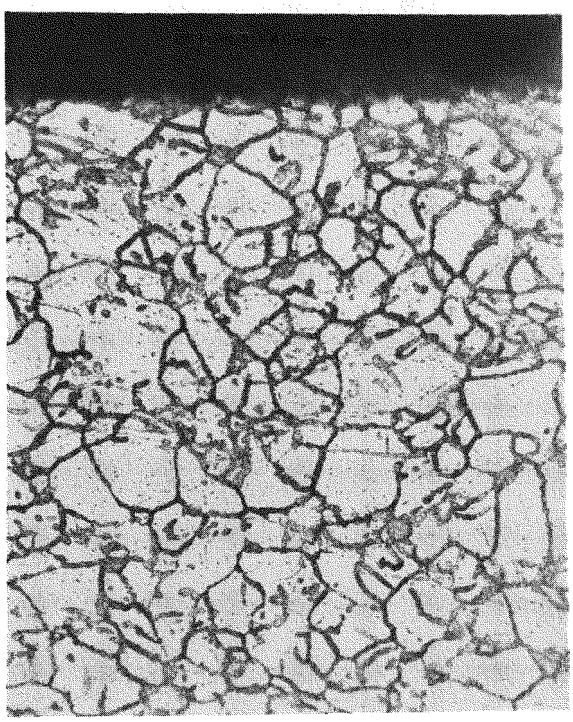

(B) 10% Oxalic Acid Etch

Figure 4-9. (A) 200X* Photograph of tube area at 0° 1/2 in. below tubesheet simulator sludge cup. (B) 500X* Photograph of same area.

*Please note that the illustration(s) on this page has been reduced 10% in printing.

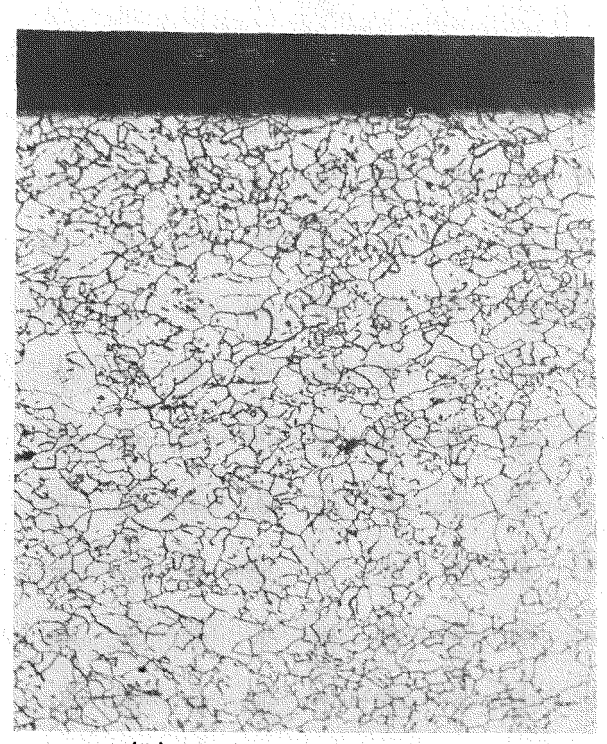

(A) 10% Oxalic Acid Etch

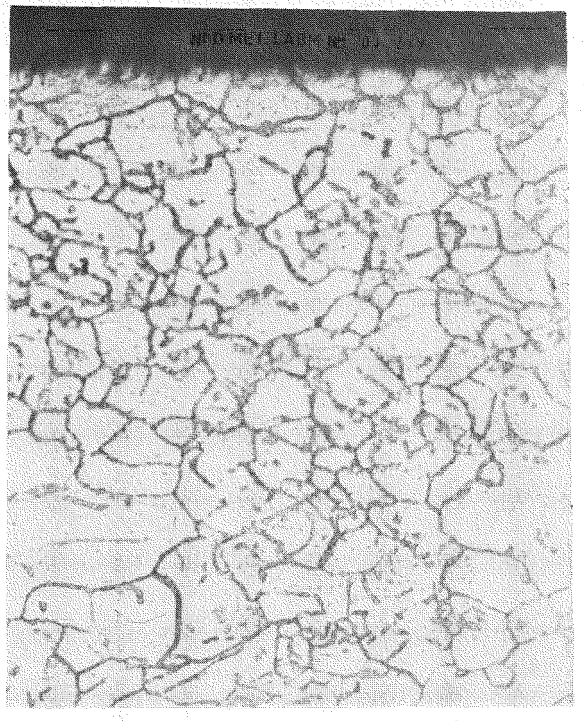

(B) 10% Oxalic Acid Etch

Figure 4-10. (A) 200X*Photograph of tube area at 0° mid-section of tubesheet simulator. (B) 500X* Photograph of same area.

*Please note that the illustration(s) on this page has been reduced 10% in printing.

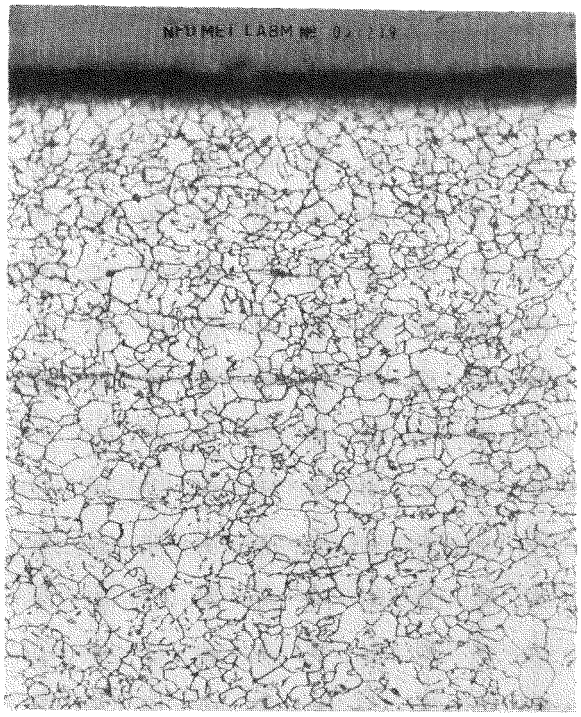

(A) 10% Oxalic Acid Etch

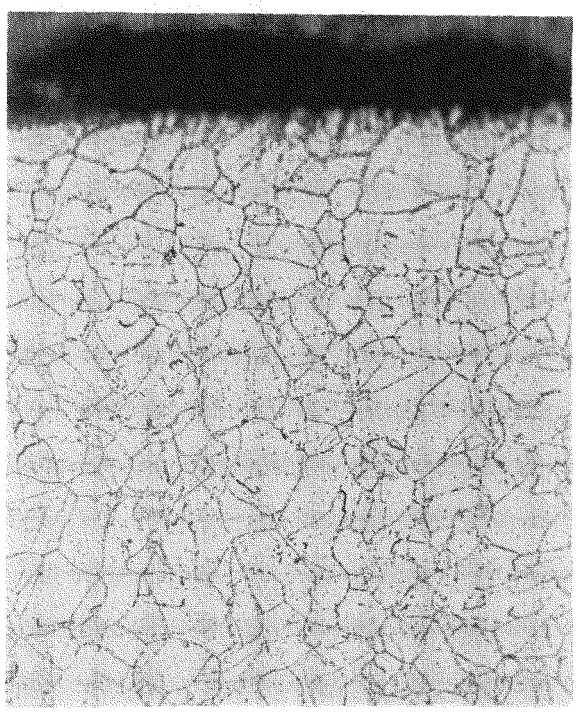

(B) 10% Oxalic Acid Etch

Figure 4-11. (A) 200X*of tube area at 0° roll transition region of tubesheet simulator. (B) 500X*of representative area in roll transition region of tubesheet simulator.

*Please note that the illustration(s) on this page has been reduced 10% in printing.

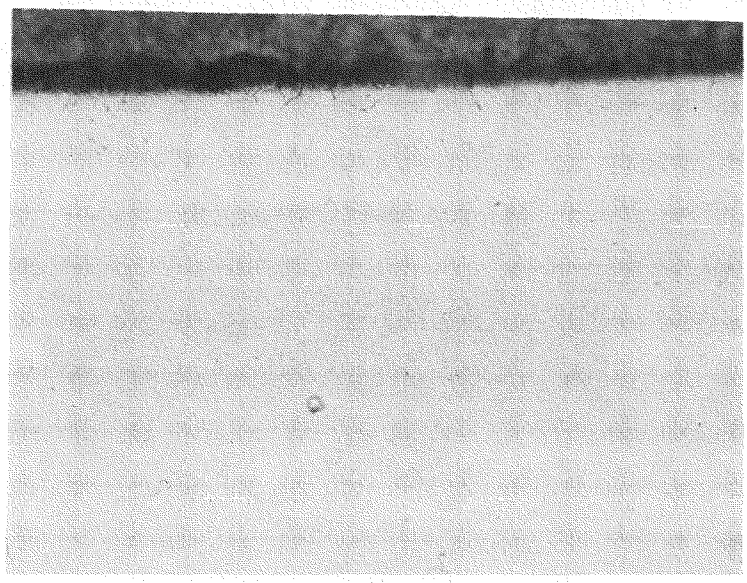

Figure 4-12. Intergranular attack one grain deep on tube at 0° at bottom of tubesheet simulator sludge cup. As polished 500X* photograph.

*Please note that the illustration(s) on this page has been reduced 10% in printing.

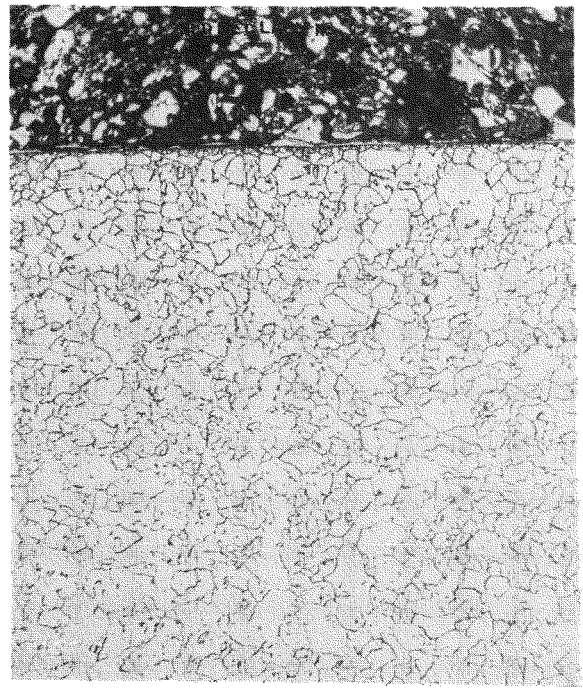

(A) 10% Oxalic Acid Etch

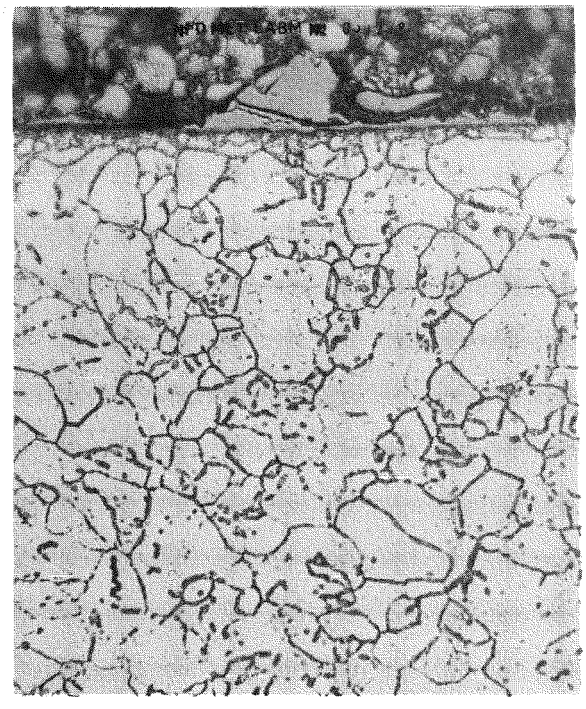

(B) 10% Oxalic Acid Etch

Figure 4-13. (A) 200X* Photograph of 90° tube area at midplane in support ring. (B) 500X* Photograph of same area.

*Please note that the illustration(s) on this page has been reduced 10% in printing.

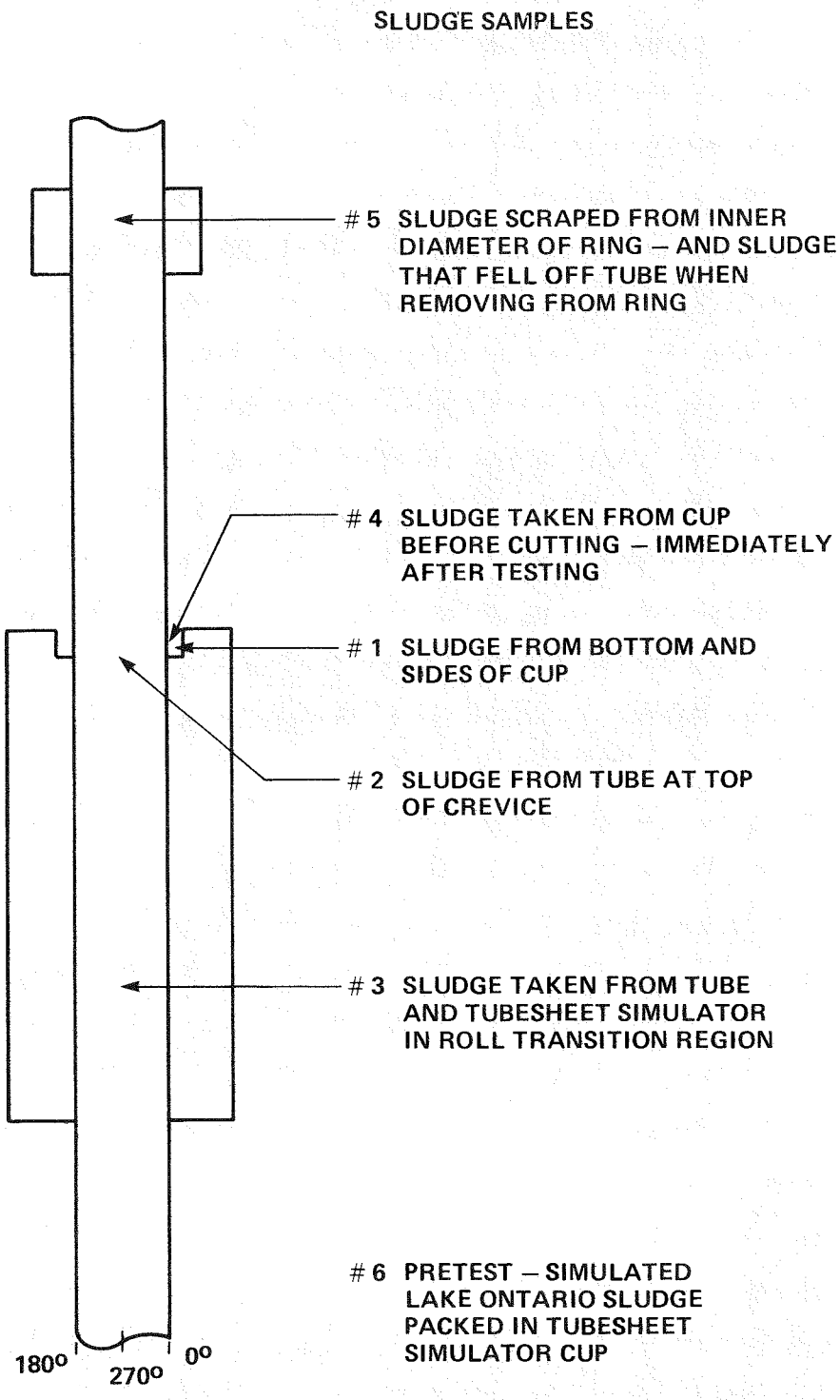

Figure 4-14. Sludge Sampling Diagram for Tube 302

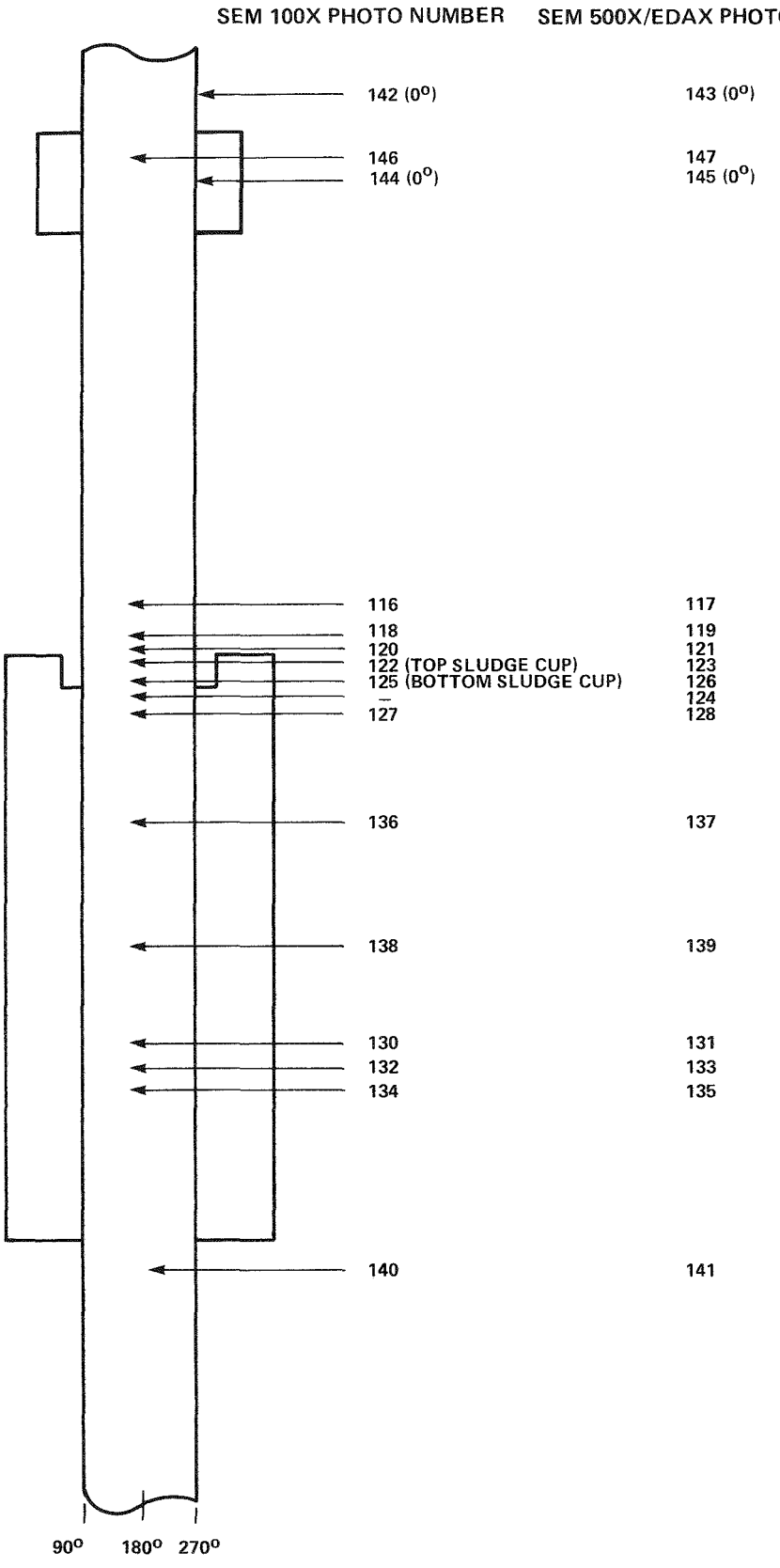

Figure 4-15. Map of Tube 302 SEM/EDAX Analyses

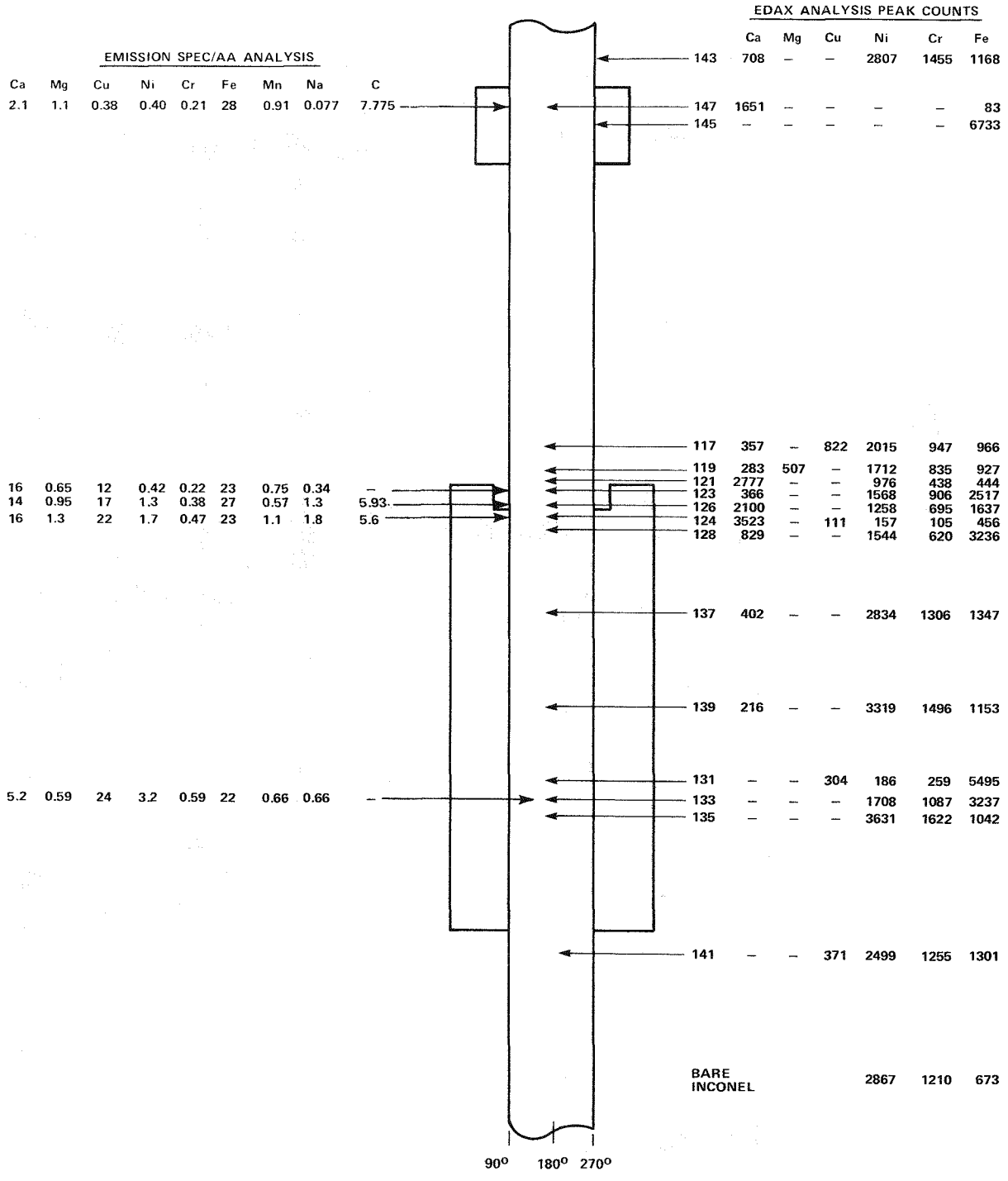

Figure 4-16. Summary of Tube 302 Task 200 Sludge Analysis Results by Location

Table 4-4

SLUDGE ANALYSIS BY EMISSION SPECTROSCOPY, ATOMIC ABSORPTION, AND TOTAL CARBON

	Weight Percentage					
Element	Sample 1	Sample 2	Sample 3	Sample 4	Sample 5	Sample 6
Al	0.11	0.14	0.11	0.082	0.33	0.15
B	<0.001	0.012	<0.001	<0.001	0.0014	<0.001
Ca	14	16	5.2	16	2.1	17
Cr	0.38	0.47	0.59	0.22	0.21	0.40
Cu	17	22	24	12	0.38	20
Fe	27	23	22	23	28	27
K	0.25	0.54	0.21	0.044	<0.03	0.008
Mg	0.95	1.3	0.59	0.65	1.1	0.68
Mn	0.57	1.1	0.66	0.75	0.91	1.2
Mo	0.021	0.034	0.0095	0.0062	0.016	<0.003
Na	1.3	1.8	0.66	0.34	0.077	0.05
Ni	1.3	1.7	3.2	0.42	0.40	2.5
Pb	0.047	0.052	0.14	0.020	0.071	0.077
Si	0.72	0.77	0.38	0.47	0.47	0.44
Sn	0.082	0.079	0.084	0.047	<0.01	0.091
Ti	0.14	0.20	0.17	0.071	0.16	0.027
V	0.033	0.048	0.052	0.021	0.097	0.056
C	5.93	5.62	*	*	7.75	2.22
Total	69.83	74.86			42.07	71.89

*Insufficient Sample for Analysis.

Table 4-5

ION CHROMATOGRAPHY ANALYSIS OF ACID LEACHABLE SLUDGE COMPONENTS

	ppm in Sludge		
Sample #	Fluoride	Chloride	Sulfate
1	122	853	694
4	57	1286	446
6	<10	201	317

*Samples #2, #3, #5 had insufficient sample for Dionex Analysis.

Table 4-6

SLUDGE X-RAY DIFFRACTION ANALYSIS RESULTS

Sample*	Description	Compounds Detected
1	Scraped from Sludge Cup	Fe_3O_4, α-Fe_2O_3, Cu
2	Scraped from Tube at Sludge Cup Bottom	Fe_3O_4, Cu
3	Scraped from Tube and Simulator-Roll Transition Region	Fe_3O_4, Cu
4	Hard Flakes Taken from Sludge Cup Immediately After Testing	Fe_3O_4, Cu
5	Sludge from Support Ring	Fe_3O_4, α-Fe_2O_3
6	Simulated Lake Ontario Sludge (Pretest)	Fe_3O_4, $CaCO_3$, Cu

*Samples 1-4 had initial composition shown in Table 3-6. Sample 5 had an initial Fe_3O_4 composition.

the sludge cup to the bottom of the sludge cup, a varying black and white deposit mixture covered the tube (Figures A-3 through A-10). EDAX analyses showed high concentrations of Ca and Fe in varying amounts in this region. Just below the sludge cup bottom a white deposit consisting almost solely of Ca covered the tube. Below this area, 1-2 in. deeper into the crevice, the deposits had a silver-gray metallic appearance. EDAX analysis showed decreasing amounts of Ca and Fe as the deposits became thinner (Figures A-11 through A-18) going deeper into the tubesheet crevice. At the beginning of the roll-transition region no Ca was detected in an area which consisted of a black crystalline deposit covered by a thin layer of orange colored material. High concentrations of Fe were measured along with a small amount of Cu. Figures A-19 to A-24 show that the amount of Fe deposited on the tube decreases from the top of the roll transition to the fully expanded area.

The EDAX analyses discussed above show that the major components of tubesheet sludge in this test are Fe, Ca, and Cu. X-ray diffraction analyses identified the Fe containing compounds as Fe_3O_4 at all sample locations with some α-Fe_2O_3 present in the sludge cup. Copper was found to be present only in the metallic form. The presence of high Ca concentration along with high concentrations of carbon (by total carbon analysis) in the sludge leads to the conclusion that Ca is present as $CaCO_3$ even though none was detected by X-ray diffraction. Emission spectroscopic analysis also detected small amounts of Mg, Mn, Na, Ni, and Cr in the sludge samples. Analysis by ion chromatography of soluble sludge components dissolved in dilute nitric acid showed the presence of small amounts of fluoride, chloride, and sulfate. No sulfite was found. The detection of phosphate, nitrate, and thiosulfate was not possible due to the small amount of sample available.

Deposits on the tube section beneath the support ring were also analyzed by EDAX and for total carbon and found to consist mainly of Fe and C with a small amount of Ca. Compared to the tubesheet deposits, sludge under the support ring was much lower in Ca and Cu but higher in Fe and C. High Fe concentrations and lower concentrations of other elements were expected in the support ring crevice because it was prepacked with only Fe_3O_4. X-ray diffraction showed that Fe was present as Fe_3O_4 and α-Fe_2O_3. Since the concentration of carbon was so high, Ca and Fe were probably present in the carbonate form. Typical SEM/EDAX photographs of Fe and Ca deposits are shown in Figures A-25 to A-28.

Upon completion of the tube sludge analysis, the 150^{o}-180^{o} tubesheet section was descaled. Open tube surfaces were cleaned readily but crevice surfaces were covered with a tenacious black film even after six cycles of the chemical cleaning procedure (18% NaOH + 3% $KMnO_4$/rinse/5% oxalic acid/rinse/10% ammonium citrate dibasic/acetone alcohol rinse). Most of the tube crevice surfaces were obscured but clean areas that were visible showed no sign of SCC/IGA.

Sludge deposits in the Task 200 Model Boiler Test were compared with sludge samples taken from tubesheet regions at Point Beach (Unit 1, Steam Generator A) and Ginna (Steam Generator B) where intergranular attack of Alloy 600 tubing has occurred. As previously discussed, the major components of the model boiler tubesheet sludge were Fe, Ca, Cu and C with small amounts of Mg, Mn, Na, Ni, and Cr. The compounds associated with the major components were probably $FeCO_3$, $CaCO_3$, Fe_3O_4 and Fe_2O_3 while copper was present as the metal. Optical emission spectrographic analyses conducted on deposits obtained from honing hot leg tubesheet holes of steam generator A of Point Beach Unit 1, which had IGA penetrations of up to 85%, showed that the major sludge components ($\geq$5 w/o) were Al, B, Na, P, and Si with minor components ($\geq$1 w/o) Ca, Cu, K, Mg, Mn, Pb, and Ti. When sludge on the honing brushes was analyzed, the major elements ($\geq$5 w/o) found were Cu and Zn with minor elements ($\geq$1 w/o) Ca, Mg, Mn, Na, and Si. Sludge scraped from a hot leg tubesheet tube was analyzed by x-ray diffraction and found to contain Na_2SO_4 and a spinel structure (1). Also, earlier Point Beach analyses showed 1.09 w/o carbon in a tubesheet sludge pile cored sample collected in December 1975 which if present as carbonate represents ~5.5 w/o of the sludge. Similar carbon concentrations were measured in the Task 200 sludge.

Analysis of hot leg samples with IGA (~50% through wall) from the "B" steam generator at RGE Ginna Station by SEM/EDAX showed the presence of Al, Na, P, Si, Ca, and S with lower levels of K and sporadic Cl signals. Emission spectrographic analysis of deposits removed from tube sheet holes from which the hot leg tubes were pulled revealed that the major constituents (~10 w/o) in the tubesheet deposits were Fe and Cu with moderate amounts (>1 w/o, <10 w/o) of Ca, Mg, Si, Ni, Zn, Al, and Na. However, the Si values are questionable since Si is a constituent of the silicon carbide hone.(2)

Besides the Alloy 600 components, Fe, Ni, and Cr, the model boiler tubesheet deposits had Na, Mg, Ca, and Cu in common with the Point Beach and Ginna sludge.

The major elements present in Point Beach and Ginna sludges but not added to the model boiler test were Al, Si, P, and Zn. With the exception of Si these elements are not found in significant quantity in Lake Ontario Water. Therefore, the Task 200 model boiler test had an elemental deposit composition similar to a steam generator with Lake Ontario water inleakage. At both Point Beach and Ginna the ingress of lake condenser cooling water was implicated as the source of sludge contaminants consistent with the elements analyzed. The hypothesis is that these contaminants, when concentrated in the tubesheet crevice, have the ability to increase alkalinity and thus cause caustic initiated intergranular attack and stress corrosion cracking. Concentration of the simulated Lake Ontario water constituents did create a caustic tubesheet crevice in the Task 200 Model Boiler test as evidenced by a pH of 10 which was measured in the sludge cup with pH paper. In addition, the hideout return data obtained during thermal cycling (Table 5-3) showed an increased pH during down power operations indicating the release of caustic from crevices to the bulk water. Since the tubesheet crevice was apparently alkaline and no SCC/IGA occurred in the model boiler test, it appears that more than just the presence of caustic is necessary for SCC/IGA. In fact, it has been shown in model boiler tests that through-wall SCC and small amounts of IGA can be produced by a threshold concentration of 0.3 ppm Na_2CO_3 (in makeup water) in the presence of simulated plant sludge with or without low hydroxide concentrations (0.5-1.0 ppm OH).

To determine why no SCC or IGA occurred in this test, it is instructive to also compare, in Table 4-7, the Task 200 model boiler test with a Westinghouse reference cracking test, Tube 253, which cracked through the wall (no IGA) in seven days.

Table 4-7

DIFFERENCES BETWEEN THE TASK 200 TEST AND THE REFERENCE CRACKING TEST

Tube 302 Task 200 Model Boiler	Tube 253 Model Boiler
Thermal cycling	No thermal cycling
1.5% Cu_2O in sludge	4.5% CuO in sludge
1/4 in. deep sludge cup	7/8 in. deep sludge cup
1.0 ppm hydroxide as NH_4OH	No hydroxide added
0.5-2.0 ppm carbonate	1.7 ppm carbonate
Average Bulk Water pH = 8.35	Average Bulk Water pH = 9.80
50 ppb hydrazine	50 ppb hydrazine
No SCC/IGA	Through wall SCC in 7 days

Both Tube 302 and Tube 253 were tested under the same thermal and hydraulic conditions with approximately the same amount of carbonate. However, the carbonate was added as Na_2CO_3 in the Tube 253 test, while it entered the boiler as Na, Ca, and Mg carbonate in the Task 200 test. The hydrolysis of carbonate in the first case was much more complete, evidenced by the pH in the Tube 253 test (pH - 9.80) which was much higher than the Task 200 test (pH = 8.35) in which 1.0 ppm hydroxide as NH_4OH was also added. Another difference between the tests was in sludge composition. A greater amount of oxidant was present in the Tube 253 test since 4.5% of the sludge was CuO and only 1.5% of the sludge in this test was Cu_2O. In addition, because the sludge cup was 1/4 in. deep, only 1.5 grams of sludge was used in this test compared to 10-12 grams used in the 7/8 in. sludge cup of the Tube 253 test. Finally, thermal cycling was conducted on Tube 302 which increases tube stresses but allows crevice flushing and hideout return to reduce the crevice alkalinity. No thermal cycling was done on Tube 253. Based on these observations, it is believed that the Task 200 model boiler test did not develop SCC/IGA while Tube 253 cracked through the wall in 6 days because of the absence of a suitable oxidizing environment (provided by copper oxide in the Tube 253 case) which fixes the electrochemical potential in the cracking regime. Also, the alkalinity necessary for SCC/IGA was not developed due to the inhibition of carbonate hydrolysis by precipitation of $CaCO_3$ and $MgCO_3$ and thermal cycling which flushed the crevice of alkaline solution and deposits.

SCREENING TESTS (TASK 300)

The objective of the testing in this Task was to evaluate the effect of various additives, either singly or in combination, on the susceptibility of Alloy 600 to intergranular attack. The reference environment against which the effect of all additives was compared was 40% NaOH + 10% KOH (by weight) at 650°F. Table 4-8 contains the test number and chemical composition of each test environment. Table 4-8 also indicates the subtask under which environments were evaluated.

In general, the selection of the chemical species shown in Table 4-8 was based on the identification of various elemental constituents in EPRI S138-2 and S138-3 project reports on analysis of IGA affected tube specimens from operating plants (1,2). The concentration of the additives was established at 12% to assure saturation conditions at test temperatures. Although solubility data for the various contaminant species in the reference chemistry (40% NaOH + 10% KOH) is almost nonexistent, it was our best estimate that a level of 12% should provide a

Table 4-8

TEST MATRIX FOR TASK 300 ELECTROCHEMICAL,
MINI-AUTOCLAVE AND CAPSULE SCREENING TESTS
(All values are % by weight)

Test No.	Subtasks 301	302A	302B	40% NaOH + 10% KOH	Other Additives
1	X	X	X	X	
2			X[a]		12% $MgSO_4$
3			X[a]		12% Na_2SO_4
4			X[a]		12% SiO_2
5			X[a]		12% Na_2CO_3
6			X[a]		3% $NaNO_3$ + 3% $CaSO_4$ + 3% SiO_2 + 3% NaCl + 3% Na_2HPO_4
7			X[a]		12% $NaNO_3$
8			X[a]		12% NaF
10			X	X[c]	12% Na_2SO_4
11			X	X	12% $CaSO_4$
12	X	X	X	X	12% SiO_2
13			X	X	12% $MgSO_4$
14			X	X	12% Al
15			X	X	12% NaCl
16			X	X[c]	12% Na_2HPO_4
17			X	X[c]	3% $NaNO_3$ + 3% $CaSO_4$ + 3% SiO_2 + 3% NaCl + 3% Na_2HPO_4
18	X	X	X	X	12% $NaNO_3$
19	X	X	X[b]	X	7% CuO + 3% ZnO
20			X	X[c]	12% Na_2CO_3
21			X	X	12% Cr_2O_3
22			X	X	12% NaF
25			X[b]	X	12% Na_2SO_4 + 7% CuO + 3% ZnO
26	X	X	X[b]	X	12% SiO_2 + 7% CuO + 3% ZnO
27			X[b]	X	12% NaCl + 7% CuO + 3% ZnO
29			X[b]	X	12% $NaNO_3$ + 7% CuO + 3% ZnO

[a] Single rather than duplicate capsules.

[b] Single capsule performed for proof testing.

[c] One of two duplicate samples to contain A508 slug.

saturated solution for most of the materials under consideration. Exceptions to this would be materials such as SiO_2, Al, and ZnO which are expected to have higher solubilities than the 12% value.

Electrochemical Tests (Subtask 301)

Reference Environment: 40 wt % NaOH + 10 wt % KOH, 650°F. The results of two separate tests (Tests 1 and 5) in this environment (designated as Test 1, Table 4-8) are summarized in Table 4-9. In Test #1, specimens 1-3 were plastically deformed C-rings of Alloy 600 which were maintained anodically polarized for one day before restoring free corrosion conditions for the remainder of the four-week exposure. Specimen #1 was held for one day at the active peak potential (+205 mV vs. Ni); specimen #2 at a potential in the middle of the active range (+100 mV vs. Ni); and specimen #3 at a potential in the active-passive transition range (+215 mV vs. Ni). The selection of potential values was based on the previously determined polarization shown in Figure 4-17 with the aim of accelerating initiation of IGA. Specimens #1 and #3 both exhibited extensive SCC as well as shallow IGA over the entire exposed stressed surface. In addition, a similar degree of IGA was observed along all the cracks within the specimens. Specimen #2 exhibited no SCC and only a few isolated and very shallow patches of IGA. These observations are illustrated in Figures 4-18 and 4-19.

Specimen #4 was identical to specimens 1-3 and used as a control specimen to allow evaluation of the effects of the one-day polarizations. This specimen exhibited uniform IGA over the entire stressed surface to a depth of ~2.5 mil as shown in Figure 4-20(a). No discrete cracks were observed. Specimen #5 was similar to specimen #4 except that the applied stress was reduced to ~ Y.S. After the 4-week exposure under free corrosion conditions, specimen #5 exhibited uniform IGA to a depth of 1.5 mils (Figure 4-20(b)).

Specimens #6 and #7 were prepared using 2 in. lengths of Alloy 600 tubing (heat 9837) which were stressed in the central region by means of 1/2 in. long carbon steel internal expansion plugs. The expansion produced ~0.5% strain. Specimen #6, which was given a 5 hour 1200°F heat treatment which resulted in sensitization exhibited uniform surface IGA to a depth of 1.6 mils. In contrast, specimen #7, which was given a 5 hour 1200°F heat treatment which resulted in sensitization, exhibited neither IGA nor SCC, as shown in Figure 4-21. It was also observed

Table 4-9

RESULTS OF A 4 WEEK EXPOSURE OF ALLOY 600 TO A DEAERATED 40 wt % NaOH + 10 wt % KOH AQUEOUS MIXTURE AT 650°F

	Specimen No.	Heat No.	Specimen Condition	Test Conditions	Max. Depth of IGA (mil)	Max. Depth of SCC (mil)
Test 1	1	9955	Mill Annealed (MA) Closed C-ring σ_{app} >> Y.S.	1 day at +205 mV (active peak) + 27 days at FCP	2.5	44
	2	9955		1 day at +100 mV (active range) + 27 days at FCP	0.9	--
	3	9955		1 day at +215 mV (act/pass range) + 27 days at FCP	1.3	44
	4	9955	σ_{app} >> Y.S. MA C-rings	28 days at FCP	2.5	--
	5	9955	σ_{app} ~ Y.S. MA C-rings	28 days at FCP	1.5	--
	6	9837	MA 2 in. long tube with carbon steel expansion plug	28 days at FCP	1.6	--
	7	9837	Sens. ~0.5% ε 2 in. long tube with carbon steel expansion plug	28 days at FCP	--	--
Test 2	1	9955	MA closed C-ring σ_{app} >> Y.S.	1 hr at +350 mV (passive range) + Remaining exposure at FCP	0.3	--
	2	9955		1 day at +350 mV (passive range) + Remaining exposure at FCP	0.9	45
	3	9955		3 day at +350 mV (passive range) + Remaining exposure at FCP	0.4	--
	6	9955			0.4	--
	7	9955	MA C-ring σ_{app} ~ Y.S.	28 days at FCP	0.2	--
	8	9955	MA 2 in. long tube with carbon steel expansion plug (~0.5% ε)	28 days at FCP	1.5	--
	11	9837	MA closed C-ring σ_{app} >> Y.S.	28 days at FCP	0.9	--

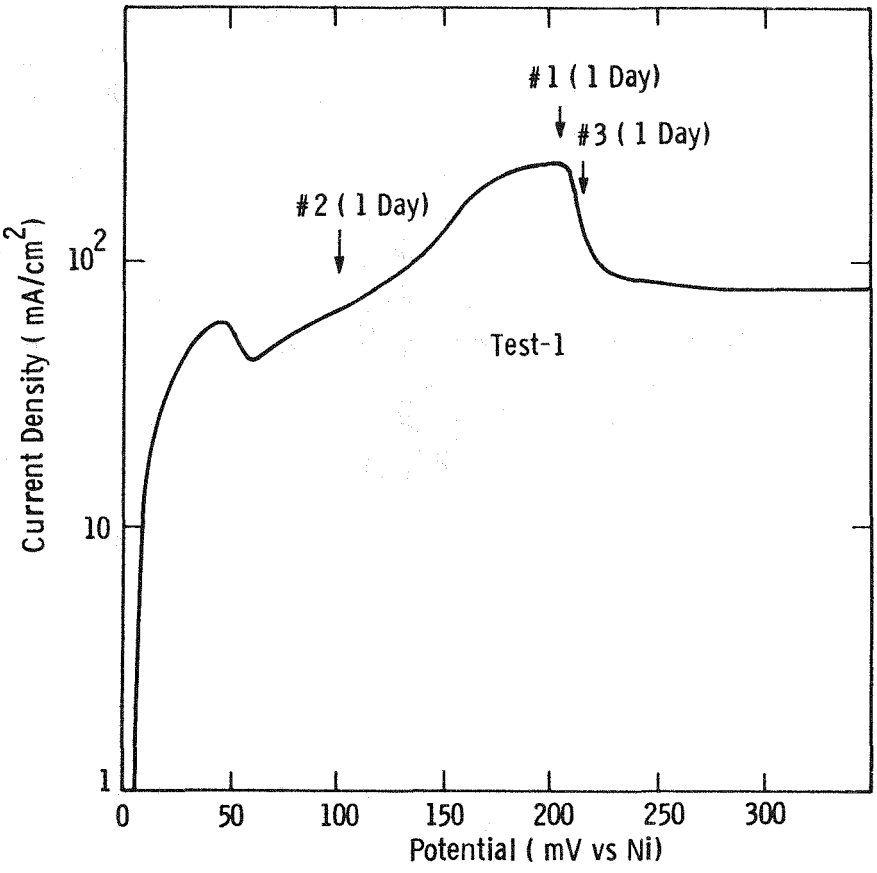

Figure 4-17. Anodic polarization curve for mill-annealed Alloy 600 (Ht. 9955) in the reference environment (40 wt % NaOH + 10 wt % KOH) at 650°F. Scan rate: 10 mV/min. The holding times and potentials for specimens 1-3 in Test 1 are indicated.

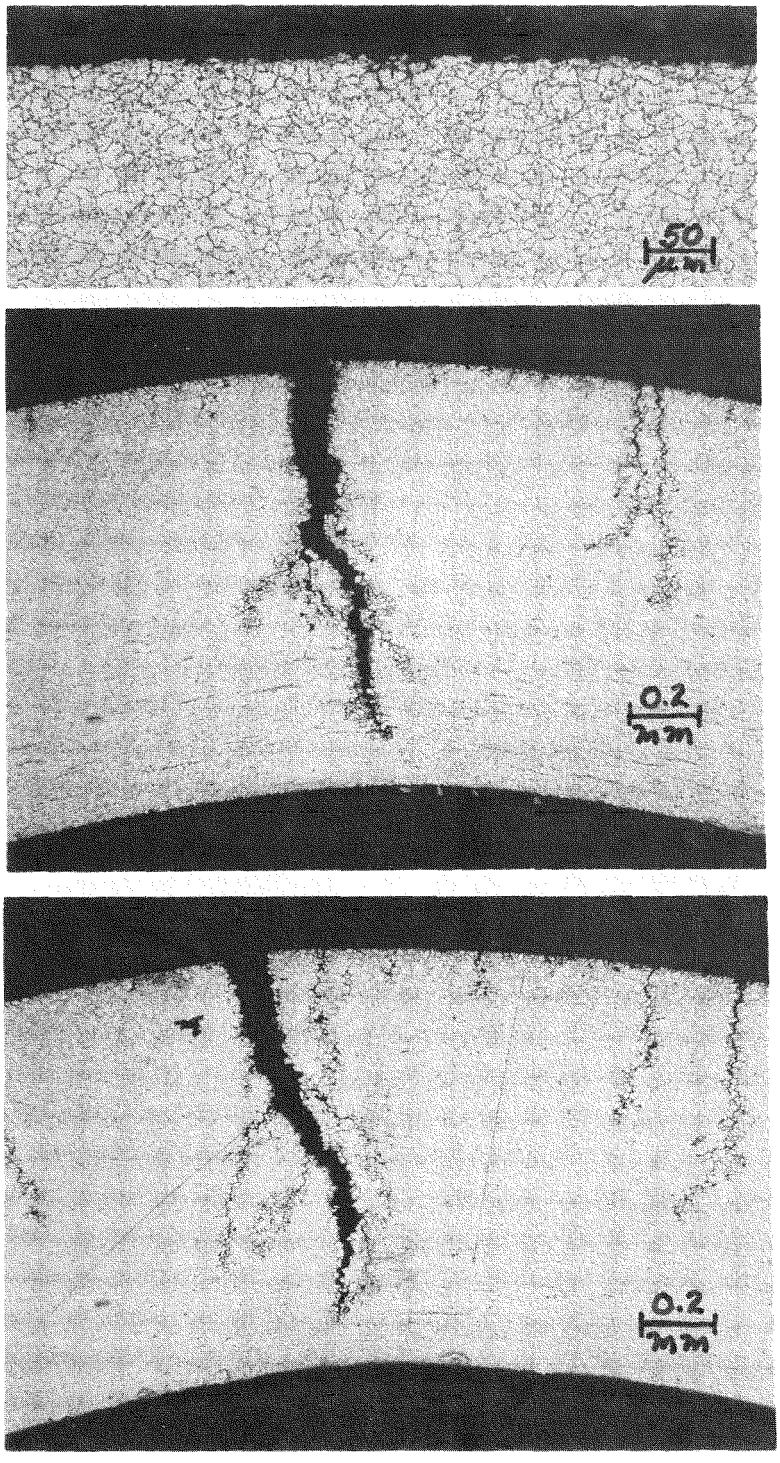

(a)

(b)

(c)

Figure 4-18. Localized attack on mill-annealed Alloy 600 (Ht. 9955) closed C-rings after exposure to the reference environment (40 wt % NaOH + 10 wt % KOH) at 650°F (Test 1). (a) Held 1 day at +100 mV vs. Ni and 27 days under open circuit conditions. Maximum penetration: 0.9 mils. (b) Held 1 day +205 mV vs. Ni and 27 days under open circuit conditions. Maximum penetration: 44 mils. (c) Held 1 day at +215 mV vs. Ni and 27 days under open circuit conditions. Maximum penetration: 44 mils. Electrolytic phosphoric acid etch.

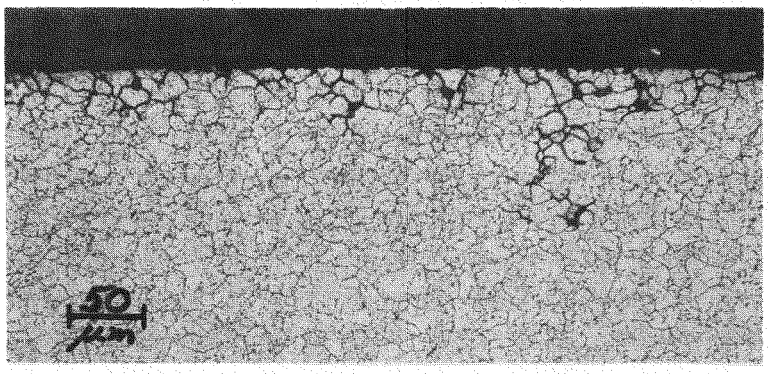

(a)

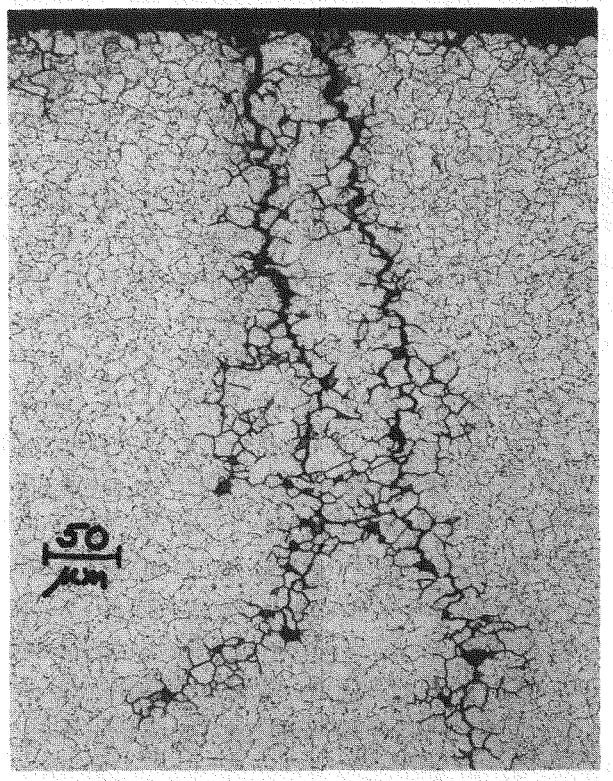

(b)

Figure 4-19. Localized attack on mill-annealed Alloy 600 (Ht. 9955) closed C-ring after 1 day at +205 mV vs. Ni and 27 days under open circuit conditions in the reference environment (Test 1). Electrolytic phosphoric acid etch.

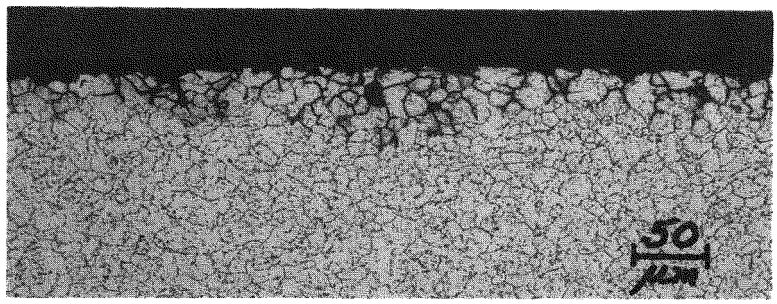

(a)

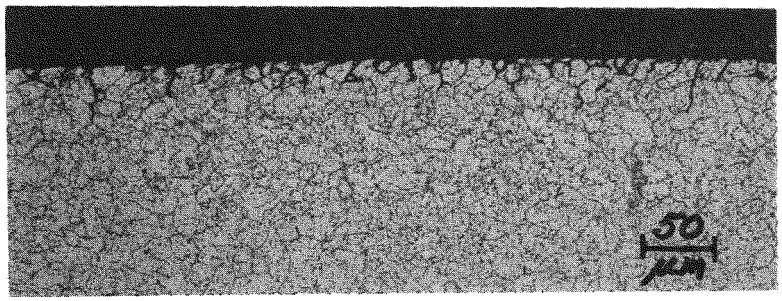

(b)

Figure 4-20. Localized attack in mill-annealed Alloy 600 (Ht. 9955) after 28 day exposure under open circuit conditions in the reference environment (Test 1).
(a) Specimen #4. Maximum penetration: 2.5 mils.
(b) Specimen #5. Maximum penetration: 1.6 mils.
Electrolytic phosphoric acid etch.

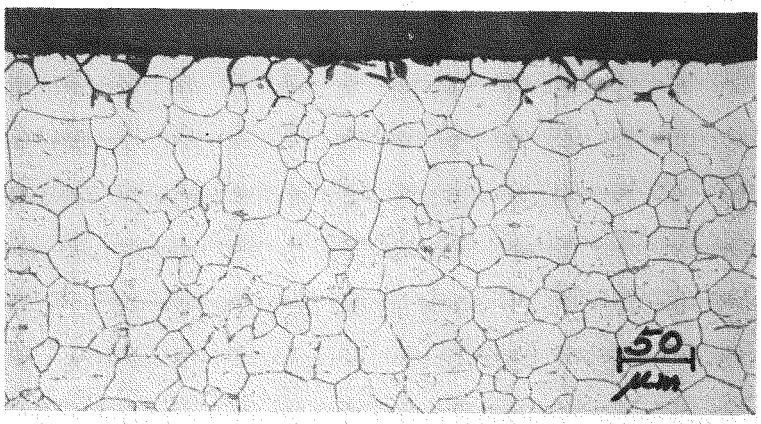

(a)

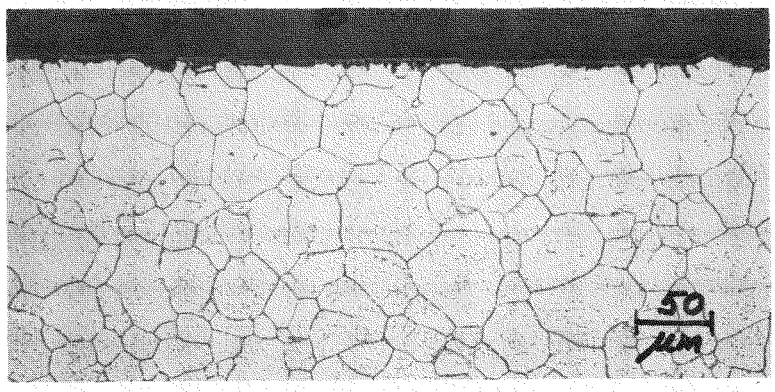

(b)

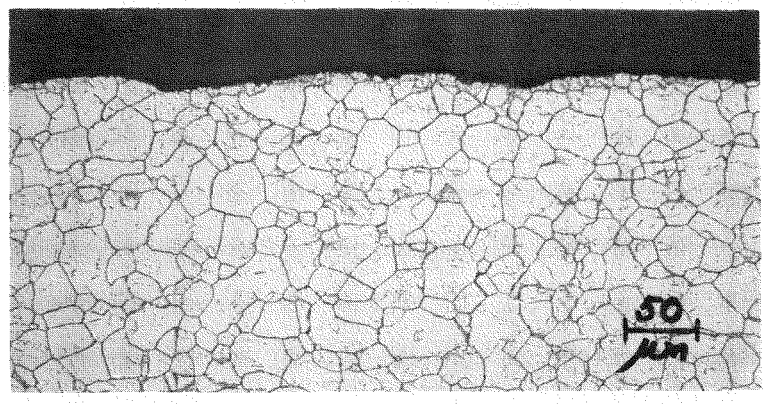

(c)

Figure 4-21. Transverse sections through tubes of mill-annealed Alloy 600 (Ht. 9837) after 28 day exposures under open circuit conditions in the reference environment (Test 1). (a) Mill-annealed specimen #6 in high stress region; (b) Specimen #6 in unstressed region; (c) Specimen #7 (mill-annealed plus 5 hr at 1200°F) in high stressed region. Electrolytic phosphoric acid etch.

(Figure 4-21) that the extent of IGA was less in those regions of the C-ring specimens which were at low applied stress.

Also included in Table 4-9 are the results of Test 5 which duplicated the test reference environment. In this test, specimens 1-3 were plastically deformed C-rings of Alloy 600 which were maintained potentiostatically in the passive range of the polarization curve (+350 mV vs. Ni - see Figure 4-17) for 1 hr, 1 day and 3 days, respectively, before restoring free corrosion conditions for the remainder of the 4-week exposure. A typical potential-decay curve is shown in Figure 4-22. The passivation treatment followed by free potential-decay was an attempt to accelerate IGA initiation by concentrating the corrosive attack on the first sites to activate during the potential-decay. As indicated in Table 4-9, this approach was unsuccessful in accelerating IGA but one specimen (#2) did exhibit extensive SCC (Figure 4-23).

Specimens #6 and #7 in Test 5 duplicated Specimens #4 and #5 in Test 1. Although IGA was observed in all the C-ring specimens, the extent of attack was much less in Test 2. However, the magnitude of IGA produced in an expanded tube of the same material (Specimen #8, Test 2), shown in Figure 4-24, did closely reproduce that observed in Test 1.

Reference Environment + 12 wt % SiO_2, 650°F. The results of two separate tests (Tests 2 and 6) in this environment are summarized in Table 4-10. Specimens 1-3 in Test 2 were plastically deformed C-rings which were held potentiostatically in the active range of the polarization curve for 2 hours or 1 day before restoring free corrosion conditions for the remainder of the 4-week exposure. The initial polarizations did not accelerate IGA but did induce extensive SCC in both Tests 2 and 6. The polarization curve for mill annealed material in this environment, shown in Figure 4-25, was noteworthy in that the current density was 4 orders of magnitude higher than that shown in Figure 4-17 for the same material in the reference environment.

As indicated in Table 4-10, similar specimens in Tests 1 and 6 exhibited very similar behavior in terms of IGA. Most notable, however, was the observation that the SiO_2 addition to the reference environment increased the extent of IGA in the high stress region by a factor of ~2. Illustrations of the IGA attack produced in the SiO_2-containing environment are given in Figures 4-26 to 4-32. As noted in

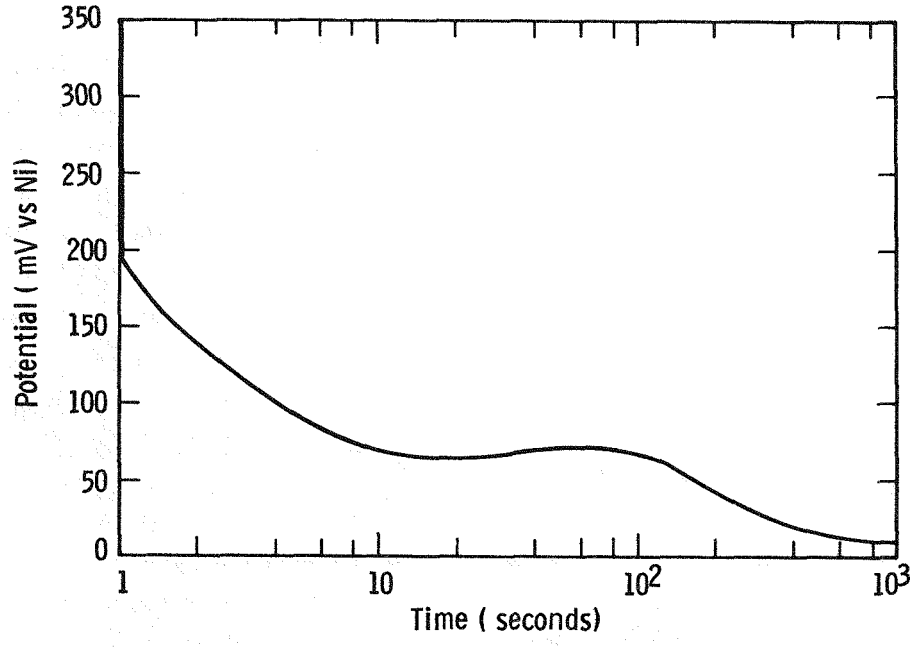

Figure 4-22. Potential decay curve for specimen #1 in Test 5 after 1 hour at +350 mV vs. Ni in the reference environment

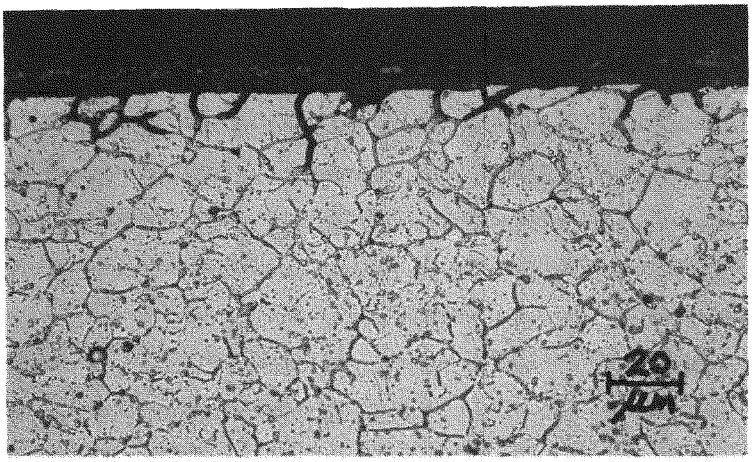

(a)

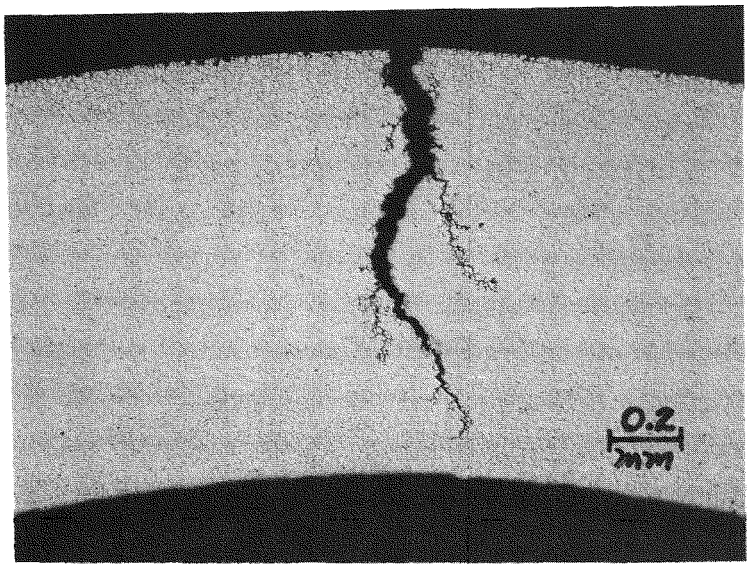

(b)

Figure 4-23. Localized attack in Test 5 of specimen #2 (mill-annealed Alloy 600 (Ht. 9955)) after 1 day at +350 mV vs. Ni and 27 days under open circuit conditions in the reference environment. (a) General surface attack; (b) Stress-corrosion cracking and IGA. Electrolytic phosphoric acid etch.

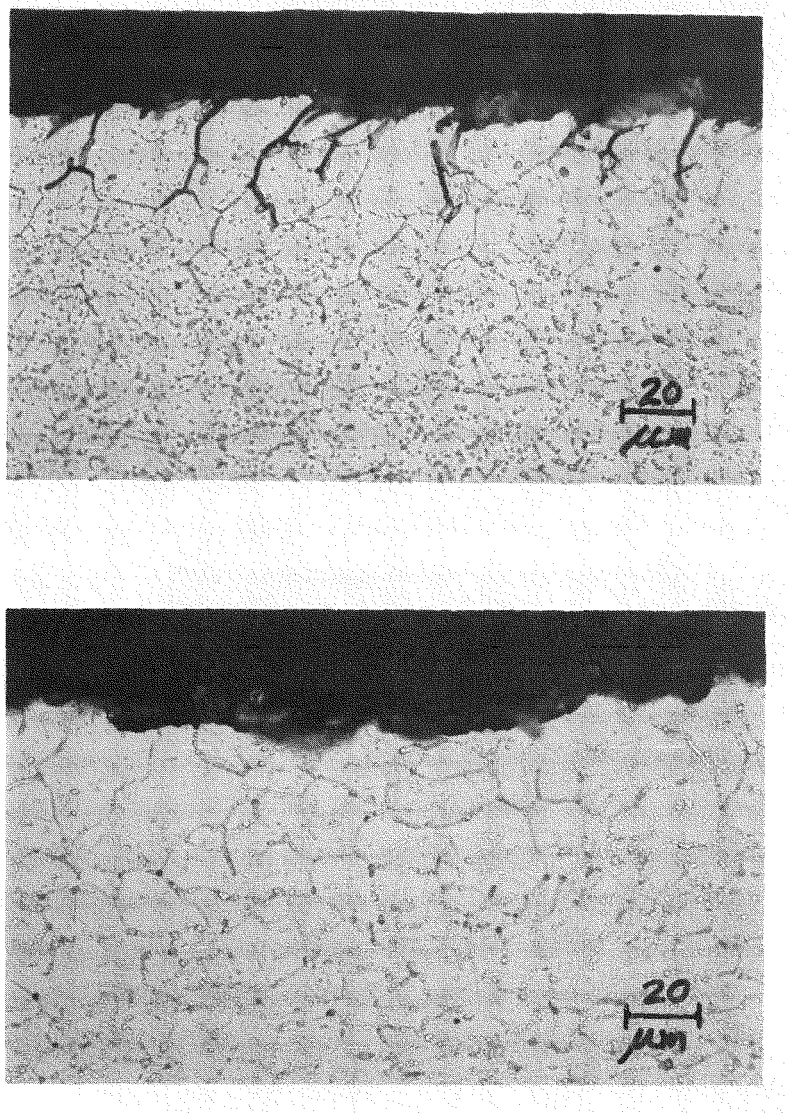

(a)

(b)

Figure 4-24. Mill-annealed Alloy 600 (Ht. 9955) tubing (specimen #8 in Test 5) after 28 days exposure under open circuit conditions in the reference environment. (a) Transverse section in high stress region (1.5 mil maximum penetration depth); (b) Longitudinal section in unstressed region. Electrolytic phosphoric acid etch.

Table 4-10

RESULTS OF A 4 WEEK EXPOSURE OF ALLOY 600 TO A DEAERATED 40 wt % NaOH + 10 wt % KOH + 12 wt % SiO_2 AQUEOUS MIXTURE AT 650°F

	Specimen No.	Heat No.	Specimen Condition	Test Conditions		Max. Depth of IGA (mil)	Max. Depth of SCC (mil)
Test 2	1	9955	Mill Annealed (MA) Closed C-ring σ_{app} >> Y.S.	1 day at +180 mV (peak potential)	Remaining Exposure at FCP	3	23
	2	9955		2 hr at +180 mV (peak potential)		2.8	--
	3	9955		1 day at +100 mV (active range)		1.3	--
	6	9955	MA Closed C-rings σ_{app} >> Y.S.	28 days at FCP		4.8	--
	7	9955				5.5	--
	8	9955	MA C-ring $\sigma_{app} \sim$ Y.S.			4.5	--
	9	9955	MA 2 in. long tube with carbon steel expansion plug (~0.5% ε)			3.5	--
Test 6	1	9837		1 day at +350 mV (passive range) + 27 days at FCP		3.8	43 (TW)
	6	9837	MA Closed C-ring σ_{app} >> Y.S.	28 days at FCP		5.1	--
	10	9955				5.0	--
	11	9955	MA C-ring $\sigma_{app} \sim$ Y.S.			4.4	--

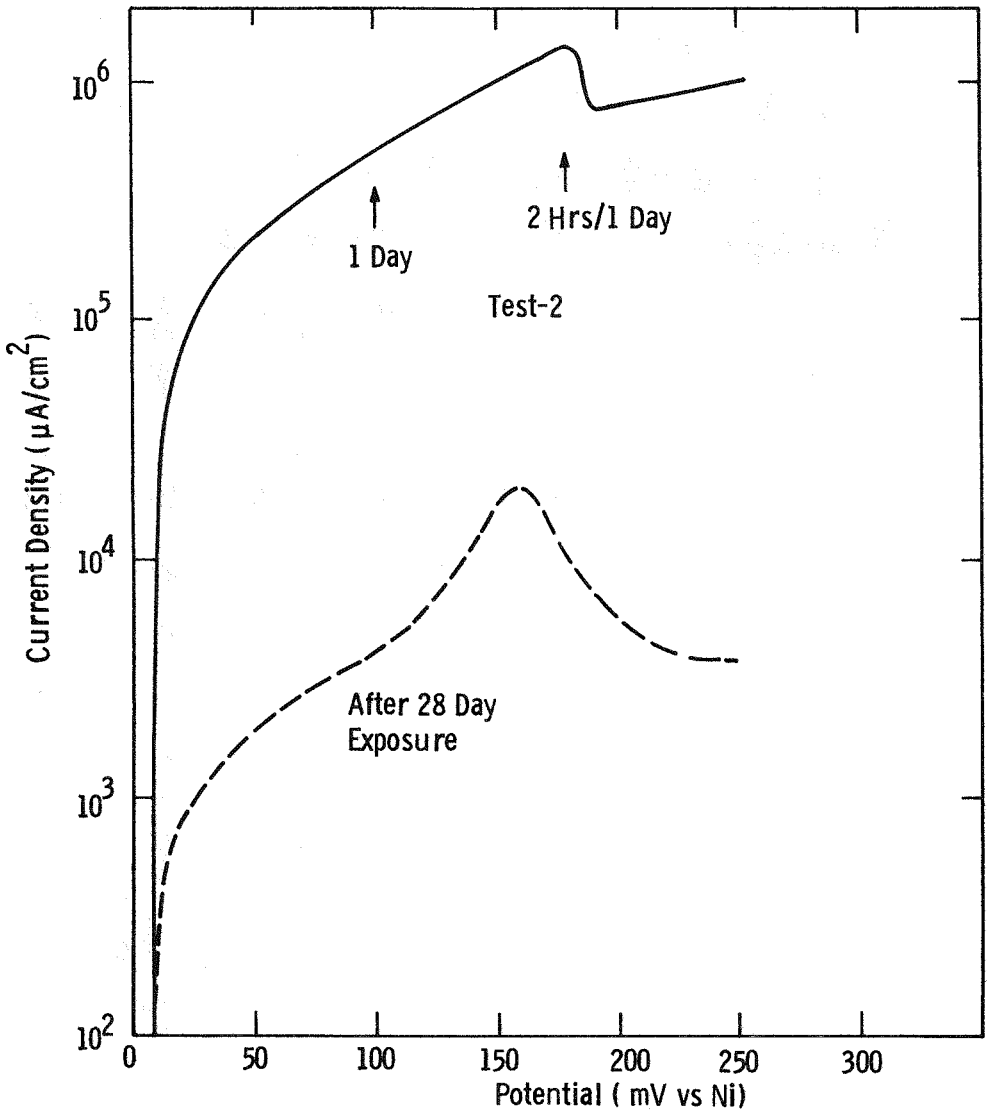

Figure 4-25. Anodic polarization curves for mill-annealed Alloy 600 (Ht. 9955) in the reference environment + 12 wt % SiO_2. Scan rate: 10 mV/min. The holding times and potentials for specimens 1-3 in Test 2 are indicated.

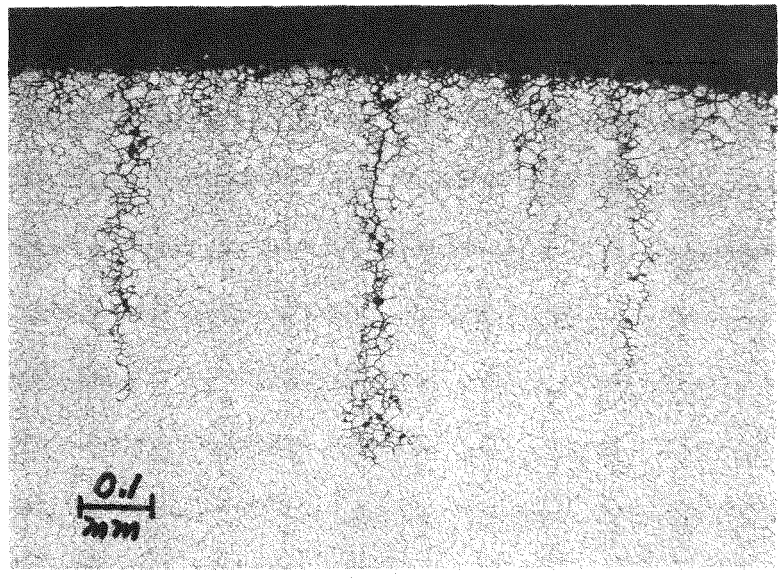

(a)

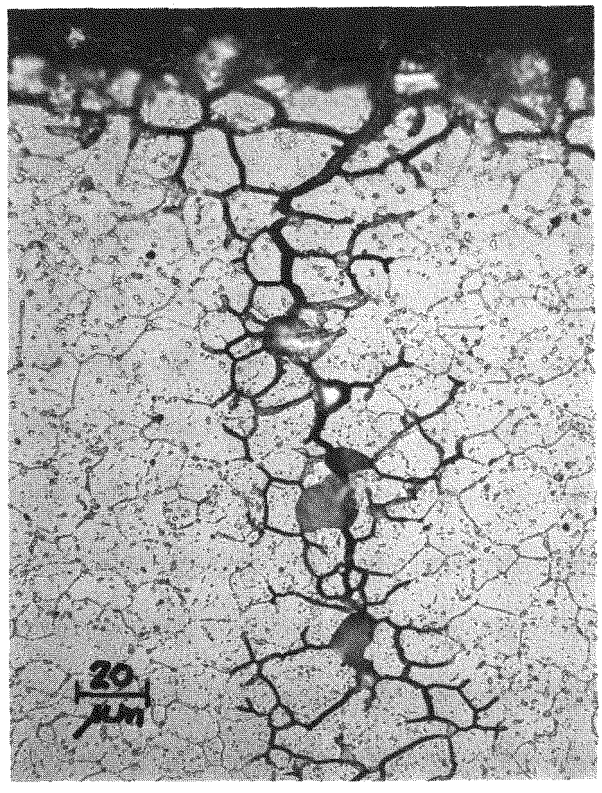

(b)

Figure 4-26. Localized attack in Test 2 of specimen #1 (mill-annealed Alloy 600 (Ht. 9955) after 1 day at +180 mV vs. Ni and 27 days under open circuit conditions in the reference environment + 12 wt % SiO_2. (a) Surface attack and multiple cracking (23 mil max.); (b) Intergranular branching from crack. Electrolytic phosphoric acid etch.

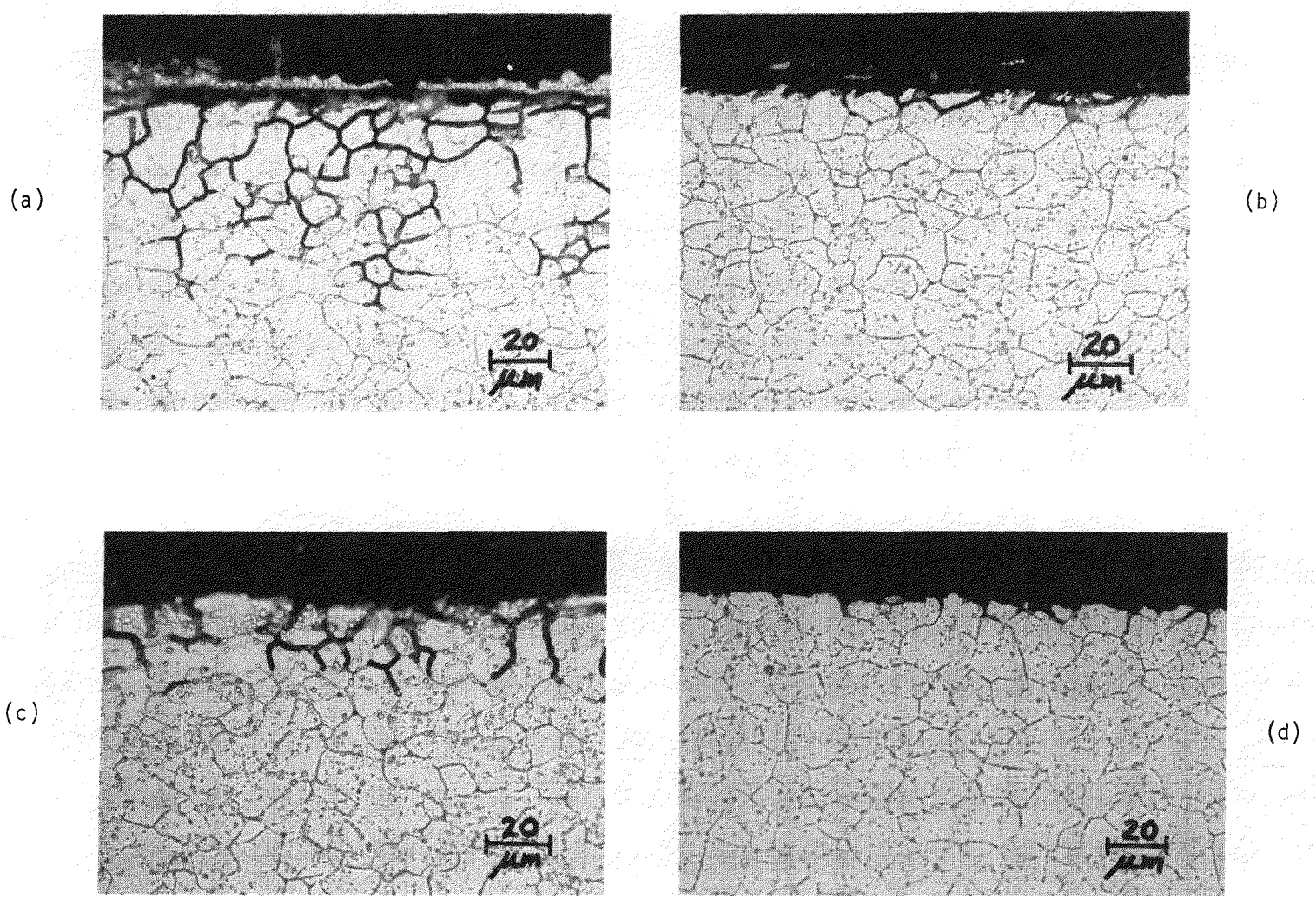

Figure 4-27. Localized attack of mill-annealed Alloy 600 (Ht. 9955) after exposure to the reference environment + 12 wt % SiO_2 (Test 2). (a) Specimen #2 in the high stress region; (b) Specimen #2 in the unstressed region; (c) Specimen #3 in the high stress region; (d) Specimen #3 in the unstressed region. Electrolytic phosphoric acid bath.

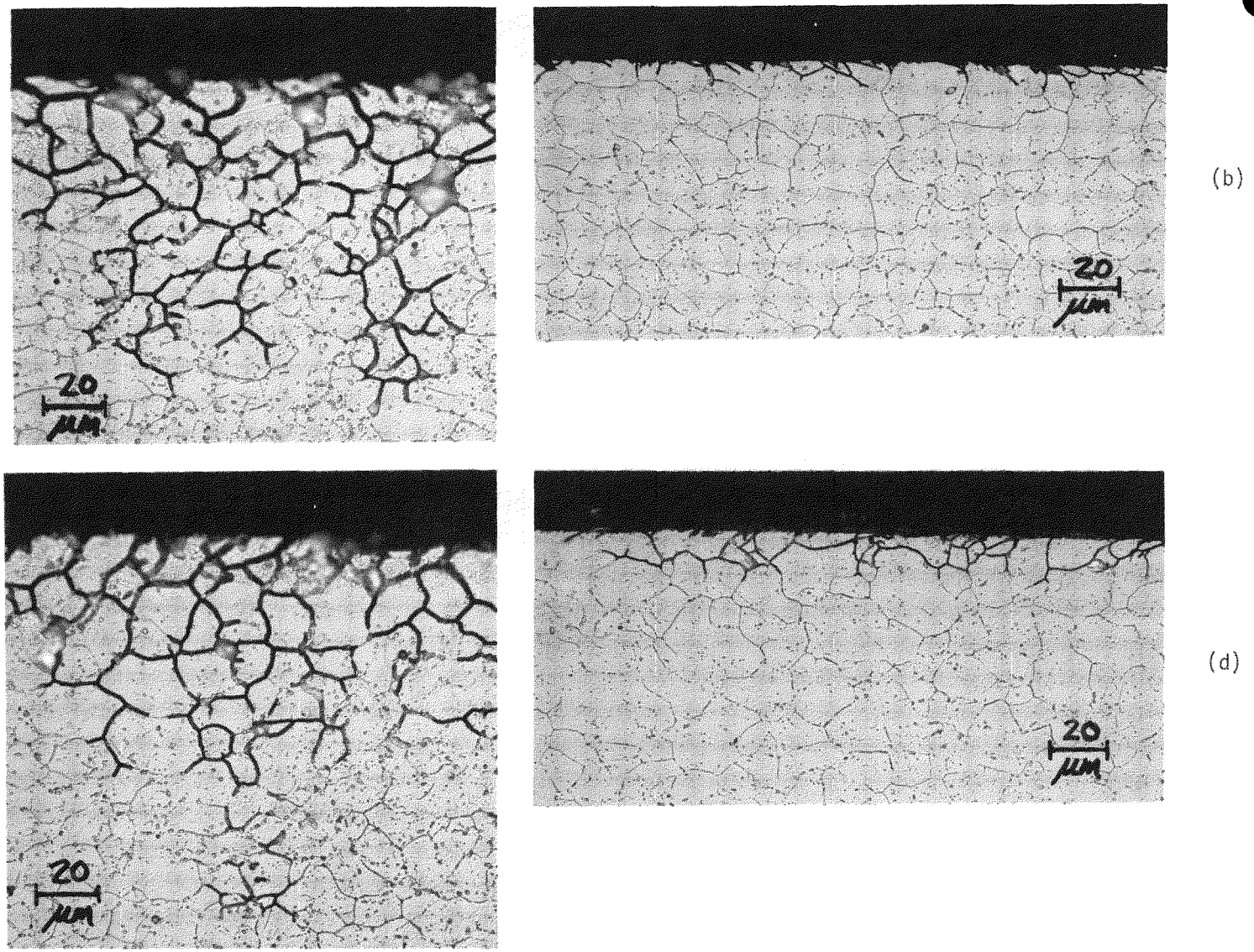

Figure 4-28. Localized attack of mill-annealed Alloy 600 (Ht. 9955) after exposure to the reference environment + 12 wt % SiO_2 (Test 2). (a) Specimen #6 in the high stress region; (b) Specimen #6 in the unstressed region; (c) Specimen #7 in the high stress region; (d) Specimen #7 in the unstressed region. Electrolytic phosphoric acid etch.

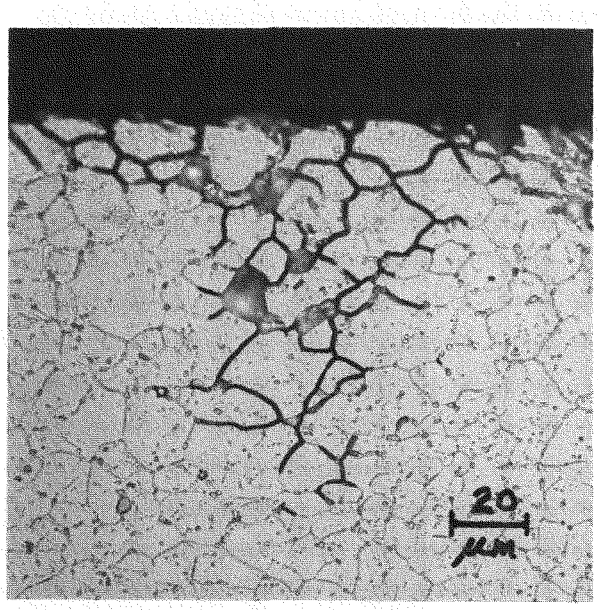

(a)

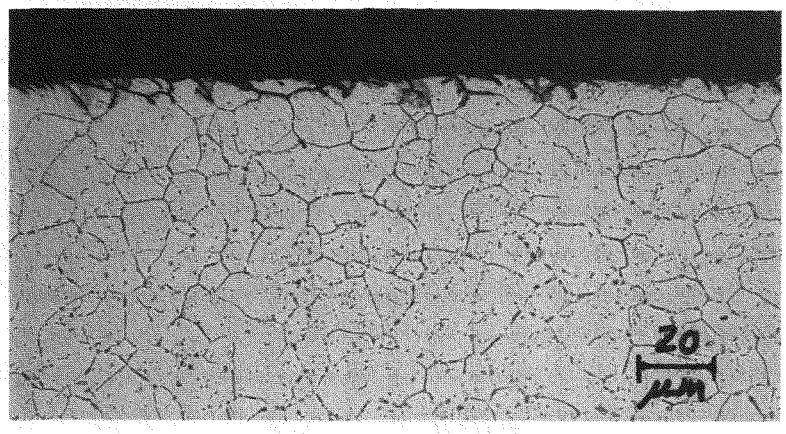

(b)

Figure 4-29. Localized attack of mill-annealed Alloy 600 (Ht. 9955) after exposure to the reference environment + 12 wt % SiO_2 (Test 2). (a) Specimen #8 in the high stress region; (b) Specimen #8 in the unstressed region. Electrolytic phosphoric acid etch.

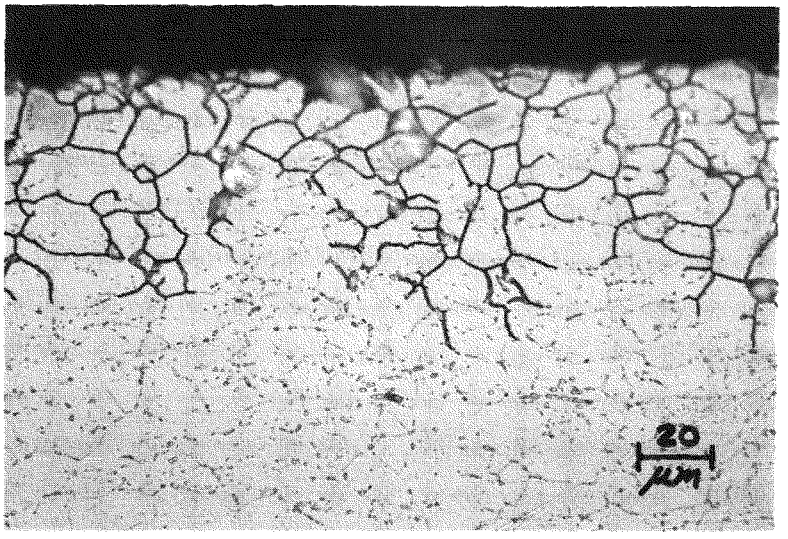

Figure 4-30. Transverse section through high stress region of mill-annealed Alloy 600 (Ht. 9955) tube (specimen #9, Test 2), after 28 day exposure in the reference environment + 12 wt % SiO_2. Electrolytic phosphoric acid etch.

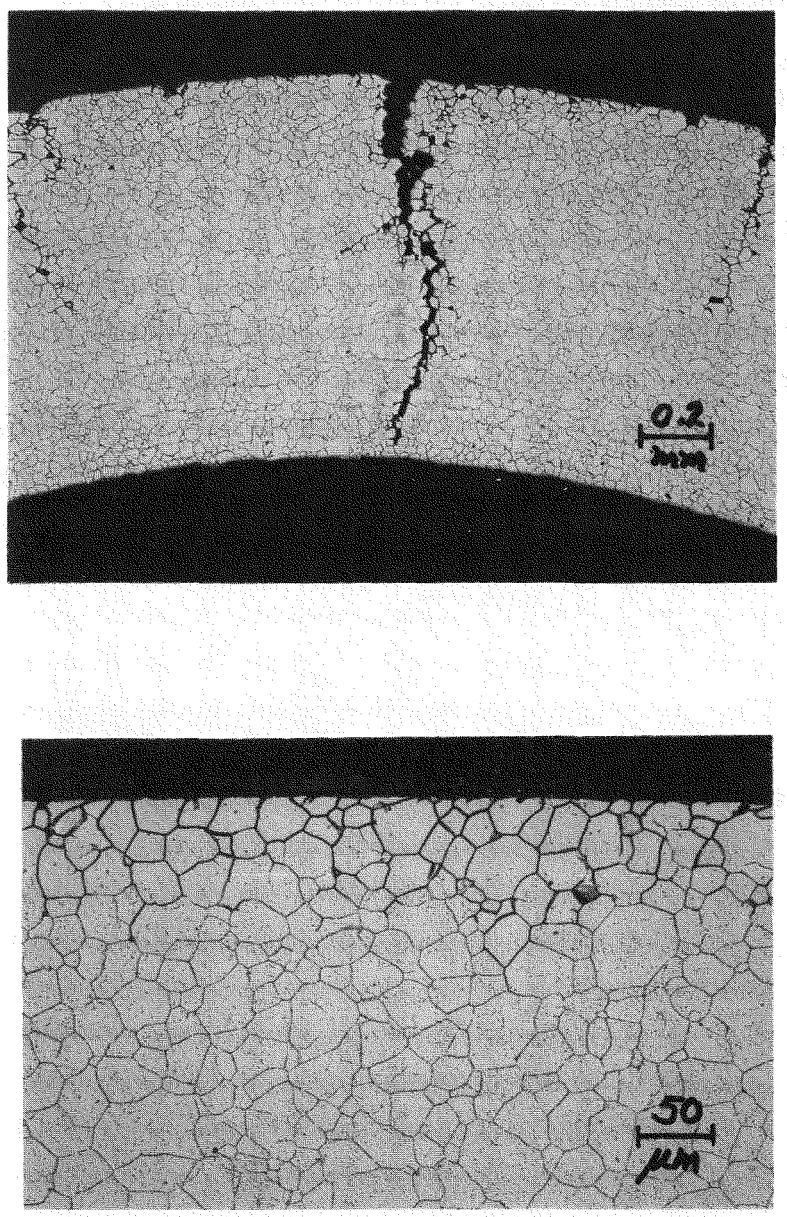

(a)

(b)

Figure 4-31. Localized attack of mill-annealed Alloy 600 (Ht. 9837) after exposure to the reference environment + 12 wt % SiO_2 (Test 6). (a) Specimen #1 in high stress region; (b) Specimen #6 in high stress region. Electrolytic phosphoric acid etch.

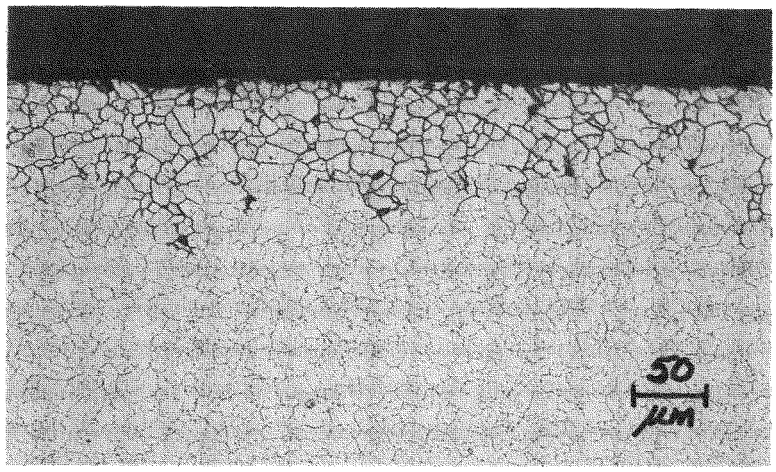

(a)

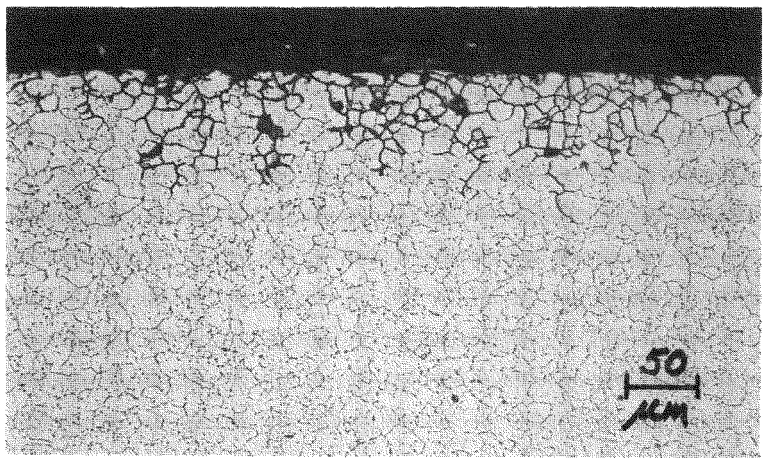

(b)

Figure 4-32. Influence of applied stress on the localized attack of mill-annealed Alloy 600 (Ht. 9955) after 28 day exposure in the reference environment + 12 wt % SiO_2 (Test 6). (a) Specimen #10 in high stress region; (b) Specimen #11 in high stress region. Electrolytic phosphoric acid etch.

the tests in the reference environment, the extent of IGA was greatest in the regions of highest applied stress.

Reference Environment + 12 wt % $NaNO_3$, 650°F. The results of testing in this environment are summarized in Table 4-11. No evidence of IGA or SCC was found on any specimen of mill-annealed Alloy 600, including those which had been initially polarized up to 350 mV more positive than the open circuit potential. However, this environment did cause general corrosion of all test specimens. The anodic polarization curve for mill-annealed Alloy 600 in this environment is shown in Figure 4-33. As was observed in the reference environment + SiO_2 (Figure 4-25) the current density was higher than in the reference environment alone (Figure 4-17) yet no IGA was observed. Figure 4-34 illustrates the typical general corrosion and absence of IGA in specimens #6 and #7 after a 4-week exposure in the $NaNO_3$-containing environment.

Reference Environment + 7 wt % CuO + 3 wt % ZnO, 650°F. This test was terminated after ~2 hours at 650°F due to a leaking thermowell gasket. The specimens under test were duplicates of those used in Test 5 (see Table 4-9). In spite of the short exposure time in this environment, two specimens exhibited extensive SCC. Figure 4-35 illustrates the SCC found in duplicate specimens of mill-annealed Alloy 600 C-rings after the few hours of exposure. No SCC or IGA was observed in other specimens in this test.

Under appropriate corrosive conditions, local differences in composition at, or adjacent to, grain boundaries will result in enhanced corrosive attack along the grain boundaries, with the grains themselves remaining virtually unattacked. The advance of the intergranular attack may be initially rapid due to the large ratios of cathodic area (exposed grain surfaces) to anodic area (advancing edges of grain boundaries). However, this form of corrosion, referred to as intergranular attack (IGA), will generally tend to slow down as it advances along the grain boundaries because the resistance of the path joining anodic and cathodic areas gradually increases. In material-environment combinations which produce IGA, the application of tensile stresses will frequently enhance the corrosion penetration along the grain boundaries, either by rupturing bridges between corroded grain boundary regions or by reducing the activation polarization at the corroding grain boundary edges (3).

Table 4-11

RESULTS OF A 4 WEEK EXPOSURE OF ALLOY 600 TO A DEAERATED 40 wt % NaOH + 10 wt % KOH + 12 wt % $NaNO_3$ AQUEOUS MIXTURE AT 650°F

	Specimen No.	Heat No.	Specimen Condition	Test Conditions		Max. Depth of IGA (mil)	Max. Depth of SCC (mil)
Test 4	1	9955	Mill Annealed (MA) Closed C-ring σ_{app} >> Y.S.	1 day at +350 mV (peak potential)	Remaining exposure at FCP	--	--
	2	9955		2 hr at +200 mV (active range)		--	--
	3	9955		2 hr at +50 mV (active range)		--	--
	6	9955	MA Closed C-ring σ_{app} >> Y.S.	28 days at FCP		--	--
	7	9955	MA C-ring σ_{app} ~ Y.S.			--	--
	8	9955	MA 2 in. long tube with carbon steel expansion plug (~0.5% ε)			--	--
	11	9837	MA Closed C-ring σ_{app} >> Y.S.			--	--

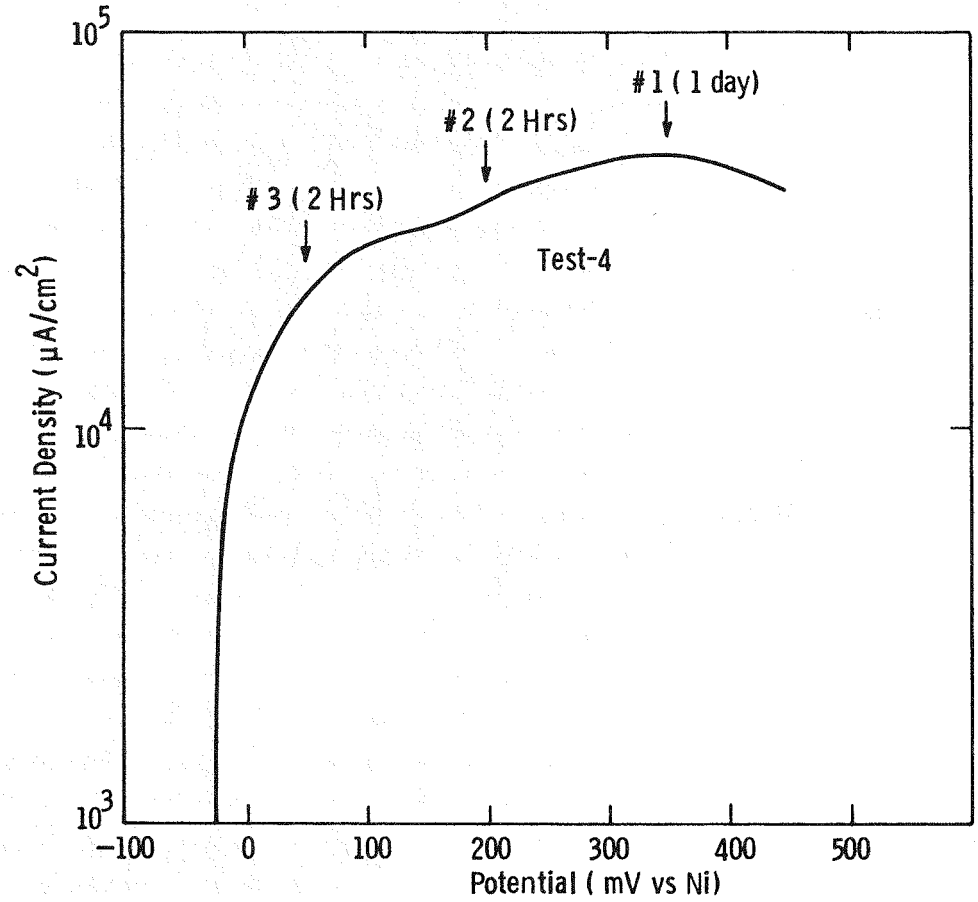

Figure 4-33. Anodic polarization curve for mill-annealed Alloy 600 (Ht. 9953) in the reference environment + 12 wt % $NaNO_3$. Scan rate: 10 mV/min. The holding times and potentials for specimens 1-3 in Test 4 are indicated.

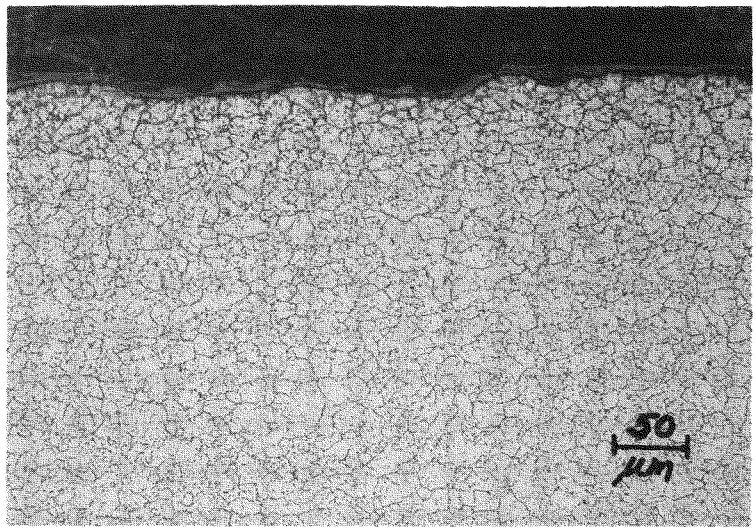

(a)

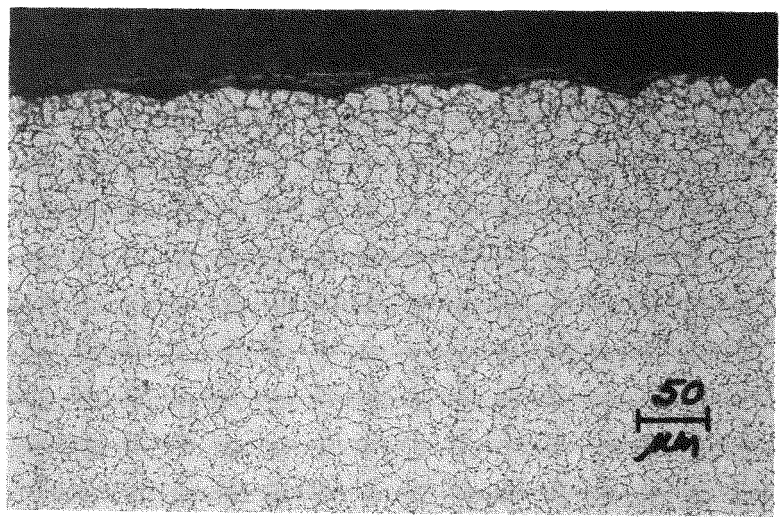

(b)

Figure 4-34. General corrosion observed on mill-annealed Alloy 600 (Ht. 9955) after 28 day exposure under open circuit conditions in the reference environment + 12 wt % $NaNO_3$ (Test 4). (a) Specimen #6 in high stress region; (b) Specimen #7 in high stress region. Electrolytic phosphoric acid etch.

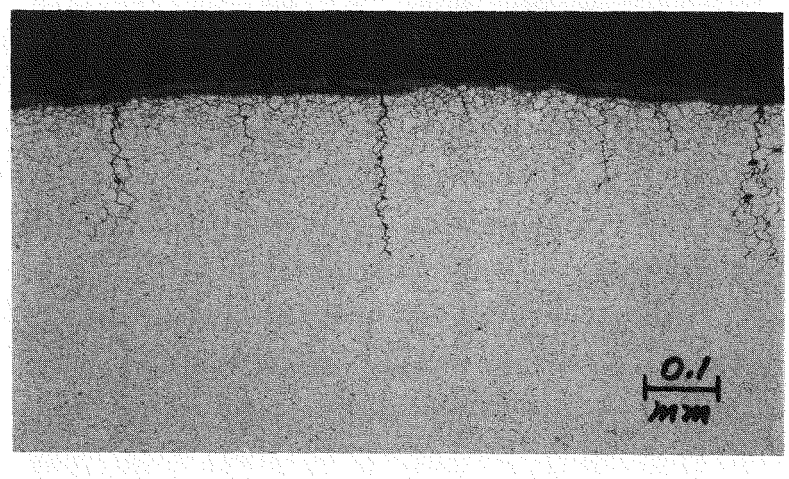

(a)

(b)

Figure 4-35. Stress corrosion cracking observed in duplicate specimen of mill-annealed Alloy 600 (Ht. 9955) closed C-rings after ∿2 hr exposure in the reference environment + 7 wt % CuO + 3 wt % ZnO at 650°F. (a) Maximum penetration 9.4 mils; (b) Maximum penetration 8.8 mils. Electrolytic phosphoric acid etch.

The results of Subtask 301, in which the effects of stress and controlled electrochemical conditions were evaluated, are essentially consistent with the generally accepted concepts of IGA described above. The application of high tensile stresses and anodic polarization, for example, resulted in severe localized intergranular cracking in highly stressed regions with minimal penetrations due to IGA over the bulk of specimen surfaces. The most severe intergranular cracking was produced by partial passivation of the surface which resulted in enhanced corrosive attack at the more active grain boundaries. Similarly, in the absence of anodic polarization, the maximum depths of IGA penetrations were always observed at regions of highest applied tensile stresses.

The reference environment alone was sufficiently aggressive to produce shallow IGA in a 4-week period, without stimulation from applied stress or anodic polarization. The observations that: (1) SiO_2 additions to NaOH/KOH solutions increase the maximum depth of penetrations associated with surface IGA; and (2) $NaNO_3$ additions to NaOH/KOH solutions or carbide precipitation treatments inhibit IGA and associated intergranular penetrations, are qualitatively consistent with published observations of Pement et al. (4).

On initial immersion, the anodic polarization curves for Alloy 600 obtained in both SiO_2- and $NaNO_3$-containing environments were characterized by significantly higher current densities than those obtained in the reference environment. However, severe corrosion was only observed after exposure to the $NaNO_3$-containing environment, and in contrast to the SiO_2-containing environment, the presence of the $NaNO_3$ inhibited both IGA and SCC. Such differences are probably associated with the facts that nitrates are quite soluble and offer little or no film forming protection while silicates often form insoluble corrosion products and as a result provide partial protection. Consequently, the presence of SiO_2 would tend to accentuate local attack (IGA and/or SCC) at unprotected surface regions. In contrast, the uniform attack in the presence of $NaNO_3$ would tend to inhibit local grain boundary attack. Such a hypothesis is consistent with the observation that the anodic polarization curve of Alloy 600 in the SiO_2-containing environment was displaced to lower current density values (1-2 orders of magnitude) after the 4-week exposure (Figure 4-25).

C-Ring Tests (Subtask 302A)

Mill-annealed Alloy 600 C-ring specimens were exposed to five of the environments listed in Table 4-8 (Test numbers 1, 12, 18, 19, and 26). The results of destructive metallographic examination of C-ring specimens exposed for up to 2688 hours (4000 hours in Test #26) are shown in Table 4-12. The results presented in this table show the depth of uniform IGA on the OD and ID surfaces of the C-ring specimens, and the maximum depth of IGA and SCC (shown in parentheses) whenever these depths exceeded the uniform depth by 50%. Figure 4-36 presents examples of uniform IGA, maximum IGA, and maximum SCC. The depth of uniform IGA was defined as the depth to which every grain boundary was affected. The depth of maximum IGA and SCC was determined as the depth to which localized regions of IGA and SCC extend from the specimen surface beyond the region of uniform IGA.

In the reference environment, 40 wt % NaOH + 10 wt % KOH, the IGA data generated at the two stress levels and at the two exposure times are so similar that an effect of these parameters (stress level and exposure length) on the depth of IGA cannot be seen. However, the effect of exposure time and stress level on SCC is evident. The extent, or depth, of SCC was greater for specimens stressed at 75% of the yield stress than at 25% of the yield stress. No SCC was observed on specimens stressed to 25% of yield. Also, for the more highly stressed specimens, the depth of SCC increased with increasing exposure time.

At the low stress levels (< yield stress) tested in this subtask, no influence of stress on IGA was apparent in any environment. The threshold stress for SCC in all environments, except the nitrate containing environment, was between 25% and 75% of yield.

When 12 wt % SiO_2 was added to the reference environment, the severity of IGA, judged by the depth of uniform attack, decreased slightly when compared to specimens with comparable exposure times and stress levels exposed to the reference environment without additives (Test 1). Concurrent with the diminished IGA, the severity of SCC increased when compared to comparable specimens from the reference test. As in the reference test, SCC was at a maximum for high stress levels and long exposure times.

A similar result, namely a reduced severity of IGA and an increased severity of SCC compared to that in the reference environment, resulted from addition of 7 wt

Table 4-12

RESULTS OF MILL ANNEALED ALLOY 600 C-RINGS
EXPOSED TO THE REFERENCE CAUSTIC ENVIRONMENT + ADDITIVES AT 650°F

Test No.	Additive to 40% NaOH + 10% KOH	Specimen No.	Stress[a]	Exposure Time, h	Uniform Depth of IGA and Maximum Depth of IGA and SCC, shown in parentheses, in mm			
					Apex		Stress Free Leg	
					OD	ID	OD	ID
1	None	DU1	0.0	2688	0.010	0.015	0.015	0.025
		D1	0.25	2016	0.025	0.025	0.020	0.025
		D4	0.25	2016	0.020 (IGA-0.1)[b]	0.020	0.020	0.035
		D2	0.25	2688	0.035	0.025	0.025	0.035
		D3	0.25	2688	0.030	0.025	0.025	0.025
		D5	0.75	2016	0.020 (SCC-0.5)[b]	0.020	0.020	0.025
		D8	0.75	2016	0.025 (SCC-0.3)	0.025	0.015	0.030
		D6	0.75	2688	0.030 (SCC-0.9)	0.025	0.025	0.025
		D7	0.75	2688	0.030 (SCC-0.6)	0.025	0.020	0.010
12	12% SiO_2	DU2	0.0	2688	0.015	0.025	0.015	0.020
		D11	0.25	2016	0.025	0.030	0.020	0.030
		D12	0.25	2016	0.010	0.025	0.010	0.025
		D13	0.75	2016	0.00 (SCC-0.8)	0.025	0.00	0.020
		D16	0.75	2016	0.005 (SCC-0.7)	0.005	0.005	0.005
		D14	0.75	2688	0.015 (SCC-1.2)	0.015	0.020	0.035
		D15	0.75	2688	0.010 (SCC-1.2)	0.015	0.010	0.020
18	12% $NaNO_3$	DU3	0.0	2688	0.00	0.00	0.00	0.00
		D17	0.25	2688	0.00	0.00	0.00	0.00
		D18	0.25	2688	0.00	0.00	0.00	0.00
		D19	0.25	2016	0.00	0.00	0.00	0.00
		D20	0.25	2016	0.00	0.00	0.00	0.00
		D21	0.75	2016	0.00	0.00	0.00	0.00
		D24	0.75	2016	0.00	0.00	0.00	0.00
		D22	0.75	2688	0.00	0.00	0.00	0.00
		D23	0.75	2688	0.00	0.00	0.00	0.00

(continued)

Table 4-12 (continued)

Test No.	Additive to 40% NaOH + 10% KOH	Specimen No.	Stress[a]	Exposure Time, h	Uniform Depth of IGA and Maximum Depth of IGA and SCC, shown in parentheses, in mm			
					Apex		Stress Free Leg	
					OD	ID	OD	ID
19	7% CuO + 3% ZnO	D27	0.25	2688	0.015	0.01	0.010	0.010
		D28	0.25	2688	0.010	0.010	0.005	0.010
		D29	0.75	2016	0.005 (SCC-0.08)	0.005	0.00	0.005
		D32	0.75	2016	0.005	0.00	0.00	0.00
		D30	0.75	2688	0.010	0.010	0.005	0.010
		D31	0.75	2688	0.00 (SCC-1.22)	0.010	0.005	0.005
26	12% SiO_2 + 7% CuO + 3% ZnO	DU5	0.0	4000	0.00	0.005	0.00	0.010
		D33	0.25	1000	0.00	0.00	0.00	0.00
		D36	0.25	4000	0.00	0.005	0.00	0.010
		D45	0.5	1000	0.00 (SCC-0.7)	0.00	*	*
		D46	0.5	1000	0.00 (SCC-0.17)	0.00	*	*
		D41	0.5	1344	0.00	0.005	0.00	0.015
		D44	0.5	1344	0.005 (SCC-0.07)	0.010	0.00	0.015
		D42	0.5	3000	0.00	0.005	0.00	0.005
		D43	0.5	3000	0.00	0.010	0.00	0.00
		D37	0.75	672	0.00 (SCC-1.2)	0.00	*	*
		D38	0.75	672	0.00 (SCC-0.8)	0.00	*	*
		D39	0.75	672	0.00 (SCC-1.3)	0.00	*	*
		D40	0.75	672	0.00 (SCC-0.7)	0.00	*	*

[a]Multiple of yield strength.

[b]Maximum IGA and SCC tabulated only when they exceed uniform IGA by 50%.

*Both legs were stenciled.

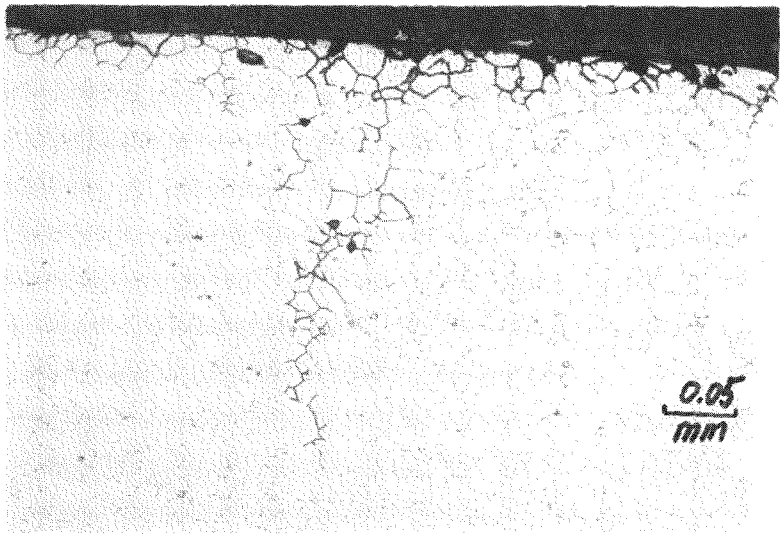

Specimen No. 32
0.025 mm = Uniform IGA
0.30 mm = SCC max.

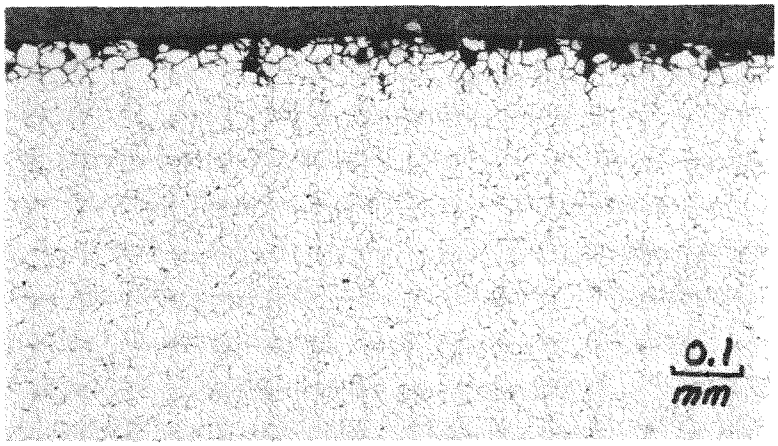

Specimen No. 37
0.04 mm - Uniform IGA

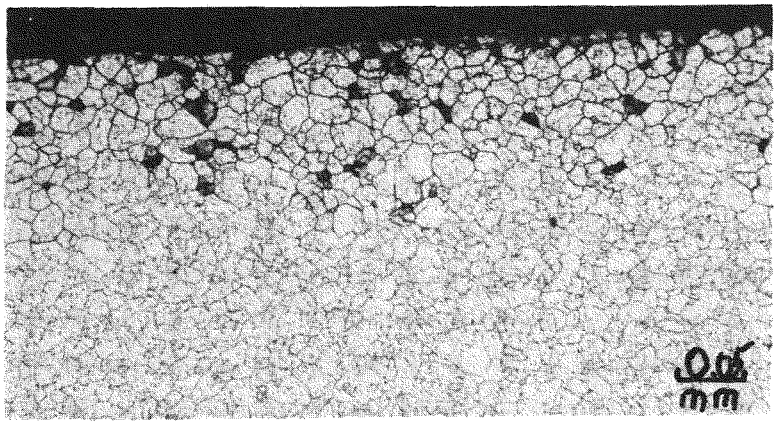

Specimen No. 38
0.14 mm = IGA max.

Figure 4-36. Typical structures and illustrations of uniform IGA, SCC max., and IGA max. Photomicrographs were taken on OD at the apex of C-rings. Electrolytic phosphoric acid etch.

% CuO + 3 wt % ZnO (Test 19). The effect of combining 12 wt % SiO_2 with 7% CuO + 3% ZnO (Test 26) was even more pronounced. The synergistic effect of these combined additives was virtual elimination of IGA and extensive, accelerated SCC. The effect was most pronounced for highly stressed specimens. Through-wall, or nearly through-wall cracking was produced on specimens stressed to 0.75 of the yield stress during the first month (672 hours) of exposure. Optical photographs of these specimens are presented in Figure 4-37. As already mentioned in the discussion of electrochemical results, the film-forming characteristic of these environments would tend to accentuate local attack at unprotected, or accessible, grain boundaries while minimizing attack at occluded grain boundaries. The net effect of this reduction in exposed grain boundary area is rapid SCC at the propagating grain boundaries.

The effect of sodium nitrate additions to the reference environment was the same as observed in the electrochemical tests (Subtask 301). No IGA or SCC was observed but general corrosion of the Alloy 600 surface was encountered. Figure 4-38 shows the OD surface of C-rings exposed in this environment. An estimate of the amount of general corrosion on these specimens was obtained by subtracting the average wall thickness of exposed C-rings from the wall thickness of the virgin tubing. A wall reduction of 0.014 mm in the reference plus nitrate environment was determined in this manner from the data in Table 4-13. The net 0.014 mm reduction in wall thickness due to general corrosion in this environment is only ~25% of the effective wall reduction of 0.060 mm due to IGA produced in the reference environment alone under comparable exposure conditions. Further work is required to evaluate the effectiveness of nitrate as an inhibitor for both SCC and IGA.

In performing the metallographic examination of C-rings used in this subtask, it was noted that localized regions of accelerated IGA were present. The IGA in these regions was significantly deeper (as much as an order of magnitude) than the uniform IGA observed elsewhere on the same specimen. These regions of accelerated IGA were located adjacent to machined surfaces, such as the holes drilled to accept the stressing bolts and the 60^{o} section cut from the tube to produce the C-ring (see Figure 4-39), and at stencil marks on the "stress-free legs". The location of these regions infers that residual stress or strain may be a significant contributing factor in accelerating IGA. Additional experimental work is required to determine the role these factors have in increasing IGA susceptibility.

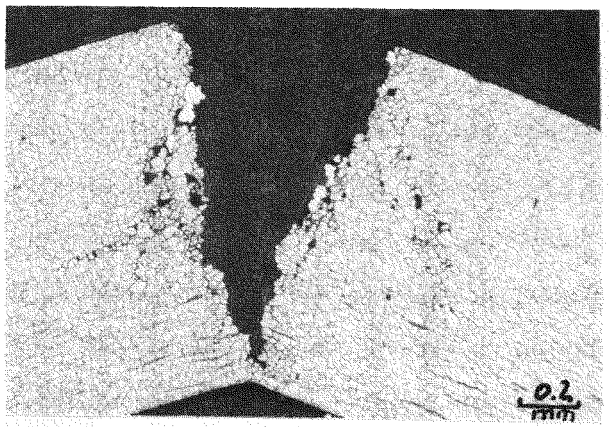

D37

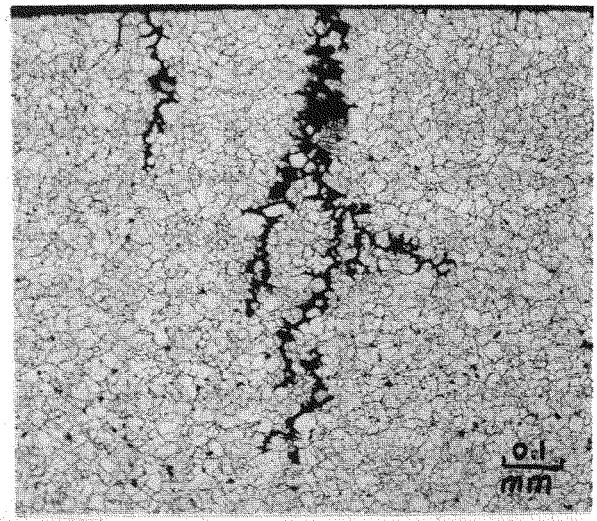

D38

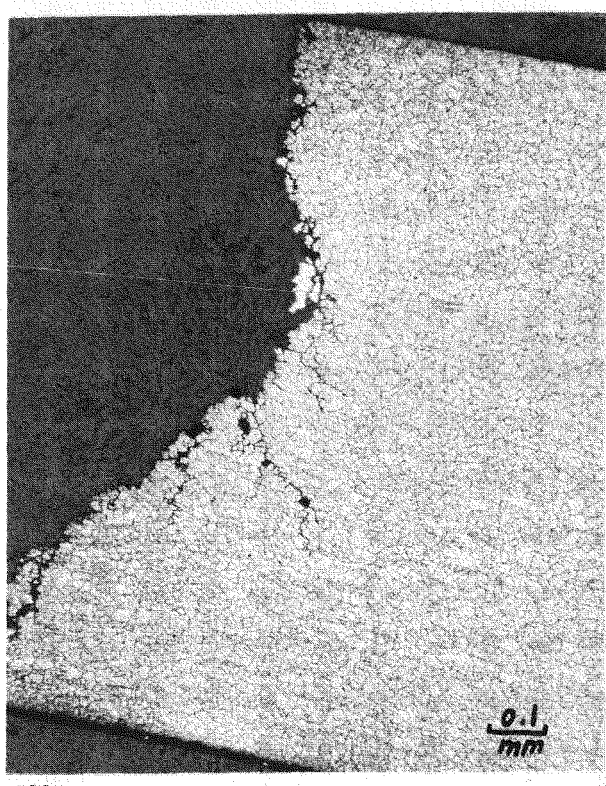

D39

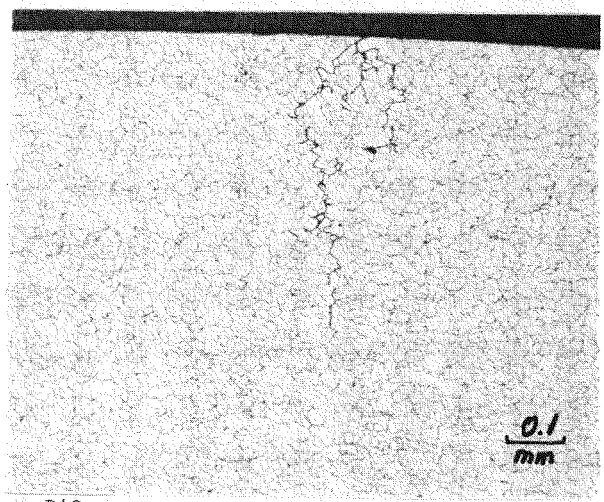

D40

Figure 4-37. SCC encountered in 4 C-rings exposed at 75% yield stress to 40% NaOH + 10% KOH + 12% SiO_2 + 7% CuO + 3% ZnO for 672 hours at 650°F (Test No. 26). OD is top surface. No IGA was observed. Electrolytic phosphoric acid etch.

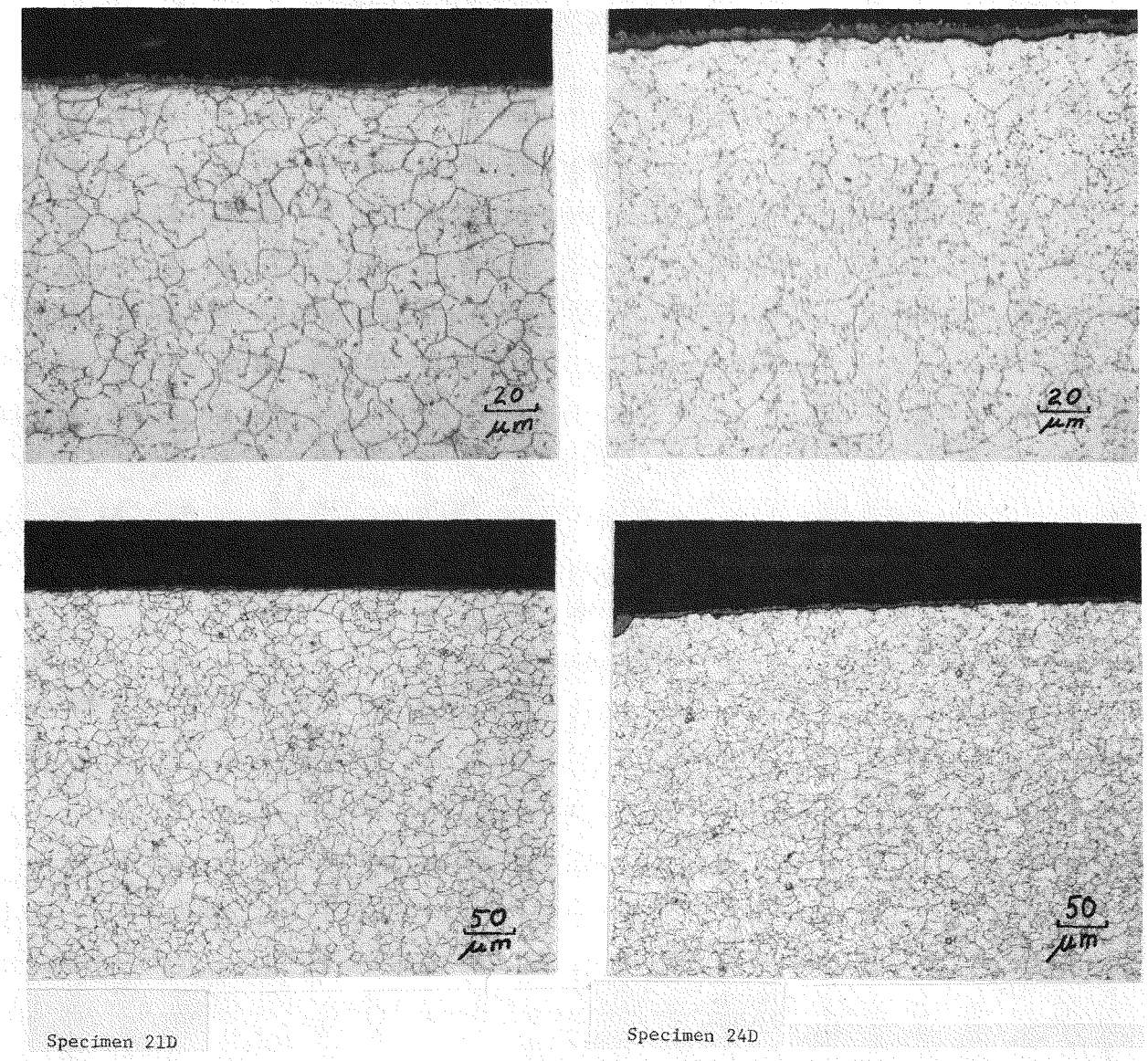

Figure 4-38. OD surfaces of rings run in 40% NaOH + 10% KOH + 12% $NaNO_3$ for 2016 hours at 650°F. Electrolytic phosphoric acid etch.

Table 4-13

WALL THICKNESSES (mm) BEFORE AND AFTER EXPOSURES TO 40% NaOH + 10% KOH + 12% $NaNO_3$

Virgin Ring from Heat 9705

1.29	
1.27	
1.24	
1.21	Average = 1.238
1.21	
1.21	
1.24	

Rings After Exposures of 2016 or 2688 h

1.19[a]	
1.23	
1.24	Average = 1.224
1.21	
1.25	

[a]Measurements at apex.

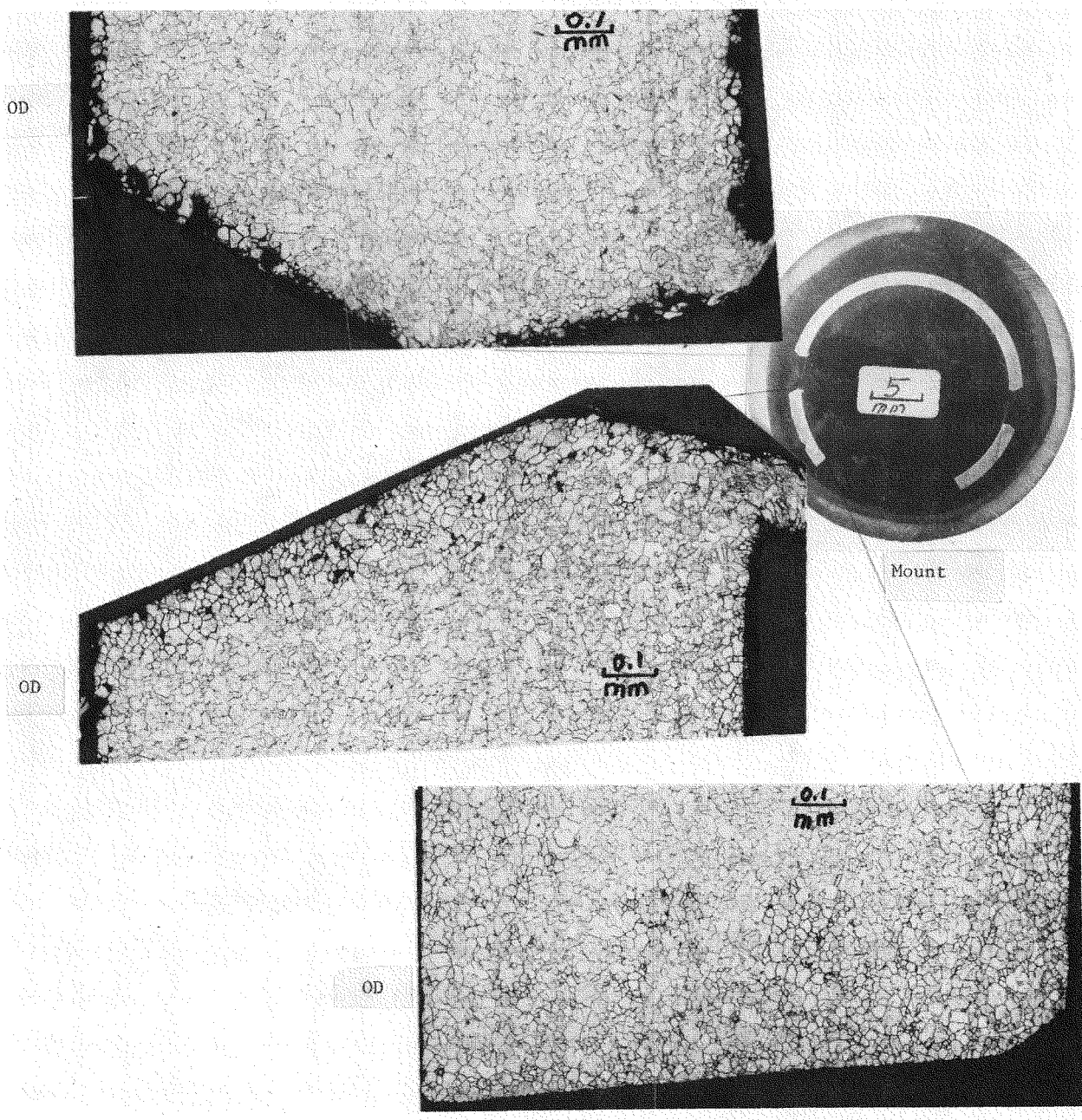

Figure 4-39. Accelerated IGA was apparent along some drilled or cut surfaces, Specimen No. 37. Bromine-methanol etch.

Capsule Tests (Subtask 302B)

Capsule Proof Tests. Prior to performance of the isothermal capsule tests identified in Table 4-8, a series of capsule proof tests was performed. These tests were necessary to identify the caustic concentration and test temperature which gave the maximum amount of IGA in the shortest period of time. These conditions would become the reference environment against which the effect of the various additives identified in Table 4-8 would be evaluated. Additionally, the desirability of using a stress promoter, such as a machined flat on the OD surface of the capsule, in all subsequent capsule testing was to be determined.

Results of earlier work by Airey (5) with C-ring specimens showed that for mill annealed Alloy 600 the depth of IGA increased and the depth of SCC decreased when the caustic concentration was increased from 10 to 50 wt % (Figure 4-40) and that in a 10 wt % NaOH solution the IGA and SCC susceptibility increased as the exposure temperature was increased from 600 to 650°F (Figure 4-41). In these figures, the mean depth of attack was defined as the depth of uniform attack in which all grain boundaries were involved, and the maximum depth of attack was defined as the maximum depth of SCC extending from the surface beyond the mean depth. Based on these results, it was presumed that a 50% solution at 650°F would be the most likely choice as a reference environment for maximizing the amount of IGA and at the same time minimizing SCC. Minimizing SCC was considered to be of utmost importance for capsule testing. If SCC initiated in an isothermal capsule the targeted exposure may not be achieved due to through-wall SCC resulting in loss of solution from the capsule.

To verify these earlier data and establish a reference test environment, a series of capsule tests with a range of caustic concentrations (50%, 10%, 5%, and 3%) was performed at 650 and 600°F. The results of these tests showed that in the ≤90 day exposures at 600°F, no IGA was observed in any of the caustic solutions. At 650°F, no IGA was produced in solutions where the caustic concentration was ≤10% and ~0.025 mm (1 mil) of uniform IGA was produced in the 50% caustic solution. Based on these results, which were in agreement with Ariey's previous work, 50% caustic at 650°F appeared to be the only choice as the reference environment.

Many of the capsules in the proof test series were unable to achieve the full 90-day exposure due to inability to contain the test environments. Frequent leaks at welds, both top and bottom, and at the Swagelok fitting were encountered. Figure 4-42 is an example of weld cracking in these tests. Several changes in welding

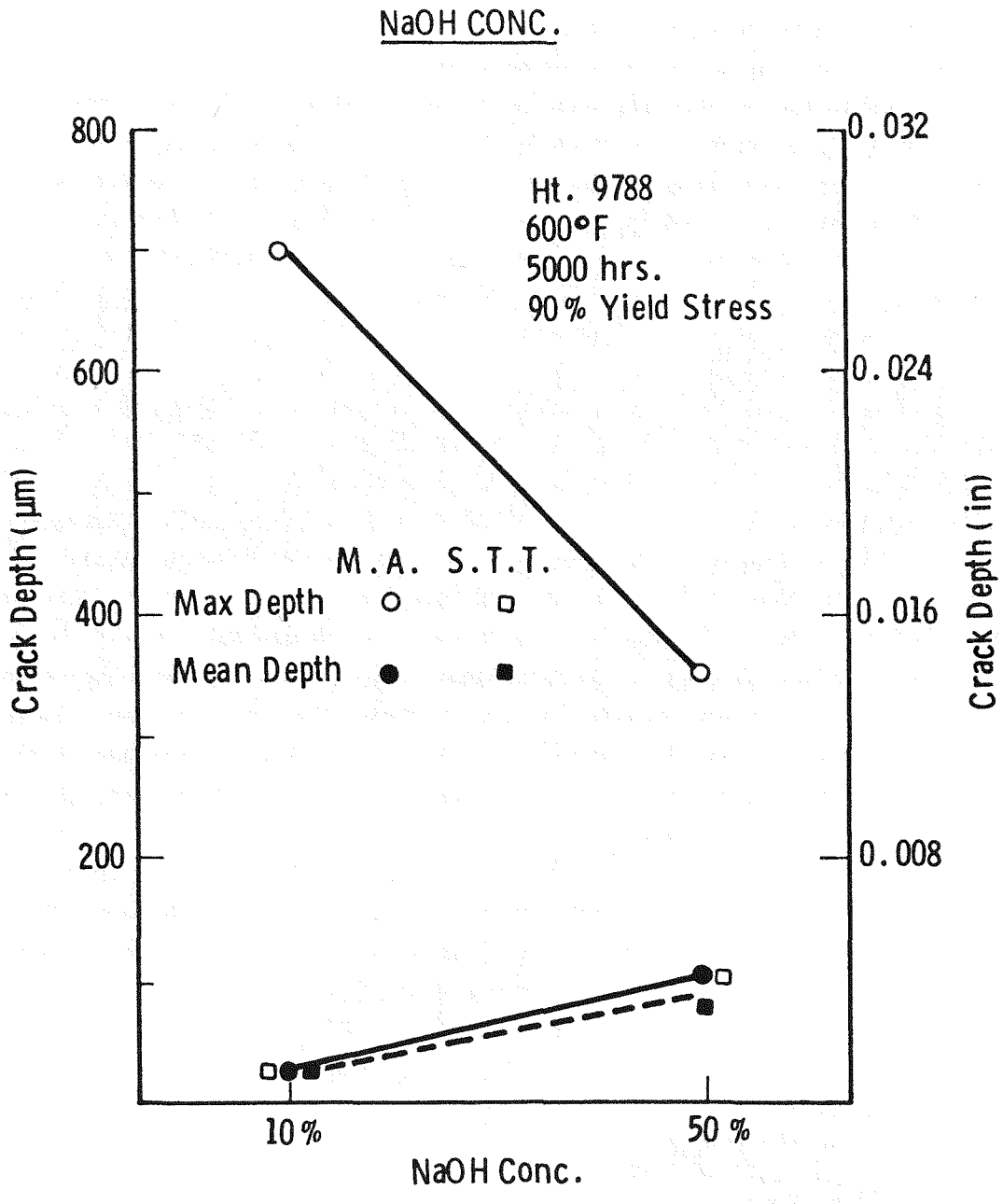

Figure 4-40. The effect of caustic concentration on SCC (maximum depth) and IGA (mean depth) susceptibility of mill-annealed and special thermally treated Alloy 600 (Reference 5).

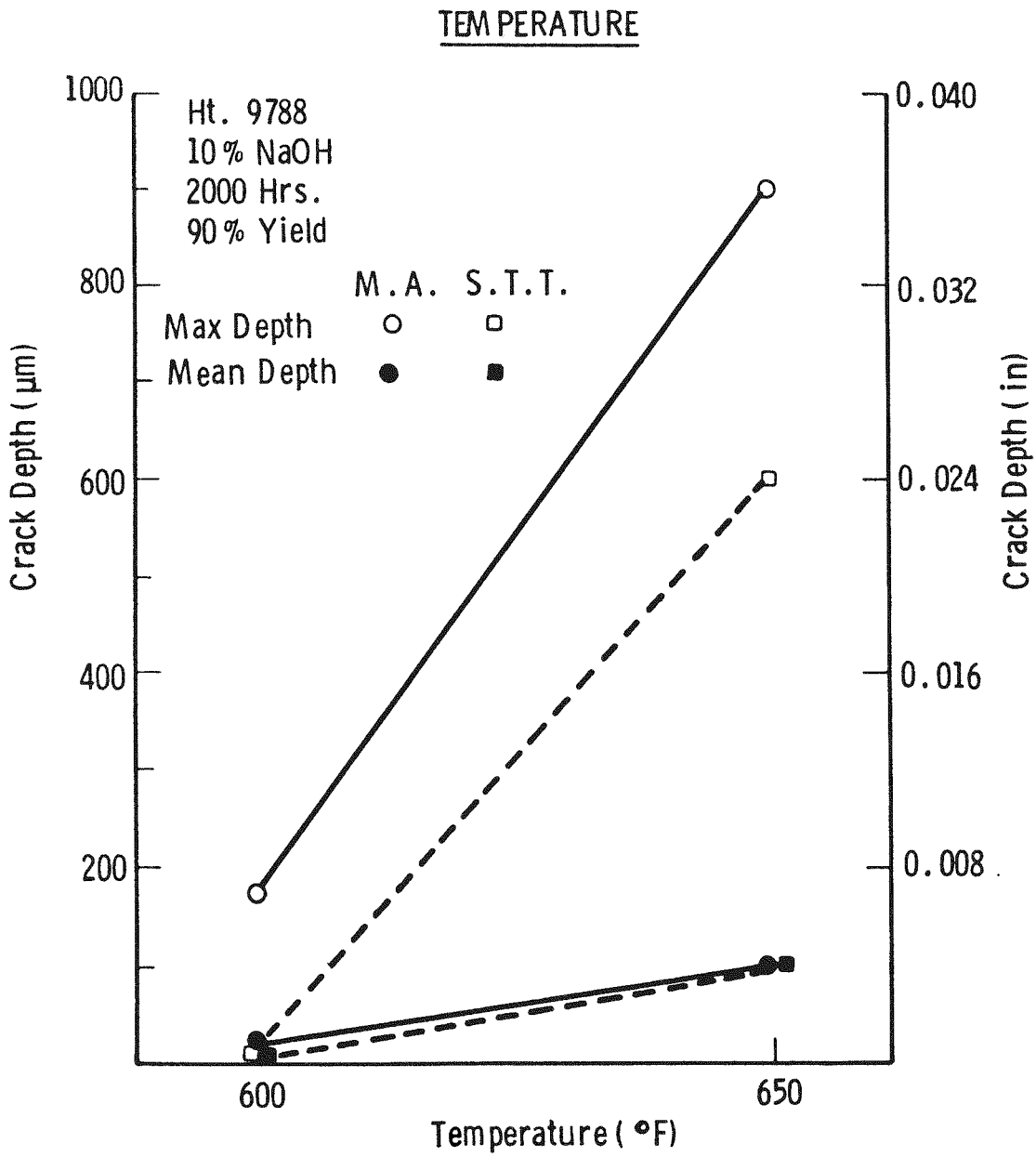

Figure 4-41. The effect of temperature on the SCC (maximum depth) and IGA (mean depth) susceptibility of mill-annealed and special thermally treated Alloy 600 (Reference 5).

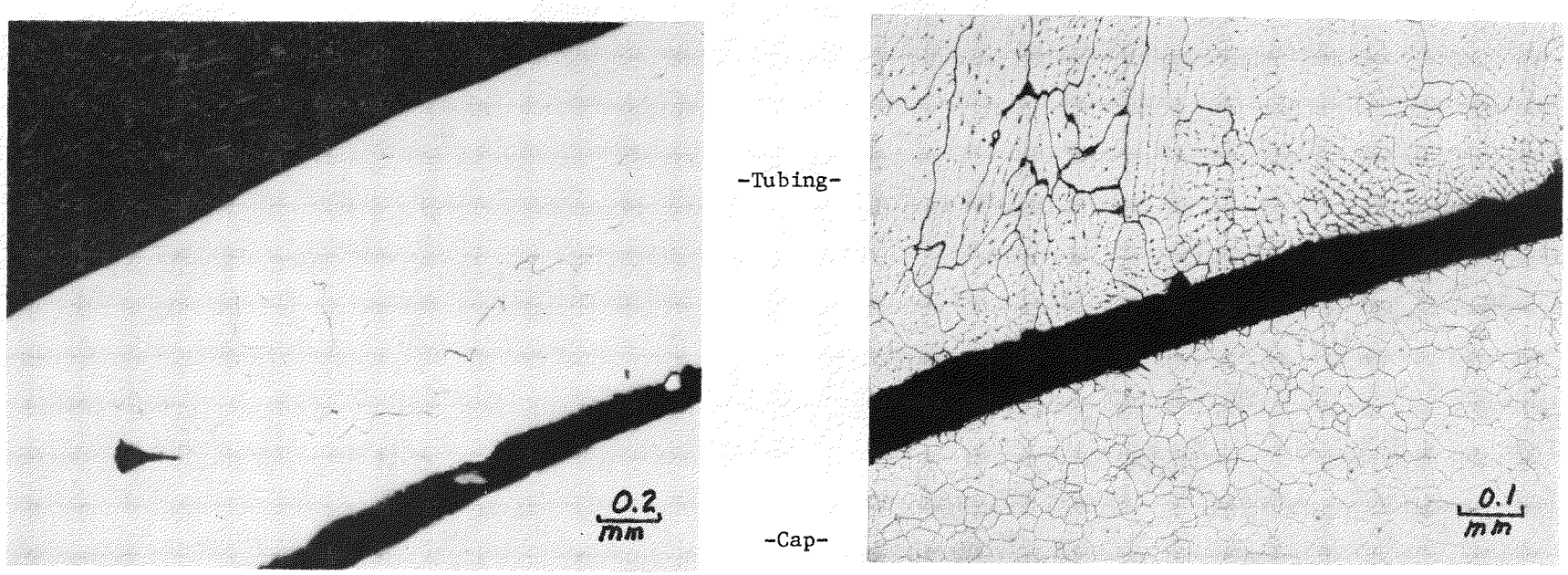

As-polished

Etched

Figure 4-42. Alloy 600 weld metal cracking in capsule NG-12 as observed at a number of locations in the top weld. Similar SCC was observed in the bottom weld. Etchant: electrolytic 10% H_3PO_4.

procedures, such as use of nickel-201 (decarburized) filler metal, maintenance of an inert gas welding atmosphere, and thickening the weld by using copious amounts of filler metal, were effective in lengthening exposure times by minimizing leaks at welds.

Many of the capsules in the proof test series contained flats on the OD surface and A508, low alloy, steel slugs tack welded to the bottom cap. An evaluation of these test devices and a recommendation against their use in the larger matrix of capsule tests was made based on their performance in the preliminary proof test series.

Figure 4-43 shows the location of the flat on the OD surface on some of the capsules in these series. The machining of the 0.029 inch deep surface left a wall thickness of ~0.026 inch at the center of the flat. Figures 4-44 and 4-45 are optical photographs of sectioned, mounted, and polished surfaces of a capsule which was exposed to 50% NaOH at 650°F for 77 days. The section of the tube containing the flat was sectioned longitudinally and then flattened to strain the tube ID beneath the flat. Transverse sections were then made as shown in Figure 4-44. These transverse sections showed (Figure 4-45) that the incidence of uniform IGA remained unchanged as the wall thickness at the flat decreased (right to left). However, the depth of SCC increased steadily as the wall thickness decreased. These results showed that the use of flats would do little to promote IGA and would significantly increase the incidence of SCC. In so doing, capsule lifetime would be significantly reduced.

The use of flats with lower caustic concentrations is even less desirable. Figure 4-46 shows a longitudinal section of the tube region containing the flat (a) and transverse sections through the flat (b and c) of a capsule which contained 3% NaOH. This capsule failed after 24 days at 650°F. The rupture at the flat was due to SCC. It is not known whether the increased severity of cracking in capsules containing <50% NaOH solutions is due to the more aggressive nature of the more dilute solutions (Figure 4-40), to the resultingly higher initial hoop stresses produced by the vapor pressure (6) of the caustic solutions (Figure 4-47), or to a combination of the two. Although the stress distribution resulting from a flat machined on the OD surface is complex, the calculated values shown in Figure 4-47 were approximated by assuming a uniform cylindrical wall reduction of 0.029 inches.

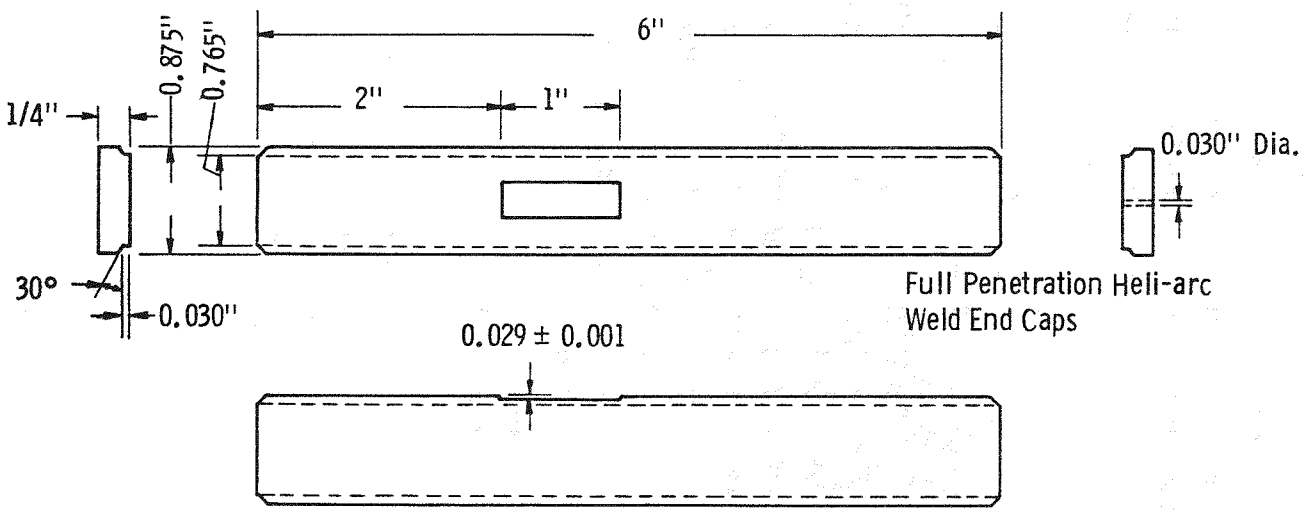

Figure 4-43. Alloy 600 capsule

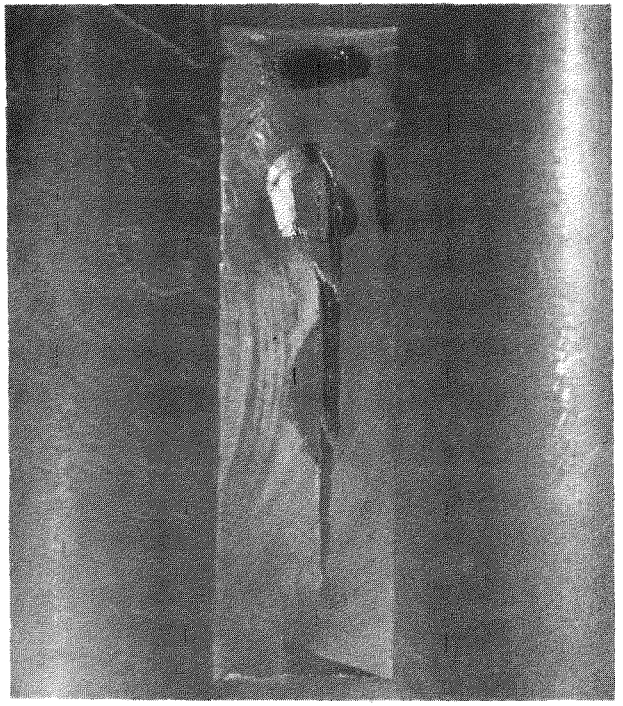

O.D.

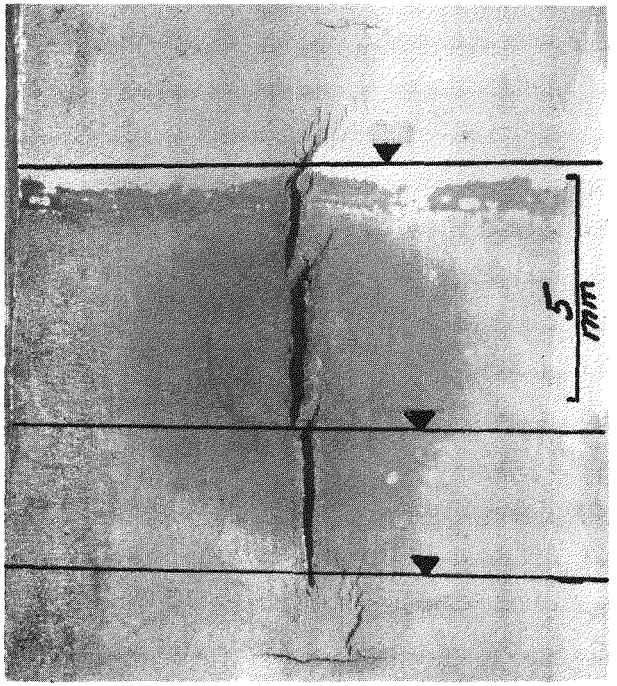

I.D.

Figure 4-44. OD and ID at flat location of capsule NG-12 after exposure and flattening to strain ID in tension. ▼ designates surface studied metallographically.

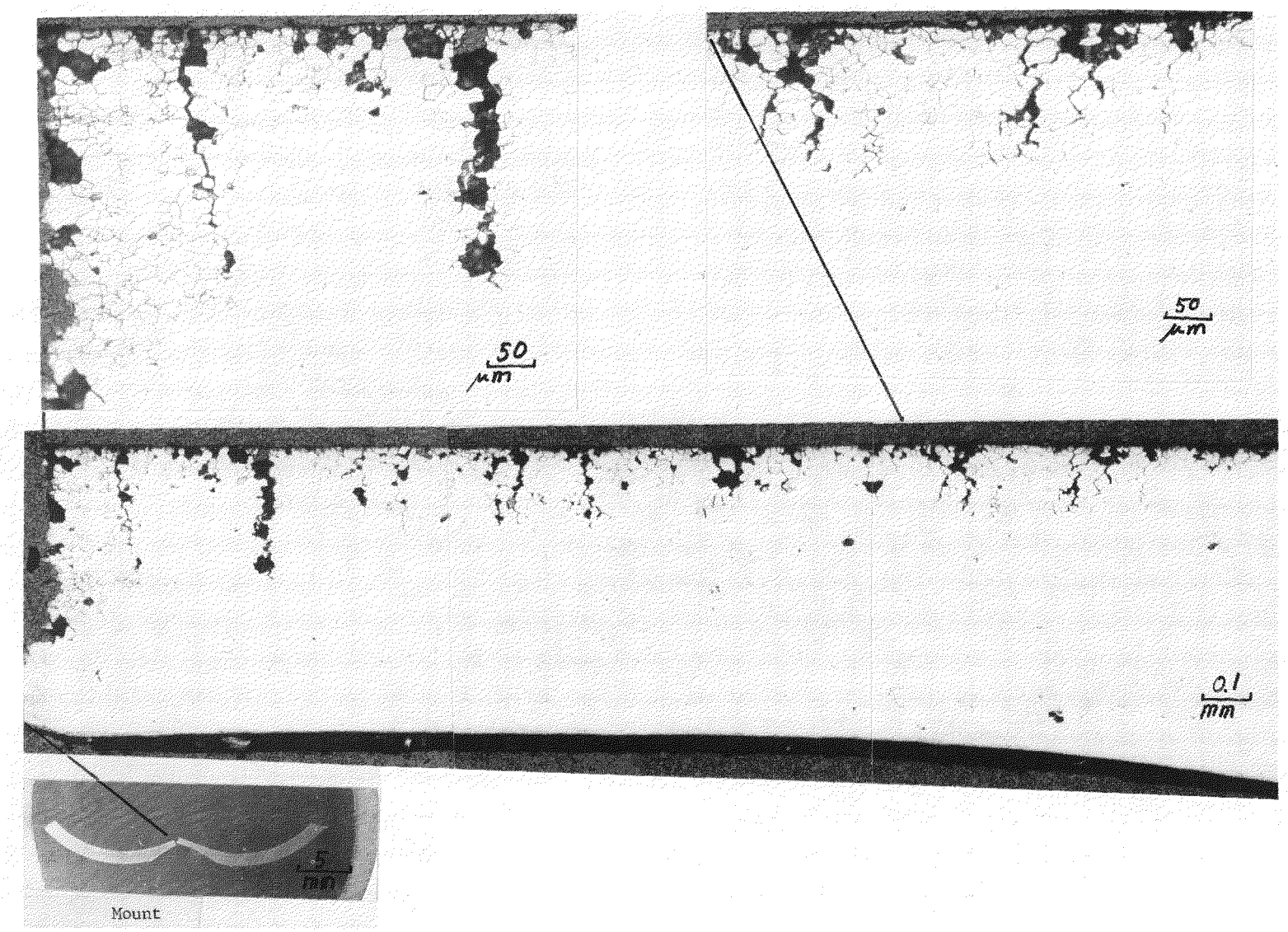

Figure 4-45. Transverse cross section through the flattened flat and in the vapor for capsule NG-12. Electrolytic phosphoric acid etch.

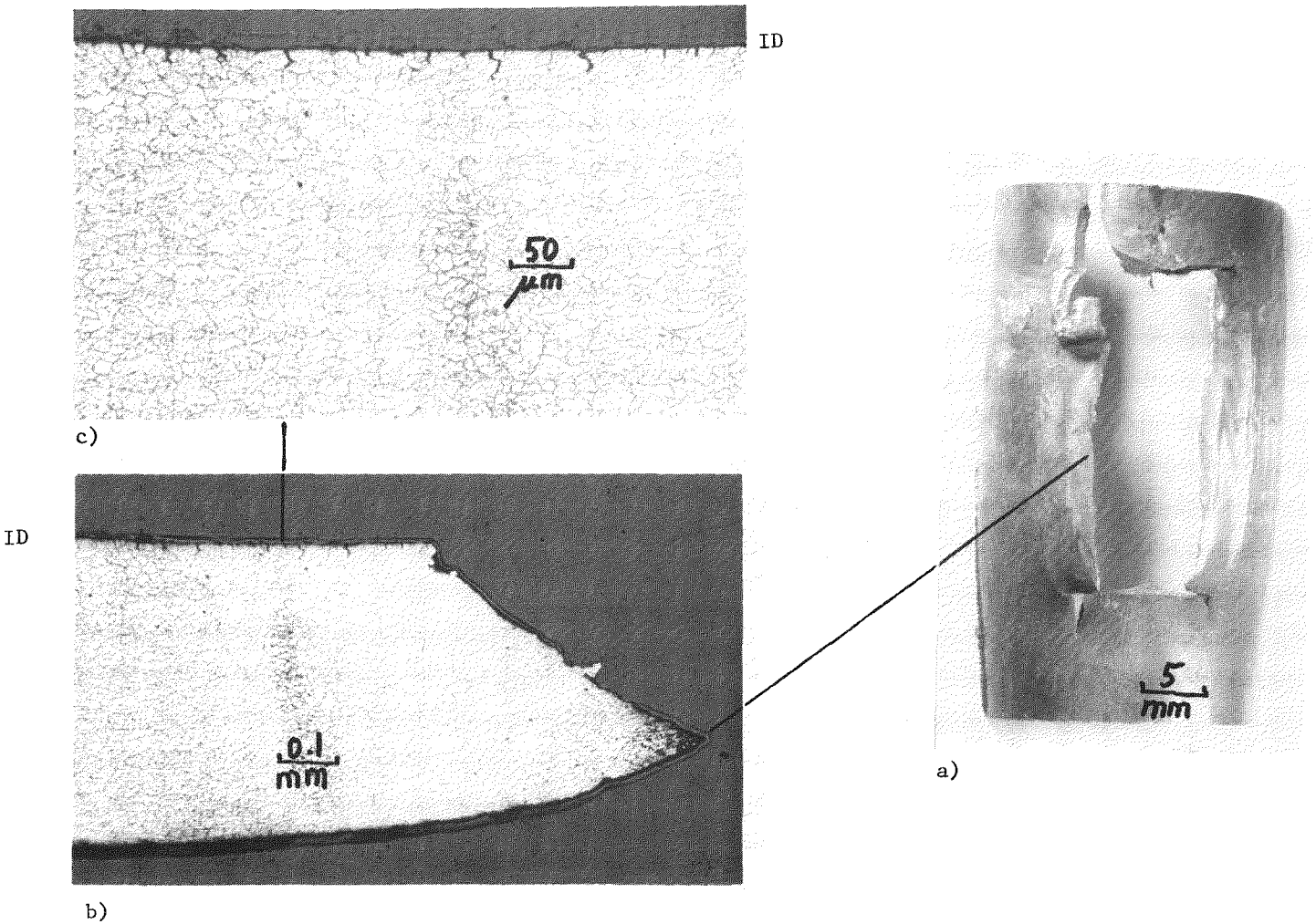

Figure 4-46. Capsule C-8: a) Blow out at flat, and (b and c) shallow SCC detected only at flat. Similar results were observed for capsule C-9. Electrolytic phosphoric acid etch.

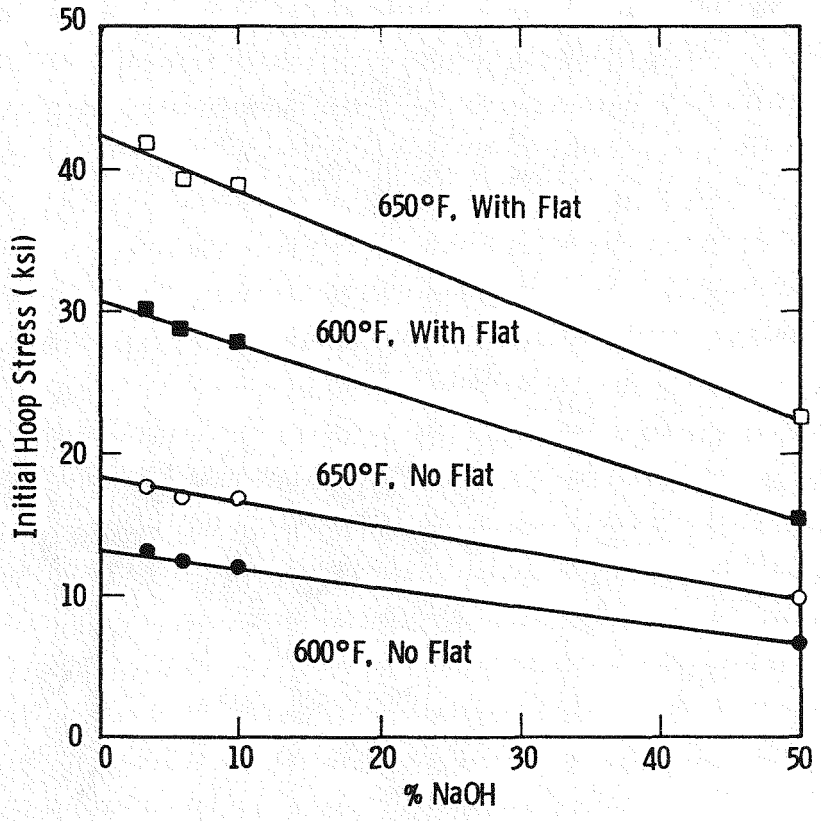

Figure 4-47. Calculated initial hopp stress valves resulting from the vapor pressure of various NaOH solutions contained within isothermal capsules with and without OD flats

Although A508 low alloy carbon steel slugs were used in some of the capsules in the proof test series to provide a galvanic couple and, therefore, simulate the plant tube-tubesheet materials combination, their use in the more extensive matrix of tests to evaluate effects of various additives was not pursued. Carbon steels are known to react rapidly with caustic according to the following reaction:

$$Fe + 2NaOH \rightarrow Na_2FeO_2 + H_2 \quad .$$

Such a reaction would have two detrimental effects in a non-refreshed, capsule environment; it would decrease the caustic concentration as the reaction proceeds, and it would increase the internal stresses by producing a hydrogen overpressure. The net effect of both these effects would be to produce a more aggressive SCC environment.

Based on the above considerations the following joint Westinghouse/EPRI decisions were made concerning all testing to follow the proof tests.

- 40% NaOH + 10% KOH solutions at 650°F were selected as the reference environment for evaluating the effect of contaminants on the susceptibility of mill annealed Alloy 600 to IGA.
- Levels of the various contaminants (see Table 4-8) were increased to levels judged to be sufficiently high to produce saturated solutions of most species.
- A 25 second, 1300 to 1400°F post-weld stress relief anneal of welds and adjacent heat affected areas was performed using induction heating equipment to further minimize the potential for stress corrosion cracking in these areas.
- Flats were not to be used on Task 300 capsules.
- Only a limited number of capsules (four) would contain A508 slugs (see Table 4-8).

Accelerated IGA Adjacent to Welds. In performing the metallographic examination of capsules from the proof test series, each capsule was cut, as previously described in Section 3, into three specimens, two cut at 45° to the capsule axis (one through the top weld and one through the bottom weld), and a one-inch long longitudinal section through that section of the tube which spanned the liquid vapor interface.

Figure 4-48 is a typical example of one of the angled cuts through the bottom weld. Enlargements of areas 3, 4, and 5 of this capsule (which was exposed to 50%

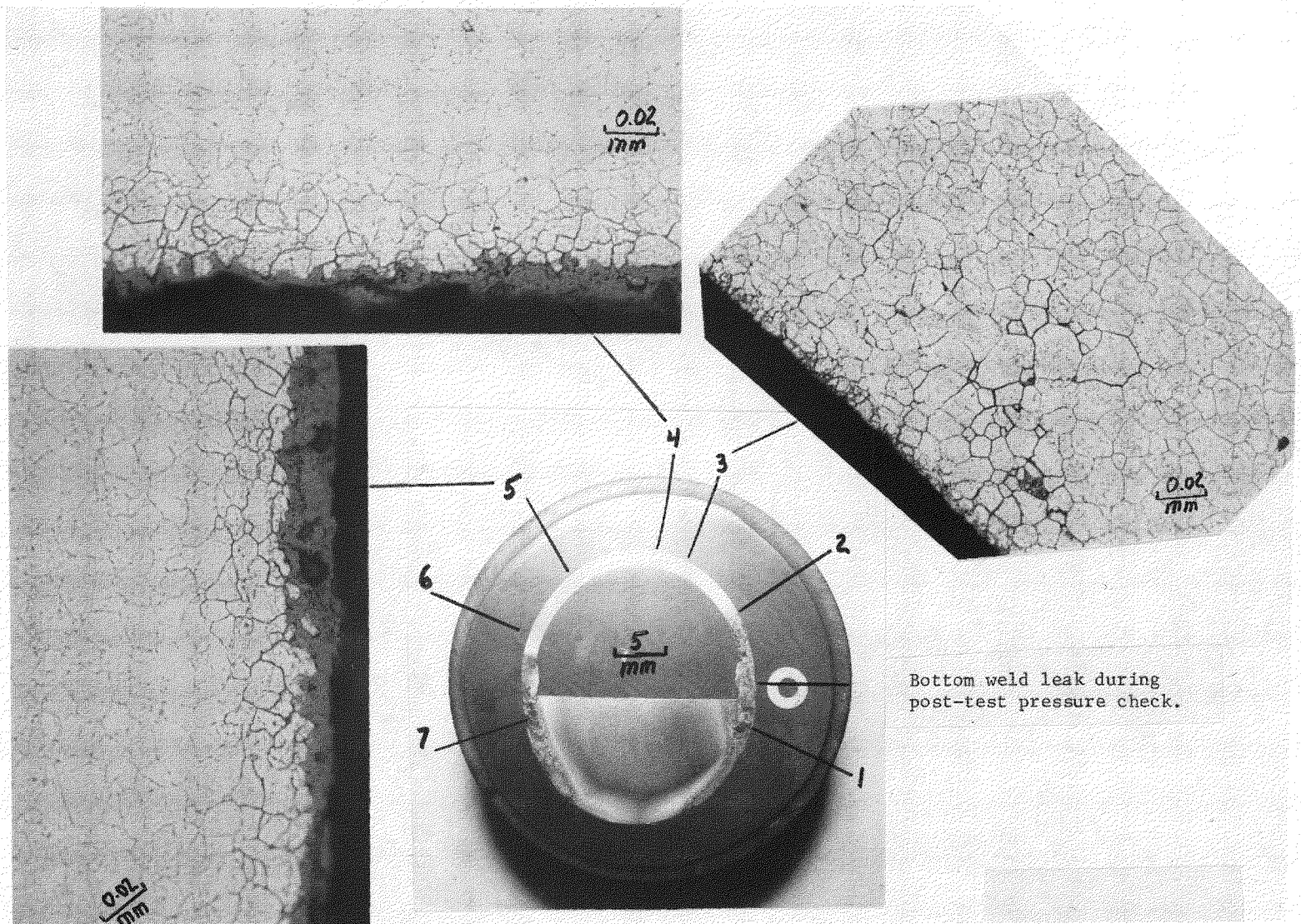

Figure 4-48. Specimen from capsule NG-14 polished on plane at 45° to capsule axis through leak indication (center). IGA at areas 3 through 5 is shown. Electrolytic phosphoric acid etch.

NaOH + 4% Na_2SO_4 at 650°F for 77 days) shows the ~0.025 mm (1 mil) IGA characteristic of the reference environment alone. No effect on IGA was attributed to the sulfate addition. Figures 4-49 and 4-50 show enlargements of regions at areas 7 and 6, respectively, of Figure 4-48. These figures show the region where the tube fused to the end cap, which is characterized by many cracks, the molten region, characterized by the dendritic structure, and the heat affected zone, characterized by large recrystallized grains. Approximately one wall thickness beyond the heat affected zone, a localized region of accelerated IGA and through wall SCC was observed. An enlargement of this region is shown in Figure 4-51. The extent of IGA in this region far exceeds the 1 mil of uniform IGA observed elsewhere in this capsule. As with the uniform IGA observed in this capsule, the localized attack cannot be attributed to the 4% Na_2SO_4 addition, since the same phenomenon was observed in other capsules run with the reference environment alone.

Another capsule which also showed localized IGA and which had run for 90 days at 650°F with 50% NaOH + 4% Na_2SO_4 was studied more extensively to attempt to understand the factors contributing to the localized attack. A longitudinal cross section through the bottom weld showed considerably more IGA localized at ~1 wall thickness above the weld than occurred elsewhere on the wetted surface of the capsule ID. This IGA penetrated 0.43 mm from the ID at ~1.7 mm above the weld and decreased to only 0.01 mm penetration at 7.8 mm above the weld, Figures 4-52 and 4-53.

Variables considered to be of possible importance in this localized attack are the metallurgical structure in the heat affected region and applied stress resulting from the combined influence of residual stress, end effects, and internal pressure. The metallurgical structure immediately behind the localized IGA is similar to that further away as observed with the SEM, Figure 4-53. To a large extent no difference is shown in the transmission electron micrographs, Figure 4-54. Some grain boundary to grain boundary variation in carbide distribtuion was noted, but overall the difference between material close to and far removed from the heat affected zone was not considered to be significant. The absence of interconnected grain boundary carbides is evidence that the alloy is not sensitized.

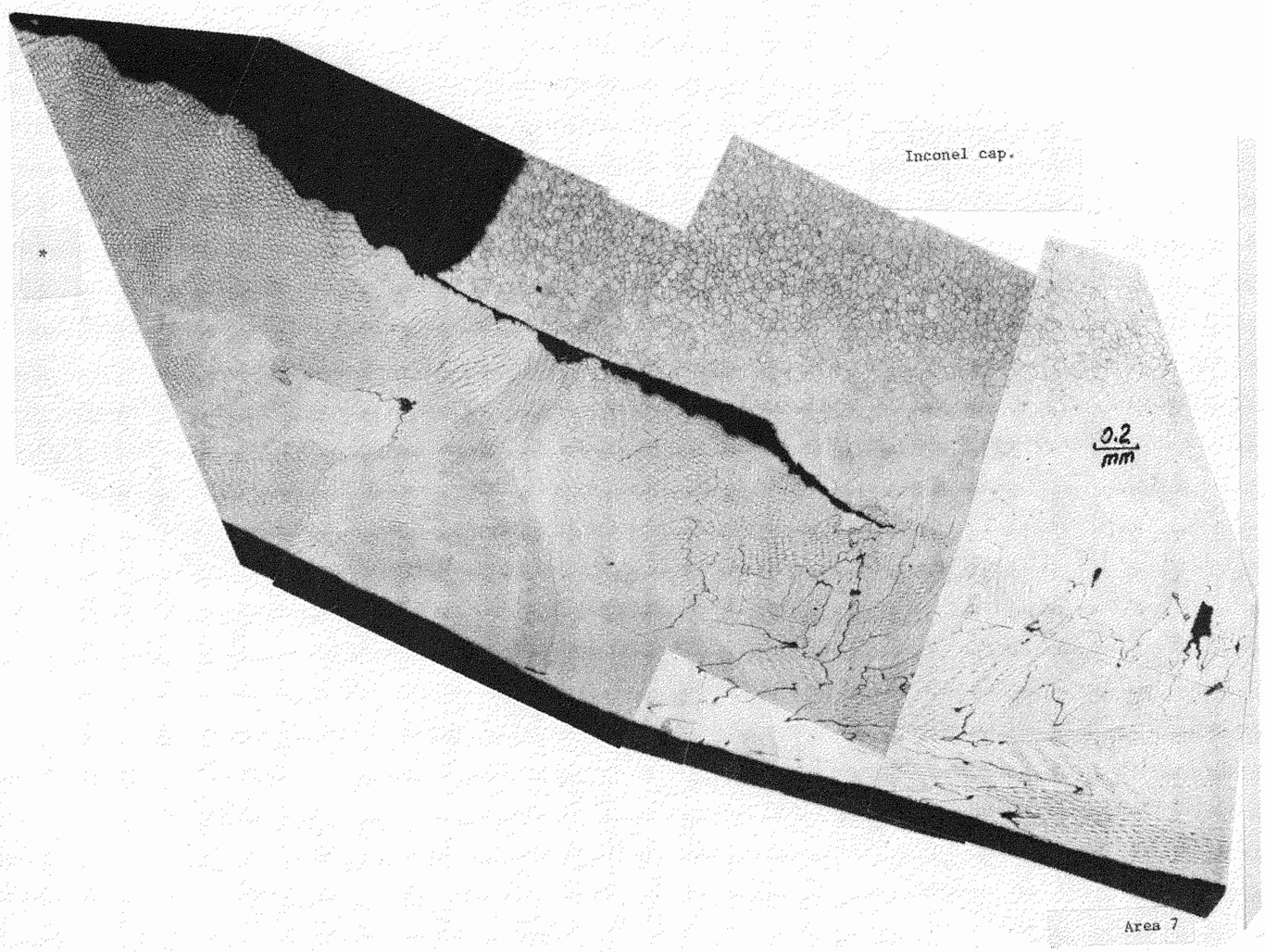

Figure 4-49. Area 7 of capsule NG-14 (Figure 4-48)
*Designates matching surface on Figure 4-50. Electrolytic phosphoric acid etch.

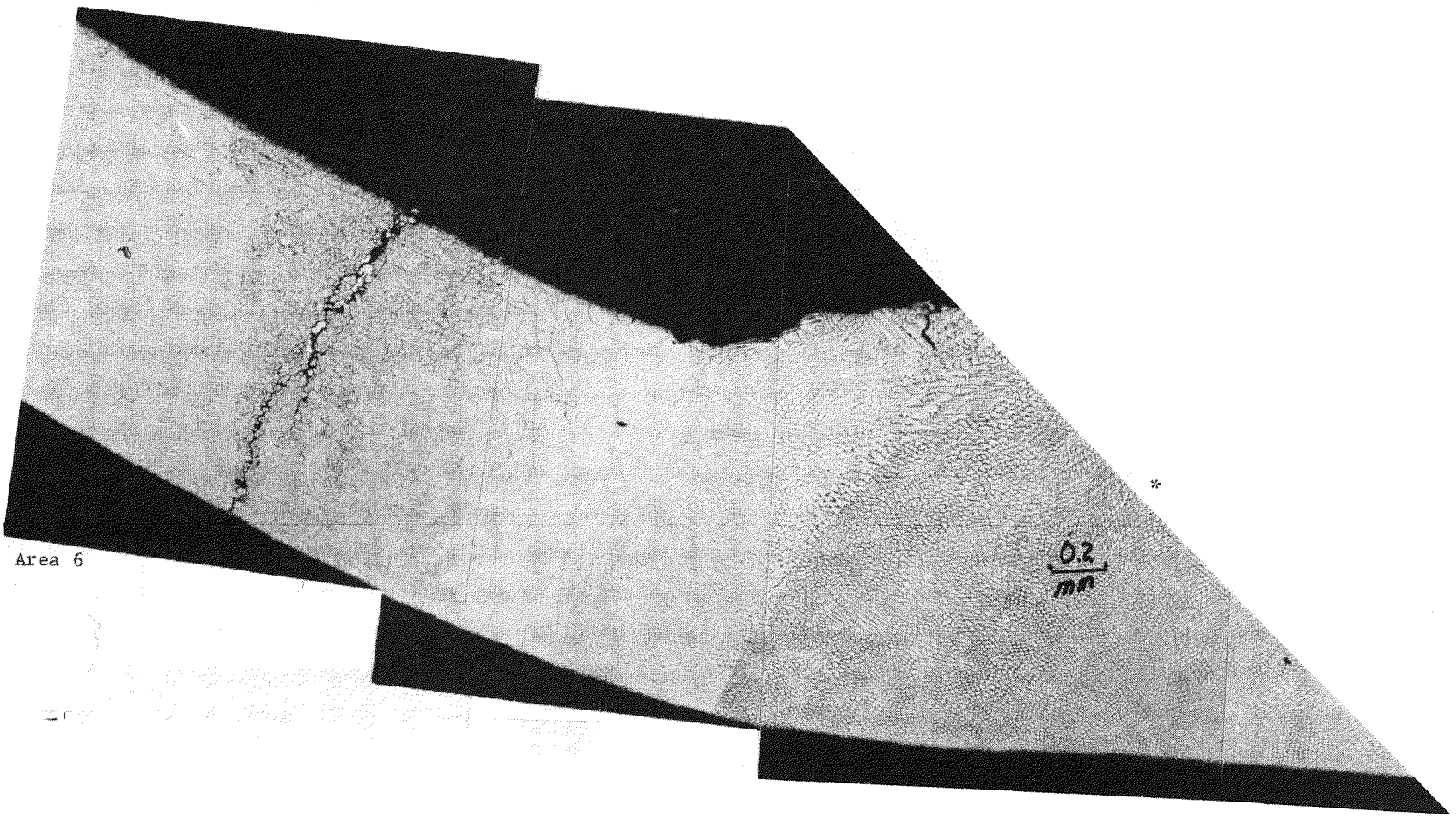

Figure 4-50. Area 6 of capsule NG-14 (Figure 4-48).
* Designates matching surface on Figure 4-49. Electrolytic phosphoric acid etch.

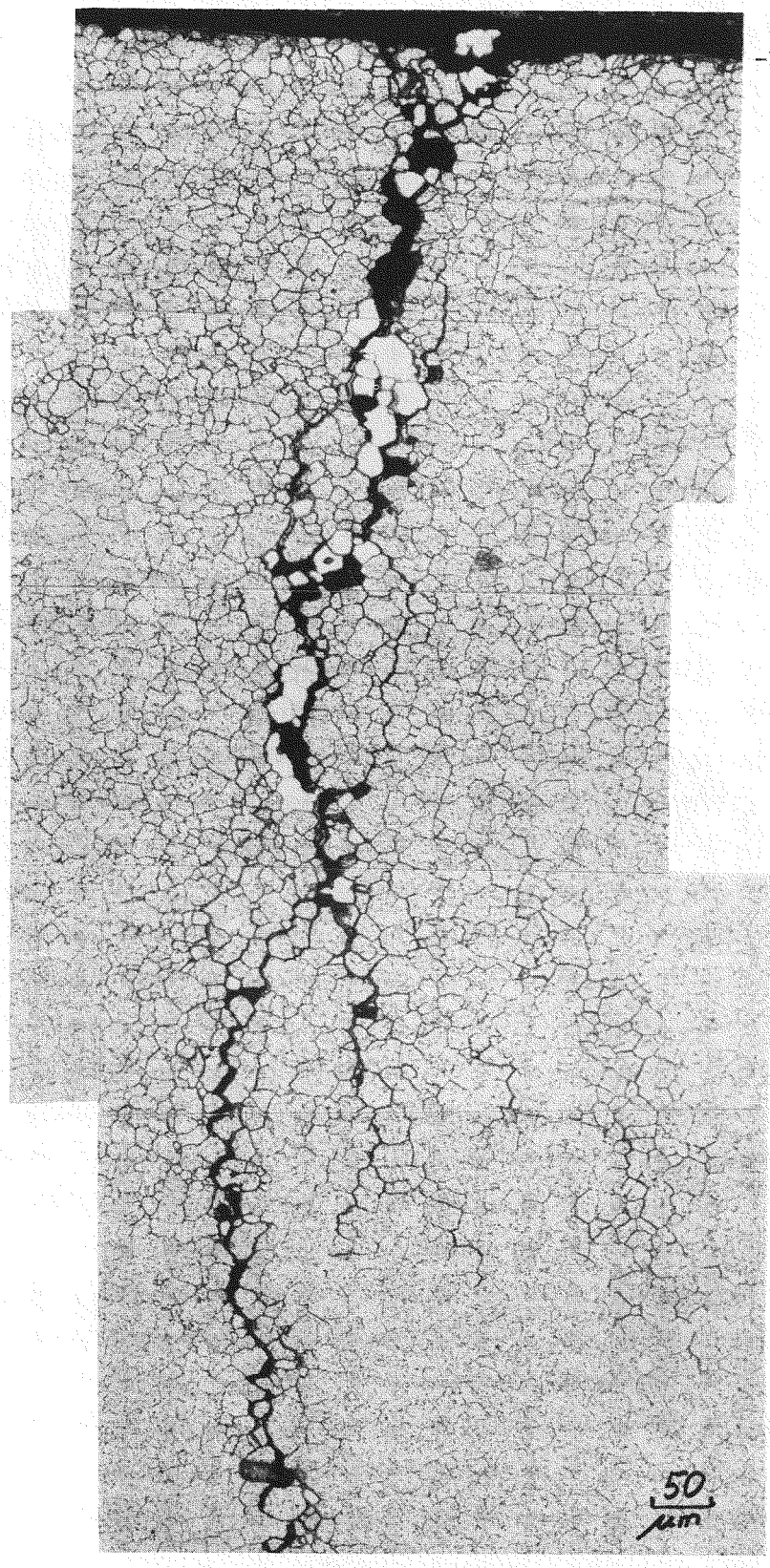

Figure 4-51. IGA near through wall crack in Figure 4-50. Electrolytic phosphoric acid etch.

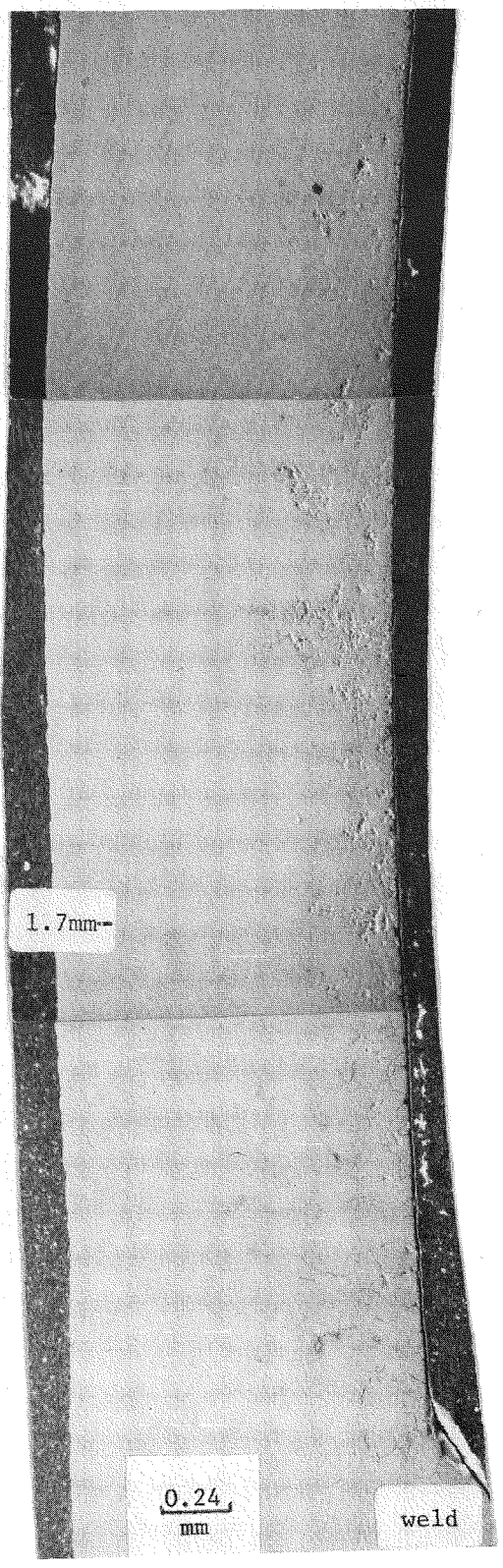

Figure 4-52. Longitudinal cross section through bottom of a capsule that had run for 90 days at 343°C and contained 50% NaOH + 4% Na_2SO_4. SEM studies were performed on the ID 1.7 mm and 7.8 mm above the bottom weld. Etchant: 5% bromine in methanol.

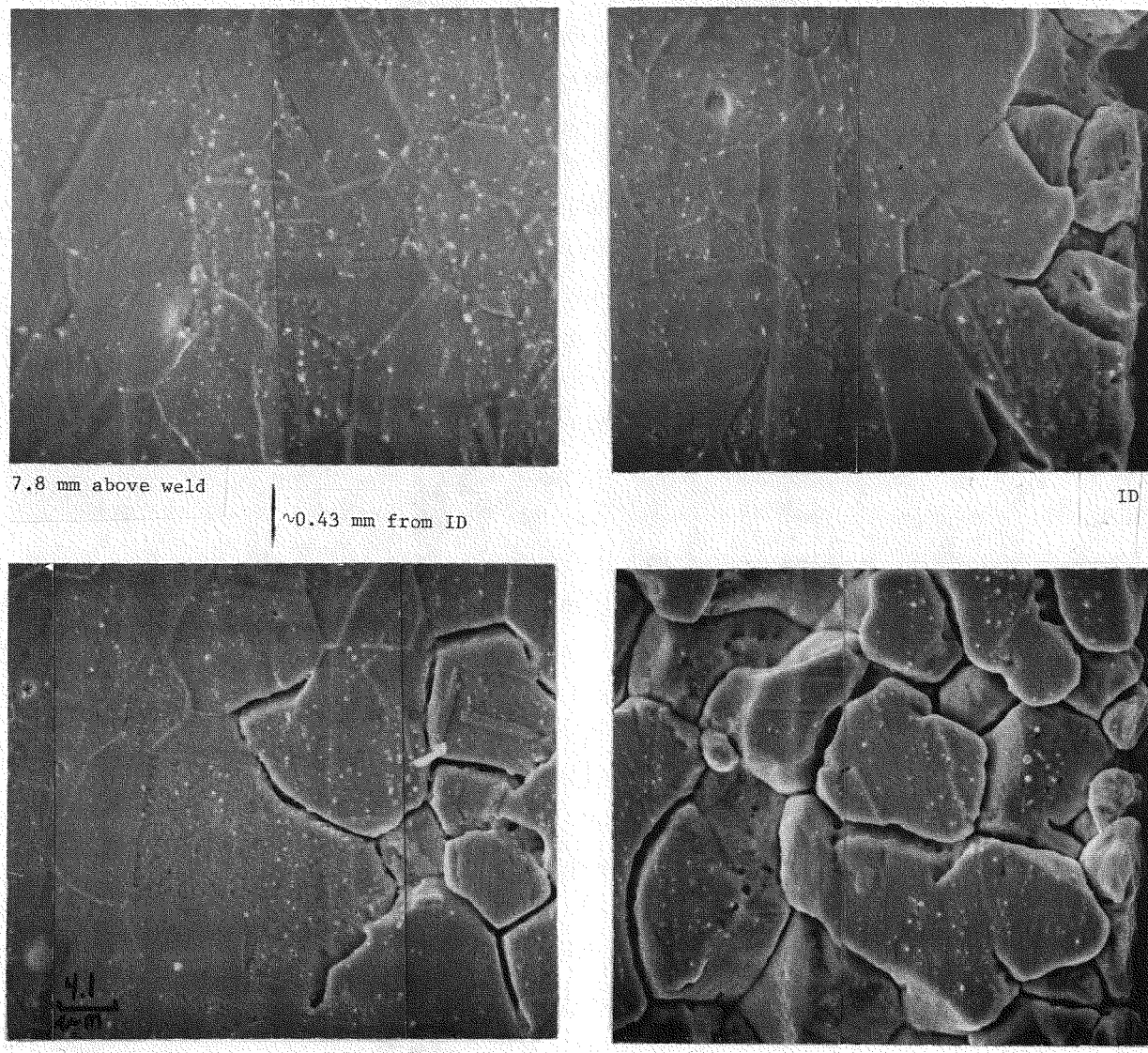

Figure 4-53. SEM photographs at the ID (right) and at ~0.43 mm (left) from the ID at distances of 1.7 mm (bottom) and 7.8 mm (top) from the bottom weld on longitudinal section of the bottom weld of the capsule.

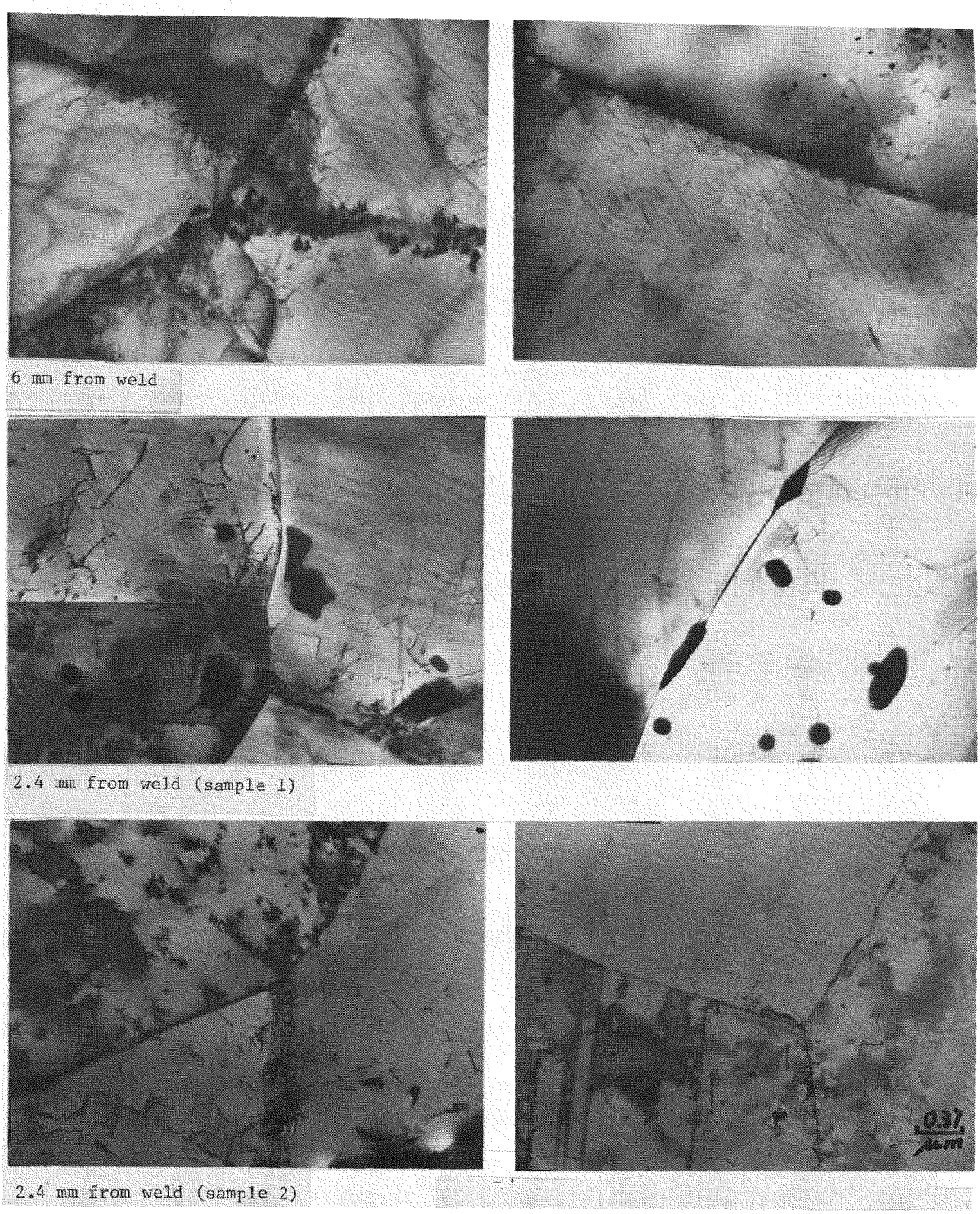

Figure 4-54. TEM photographs (mid-wall) at 2.4 mm (bottom and middle) and 6 mm (top) from the bottom weld of the capsule.

An attempt was made to study the composition of the grain boundaries at these two locations with Auger electron spectroscopy. Specimens were hydrogen charged in a sulfuric acid + sodium arsenite solution for 4 hours, held in a vacuum in the Auger chamber overnight, and strained to fracture in the morning. Fracture surfaces at both locations were partially intergranular, Figure 4-55. The Auger analyses for both areas were similar, Table 4-14. Because the grain size was fine and the fracture was mixed mode, the Auger analyses were from both intergranular and transgranular surfaces. This fact, in part, may be responsible for the similarity of results. Additional work is required to evaluate the effect of residual stress, strain, and microstructural variations on the IGA susceptibility of mill annealed Alloy 600.

Testing to Evaluate the Effect of Additives to the Caustic Reference Environment. The results of metallographic examinations of specimens prepared from capsules tested in the environments identified in Table 4-8 are presented in Table 4-15. The depth of uniform IGA measured at four locations on the three specimens prepared from each capsule is presented in this tabulation. The depth of uniform IGA at the top and bottom of the capsule was measured on the specimens cut at 45^{o} to the capsule axis (see Section 3). The measurements on these specimens were made at least 1 cm away from the weld area to preclude the possibility of confusion with the accelerated, localized regions of IGA seen next to the weld areas. Two measurements of uniform IGA were made on the specimen which contained the liquid-vapor transition region; one was in the region wetted by vapor, and one in the region wetted by liquid. The capsule environment, the capsule number (the first number of which corresponds to the test number in Table 4-8), the exposure time, and the location of leak, when one occurred, are also contained in the tabulation.

The test data in this tabulation are in three distinct groups. Capsule 1 contained the reference environment, Capsules 2 through 8 contained selected additives without the caustic addition, and Capsules 10 through 22 contained both caustic and additives. In the reference environment, 0.025 to 0.050 mm (1-2 mils) of uniform IGA was produced in the ~90 days of exposure achieved before the capsule began to leak.

In examining the data for capsules 2 through 8, it is of interest to note that some IGA was produced in these environments, even without 50% caustic additions.

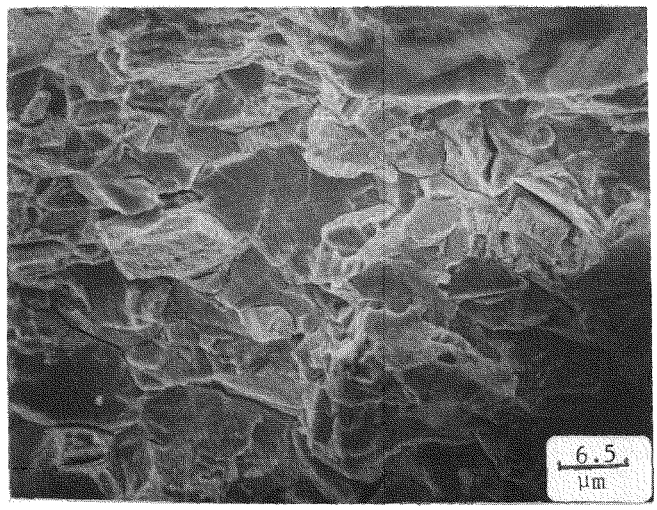

∿25 mm from weld

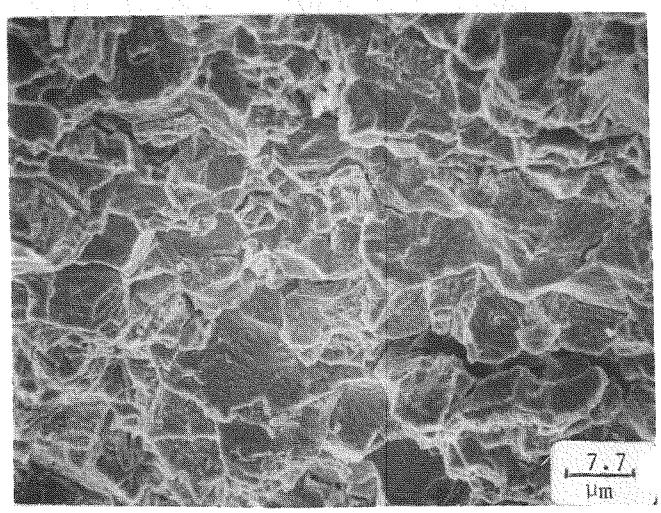

2.8 mm from weld

Figure 4-55. Fractographs of Auger specimens charged with hydrogen and pulled in tension in the Auger vacuum chamber at 2.8 mm (bottom) and at ∿25 mm from the weld (top)

Table 4-14

AES FRACTURE SURFACE ANALYSES 2.8 mm AND 25 mm FROM WELD (ANALYZED AREA WAS 20 μm x 20 μm)

	2.8 mm			25 mm		
Element	Area 1	Area 2	Area 3	Area 4	Area 5	Area 6
S	0.76[a]	1.60	2.98	0	2.80	1.26
C	6.16	13.19	16.02	7.69	17.39	15.32
O	8.30	7.38	8.18	8.90	9.10	8.76
Cr	14.26	13.03	11.39	14.23	13.32	13.84
Fe	7.98	6.92	6.46	7.61	6.72	6.62
Ni	60.21	53.84	50.34	56.35	48.03	52.59
Ti	0.71	0.83	0.65	0.82	0.64	0.66
P	0.26	0.31	0.24	0.60	0.16	0.12
B	1.34	2.90	3.75	3.79	1.85	0.18

[a]Atomic percent

Table 4-15

IGA AND/OR SCC DEPTHS IN mm FOR SUBTASK 302-B CAPSULES
EXPOSED AT 650°F TO 40% NaOH + 10% KOH PLUS DESIGNATED ADDITION

Capsule No.	% Addition	Exposure Time Days	Leak Location[a]	Depth of Uniform IGA (mm) Top of Capsule	Liquid-Vapor Transition Vapor	Liquid-Vapor Transition Liquid	Bottom of Capsule
1-2	0	84-91	B	0.025	0.05	0.05[d]	0.035
2-1	12-$MgSO_4$[b]	126-133	B	0.00	0.005	0.005	0.005
3-1	12-Na_2SO_4[b]	180	N	0.005	0.005	0.010	0.010
4-1	12-SiO_2[b]	180	N	0.00	0.00	0.00	0.00
5-1	12-$NaCO_3$[b]	35-42	T	0.015	0.015	0.020	0.005
6-1	3-$NaNO_3$+ 3-$CaSO_4$+ 3-SiO_2+ 3-NaCl+ 3-Na_2HPO_4	180	N	0.010	0.010	0.010	0.010
7-1	12-$NaNO_3$[b]	180	N	0.00	0.00	0.00	0.00
8-1	12-NaF[b]	28-35	B	0.00	0.005	0.005	0.00
10-1	12-Na_2SO_4	119-126	B	0.05[d]	0.035[d]	0.015[d]	0.06[d]
10-2[c]	12-Na_2SO_4	180	N	0.00	0.00	0.00	--
11-1	12-$CaSO_4$	70-77	B	0.015	0.015	0.015	0.015
12-1	12-SiO_2	14-21	B	0.010	0.010	0.010	0.010
13-2	12-$MgSO_4$	77-84	B	0.015[d] SCC-0.13	0.010[d]	0.015[d]	0.020[d]
14-1	12-Al	63-70	U	0.010	0.020	0.020	0.010
15-2	12-NaCl	180	N	0.035[d]	0.015[d]	0.010[d]	0.050[d]
16-1	12-Na_2HPO_4	77-84	B	0.030[d]	0.025[d]	0.020[d]	0.035[d]
16-2[c]	12-Na_2HPO_4	180	N	0.00	0.00	0.00	--
17-1	3-$NaNO_3$+ 3-$CaSO_4$+ 3-SiO_2+ 3-NaCl+ 3-Na_2HPO_4	180	N	0.01	0.00	0.00	0.00
17-2[c]	3-Na_2HPO_4	180	N	0.00	0.00	0.00	--

(continued)

Table 4-15 (continued)

Capsule No.	% Addition	Exposure Time Days	Leak Location[a]	Depth of Uniform IGA (mm) Top of Capsule	Liquid-Vapor Transition Vapor	Liquid-Vapor Transition Liquid	Bottom of Capsule
18-2	12-$NaNO_3$	180	N	0.00[f]	0.00[e]	0.00[e]	0.00[e]
19-1	7-CuO + 3-ZnO	147-161	T	0.00[f]	0.00	0.00	0.00[f]
20-1	12-Na_2CO_3	180	N	0.07[d]	0.035[d]	0.035[d]	0.09
20-2[c]	12-Na_2CO_3	180	N	0.00[d]	0.00	0.00	--
21-1	12-Cr_2O_3	92-98	B	0.180[d]	0.140[d]	0.175[d]	0.190[d]
22-1	12-NaF	63-70	U	0.02[d]	0.035[d]	0.025[d]	0.04[d]
22-2	12-NaF	180	N	0.07[d]	0.030[d]	0.030[d]	0.07[d]

[a]Location of capsule leakage determined by gas pressurization: B-Bottom weld; T-Top weld; F-Fitting; U-Unknown; N-None.

[b]No caustic was added to this capsule.

[c]Contained A508 slugs.

[d]Significant grain dropping.

[e]No IGA or SCC; however, observation of localized corrosion to a depth of 0.11-0.12 mm.

[f]Adherent deposits on surface.

The magnitude of the IGA was, generally, 1/5 to 1/10 that produced in the reference caustic environment. Environments containing SO_4^{2-} (Capsules 2, 3, and 6) showed minor intergranular involvement to a depth of 0.005 to 0.010 mm (0.2 to 0.4 mil). Shallow intergranular penetrations of only 0.005 mm (0.2 mil) resulted from exposure to the 12% NaF environment (Capsule 8). No attack was found in capsules containing 12% SiO_2 (Capsule 4) and 12% $NaNO_3$ (Capsule 7). The maximum amount of IGA found in a capsule without caustic additions was produced by exposure to 12% Na_2CO_3. The 0.005 to 0.020 mm (0.2 to 0.8 mils) of IGA was produced in the ~40 days of exposure prior to a leak developing in the capsule.

Of the additives to the reference caustic environment, several did not increase the severity of the observed IGA. Sodium, calcium, and magnesium sulfates (Capsules 10, 11, and 13), aluminum (Capsule 14), sodium chloride, sodium phosphate and sodium fluoride (Capsules 15, 16, and 22) additions to the reference environment did not promote IGA. Silica additions to caustic may have shown slightly less tendency toward IGA. This environment was also difficult to contain in capsules. Both capsules leaked during the first three weeks of exposure. These observations on silica additives are consistent with the C-ring and electrochemistry results (Subtasks 302A and 301).

As was observed in the results of Subtasks 301 and 302A, sodium nitrate additions (Capsule 18) inhibited IGA but enhanced general corrosion. Figure 4-56 shows deep localized penetrations produced in the caustic + nitrate environment. Such deep local penetrations were not observed on specimens from the electrochemistry or C-ring tests which were exposed to this environment.

Figure 4-56 also shows carbide banding which is present to some degree in all tubing specimens and which occurs most frequently near the tubing ID. Although the variation in intensity of the banding in this specimen may have been enhanced by the etching process, it shows how the banding can vary. Both regions shown in this figure are from a single specimen approximately one inch in length. There is no indication that the banding has any effect on the corrosion phenomena studied in this program. In Figure 4-56 the localized penetrations crossed the carbide bands and in Figure 4-58, a matrix of uniform IGA overlays similar carbide banding.

No IGA was observed on specimens from Capsule 19, in which copper and zinc oxides were the additives. Figure 4-57 shows adherent deposits, presumed to contain

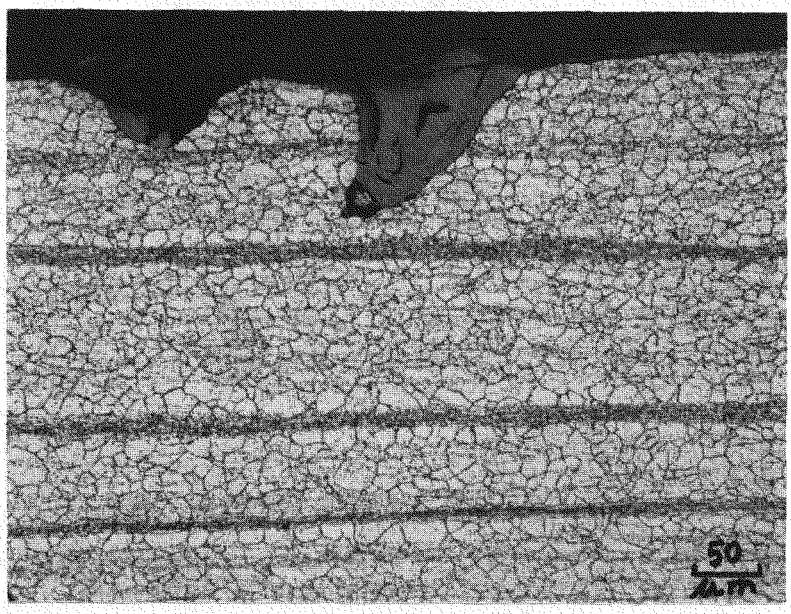

Vapor

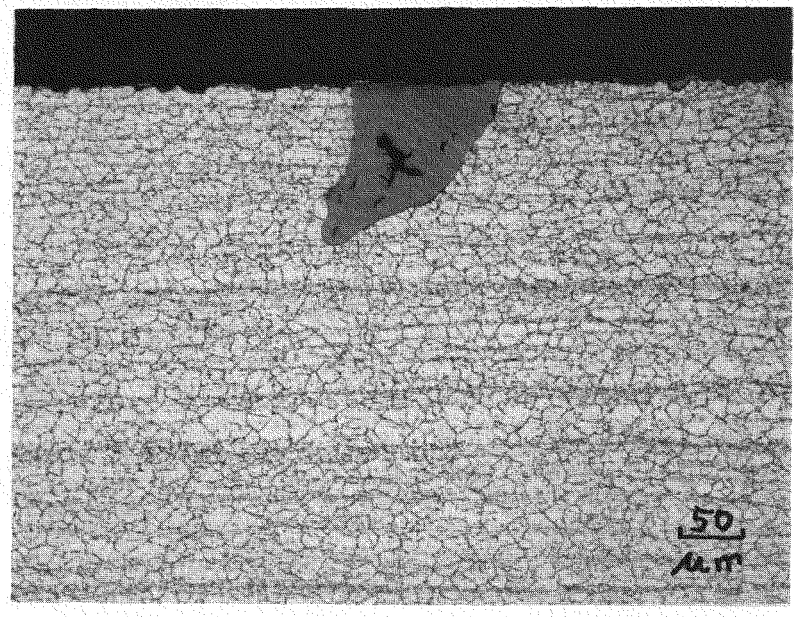

Liquid

Figure 4-56. Localized penetrations on the ID to a depth of 0.1 mm at the vapor-liquid interface of Capsule 18-2 (40% NaOH + 10% KOH + 12% $NaNO_3$, 180 days and 650°F). Electrolytic phosphoric acid etch.

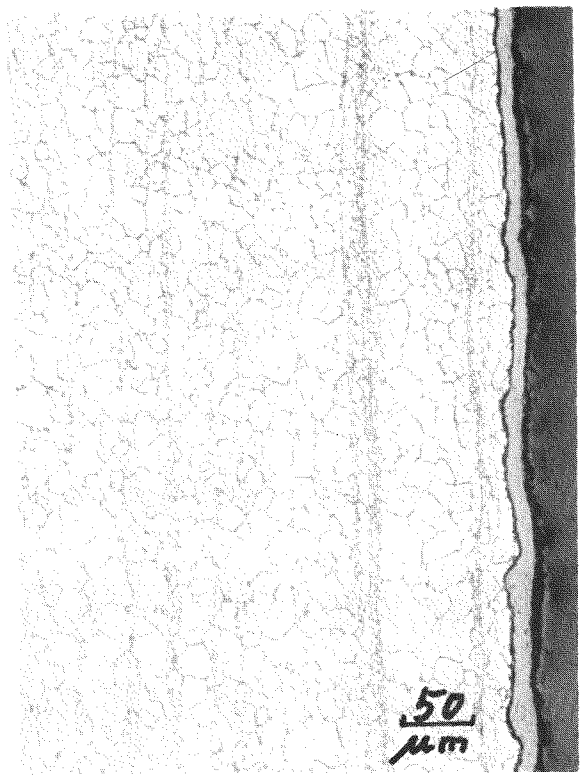

Figure 4-57. Adherent deposits on ID surfaces at lower liquid position for Capsule 19-1 run with 40% NaOH + 10% KOH + 7% CuO + 3% ZnO at 650°F for 141-161 days. Electrolyte phosphoric acid etch.

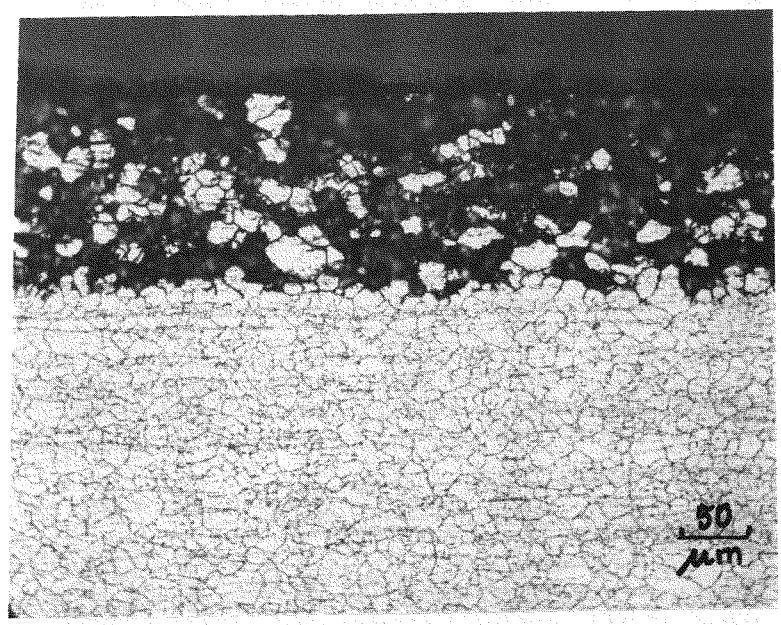

Vapor

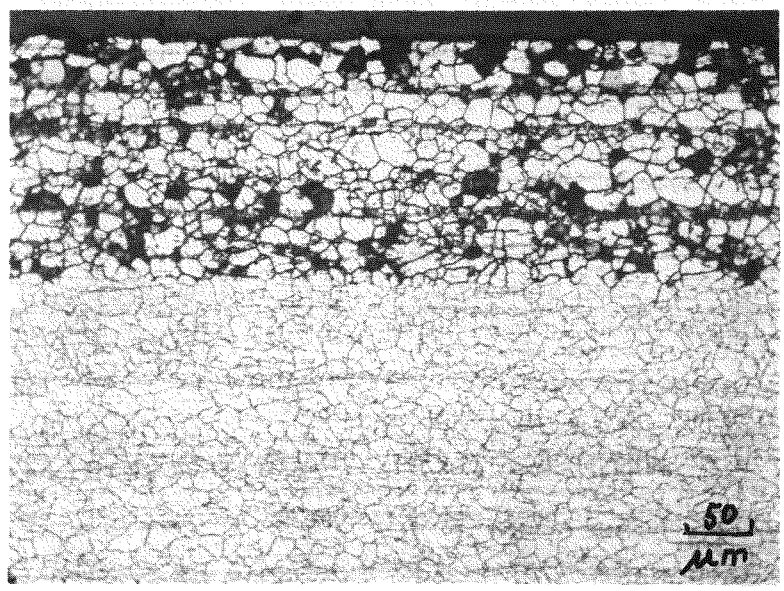

Liquid

Figure 4-58. IGA to a depth of 0.19 mm at the ID and at the vapor-liquid interface of Capsule 21-1 (40% NaOH + 10% KOH + 12% Cr_2O_3, 92-98 days, 650°F). Electrolytic phosphoric acid etch.

either copper or zinc, found on the ID surface of Capsule 19. Both capsules which contained this environment leaked through cracks in welds.

Two additives were observed to increase the amount of IGA produced when specimens were exposed to the reference environment. Although the amount of IGA observed at the liquid-vapor interface in Capsule 20 was comparable to that produced in the reference environment (Capsule 1), 0.07 to 0.09 mm (3-4 mils), or twice amount of IGA produced in the reference environment, was observed at the ends of the capsule. The effect produced by Cr_2O_3 addition was even more pronounced.

Very uniform IGA to a depth of 0.19 mm (7-8 mils) was produced in Capsule 21 after 92 to 98 days exposure to the reference environment plus 12% Cr_2O_3. Figure 4-58 shows the IGA produced at the central portion of the capsule in both the liquid and vapor phase. Because of the uniformity of the IGA produced, and the rapidity with which it was generated, Cr_2O_3 additions to caustic should be considered as a reference environment for additional testing (capsule, C-ring, or electrochemical) to evaluate potential chemical inhibitors.

It should be noted that in all the capsule tests which contained A508 slugs, no IGA was observed (see 10-2, 16-2, 17-2, and 20-1), while in the duplicate capsule tests without slugs IGA was observed. This may be a result of depletion of the caustic concentration due to caustic corrosion of the A508, or a result of the hydrogen overpressure produced during the A508 corrosion.

Figure 4-59 shows through-wall leaks which occurred in three capsules in the test series. Cracks were observed in the weld metal, at the weld-alloy interface, and in the heat affected zone. A large number of such leaks in this series, resulting in loss of test environment, occurred despite the post-weld stress relief anneal that was performed to minimize cracking.

Denting in Caustic Solutions. Many of the isothermal capsules which were exposed to the 40% NaOH + 10% KOH solutions during the capsule proof tests, and a limited number of capsules in the test series to evaluate the effect of additives (Table 4-8) contained A508 low alloy steel slugs (see Figure 3-5). After exposure of these capsules and prior to destructive examination, it was observed that the capsules were bulged in the region of the tube where the A508 slug was located. Micrometer measurements on the capsule OD surface verified the existence of the

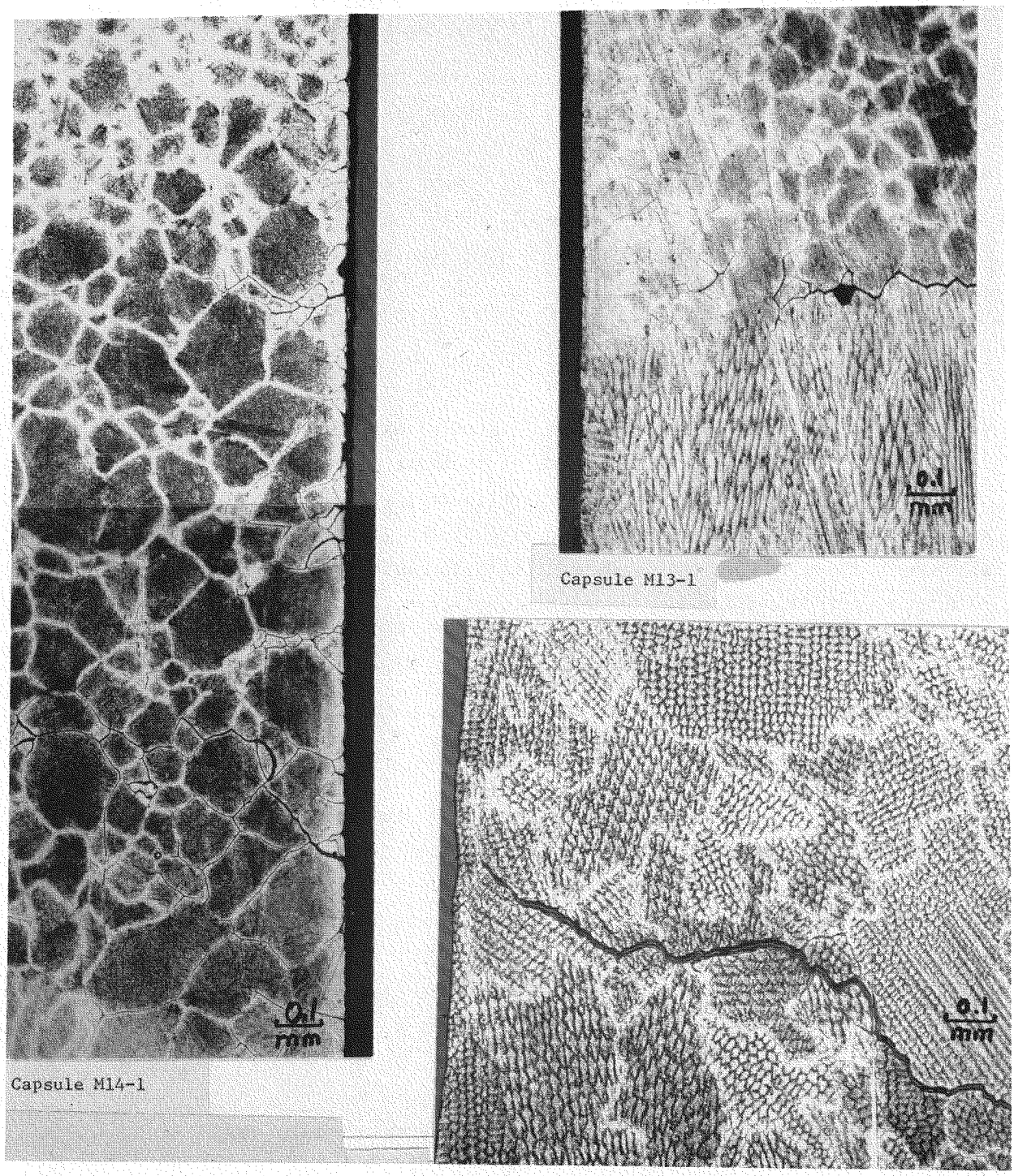

Figure 4-59. Examples of SCC at welds which occurred despite post-weld stress relief anneal. Bottom weld failures occurred through the weld (M12-1), weld-alloy interface (M13-1), and heat affected zone (M14-1). Electrolytic phosphoric acid etch.

bulges which ranged in size from 0.020 mm (0.8 mil) to 0.875 mm (35 mils). The device and technique used to measure the bulges were the same as reported previously by Economy (7).

Table 4-16 contains a summary of the bulge sizes measured at the end of the indicated exposure period for various test enviornments (solution chemistry and temperature). These results show that under the simulated tubesheet crevice conditions of these tests, the degree of tube deformation was dependent on the additive to the caustic environment. Additives such as Cr_2O_3 and CuO + ZnO increase the severity of the bulging while additives such as SiO_2 appear to decrease the severity of the bulging.

The lack of a direct one-to-one correspondence between exposure times, temperatures, and chemistries in these capsules makes further generalizations based on these results difficult. The fact that tube deformation can be produced in a caustic environment suggests that the minor denting indicated at the top of the tubesheet in some operating plants by eddy current data may have been produced by the same caustic environment thought to produce the IGA and SCC observed deeper within the tubesheet crevice.

The morphology of the oxide produced between the steel slug and tube surfaces in one of the bulged capsules is shown in Figure 4-60 as a transverse section. The banded oxide structure in this figure is very similar to that produced in aqueous acidic chloride, or hydrolyzable metal chloride environments at elevated temperatures.

This banded, alternately coarse and fine grained magnetite structure, which was first reported by Potter and Mann (8, 9, 10), has been produced in several laboratory programs which studied the denting phenomenon observed in recirculating steam generators (6, 11, 12). In these programs, an acidic environment containing chloride and oxidizing agent, such as Cu^{2+} or Ni^{2+} ions, was a necessary condition for accelerated carbon steel corrosion and denting. In contrast to the current results which produced a laminar oxide structure, Potter and Mann had reported that in 5 to 20 wt % NaOH solutions at 240 to 355°C (464 to 671°F), a double layered oxide structure was produced on carbon steel. The inner layer of this structure was compact and protective while the outer layer was coarsely crystalline and nonprotective (8).

Table 4-16

SUMMARY OF BULGING RESULTS IN CAUSTIC SOLUTIONS

Designation	Temp. (°F)	Chemistry	Exposure (Days)	Bulge (mils)
Ni + N_2 - 1	600	40% NaOH + 10% KOH	270	4.7
AR-7	600	40% NaOH + 10% KOH + 7% CuO + 3% ZnO	270	11.8
Ni + N_2 - 2	600	40% NaOH + 10% KOH + 7% CuO + 3% ZnO	270	11.8
AR-8	600	40% NaOH + 10% KOH + 4% Cr_2O_3	270	32.3
Ni + N_2 - 3	600	40% NaOH + 10% KOH + 4% Cr_2O_3	270	34.6
AR-9	600	40% NaOH + 10% KOH + 7% CuO + 3% ZnO + 4% $NaNO_3$	270	20.9
Ni + N_2 - 4	600	40% NaOH + 10% KOH + 7% CuO + 3% ZnO + 4% $NaNO_3$	270	8.7
AR-10	600	40% NaOH + 10% KOH + 7% CuO + 3% ZnO + 4% SiO_2	270	8.7
Ni-5	600	40% NaOH + 10% KOH + 7% CuO + 3% ZnO + 4% SiO_2	92	3.9
B-4[a]	650	40% NaOH + 10% KOH + 7% CuO + 3% ZnO + 4% SiO_2	224-235	0.8
B-1	650	40% NaOH + 10% KOH	337	7.0
B-3	650	40% NaOH + 10% KOH + 7% CuO + 3% ZnO + 4% Na_2SO_4	337	7.0
B5	650	40% NaOH + 10% KOH + 7% CuO + 3% ZnO + 4% NaCl	337	7.0
10-2[b]	650	40% NaOH + 10% KOH + 12% Na_2SO_4	126	3
16-2[b]	650	40% NaOH + 10% KOH + 12% Na_2HPO_4	180	1.8
17-2[b]	650	40% NaOH + 10% KOH + Mix.[c]	180	0
20-2[b]	650	40% NaOH + 10% KOH + 12% Na_2CO_3	180	1.4

[a] Partial loss of solution due to slow leak (∿33% loss).

[b] Designation used in Table 5-15.

[c] Mix. = 3% $NaNO_3$ + 3% $CaSO_4$ + 3% SiO_2 + 3% NaCl + 3% Na_2HPO_4.

Inconel 600 Steel

Figure 4-60. Laminated deposit between tube and plug on Capsule AR-8 (40% NaOH + 10% KOH + 4% Cr_2O_3)

Figure 4-61 shows an enlargement of an area within the steel corrosion product near carbon steel surface of the same specimen shown in Figure 4-60. The enlargement and the elemental mapping of the area was performed on the electron beam microprobe. An enlargement and elemental maps of an area near the tube surface is shown in Figures 4-62 and 4-63. Unlike previous studies of actively denting or bulging specimens produced in acidic-chloride environments (8), which showed that chloride was localized in the coarse grained oxide near the carbon steel surface, there is no distinct association of any elemental species in the banded structure. However, if hydroxide ions, by analogy, were concentrated in these bands, the electron beam microprobe analysis (EMA) technique would not detect them because it is insensitive to light elements such as oxygen and hydrogen.

The four capsules in Table 4-15 which contained A508 slugs (10-2, 16-2, 17-2, and 20-1) had been in testing for four weeks before bulging was noted on long exposure capsules from proof-test series. Since the occurrence of bulging was not anticipated, neither initial nor periodic bulge measurements were made up to that point. Once bulging was noted, bulge measurements were initiated and continued for the remainder of the exposure period. Plots showing the bulging behavior of these four capsules are contained in Figure 4-64.

The plots in Figure 4-64 show bulging was slow to initiate (6 to 11 weeks) and also appeared to be self-attenuating (10-2 and 20-1). Since the solution was not refreshed in any of these capsules, the apparent slowing of bulging may be a result of a change in composition of the test solution during the exposure.

Capsules 16-2 and 17-2 experienced little and no bulging, respectively. The large initial off-set from zero in the plot for capsule 16-2 is attributed to lack of an initial bulge measurement rather than to denting activity during the initial four weeks of exposure. The relatively small bulge produced in capsule 16-2 (~0.5 mils) and the lack of bulging in 17-2 may be a result of the additive used in these tests. Both environments contained Na_2HPO_4, 12 wt % in 16-2 and 3 wt % in 17-2. Other additives, as shown in Table 4-15, were present in capsule 17-2.

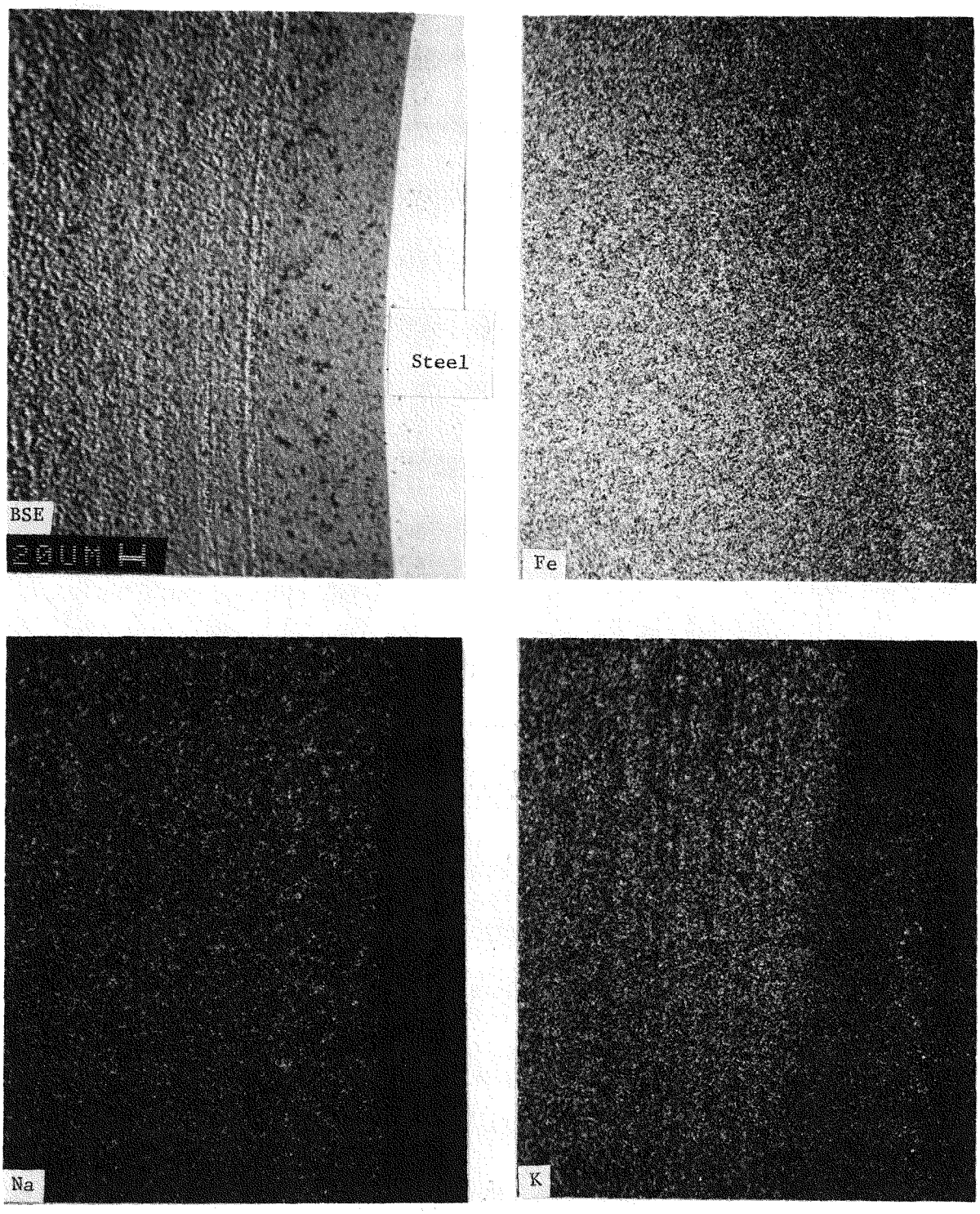

Figure 4-61. EMA area scans for various elements using K_α radiation in the deposits next to the plug in Capsule AR-8. No Cu, Cr, or Cl was detected.

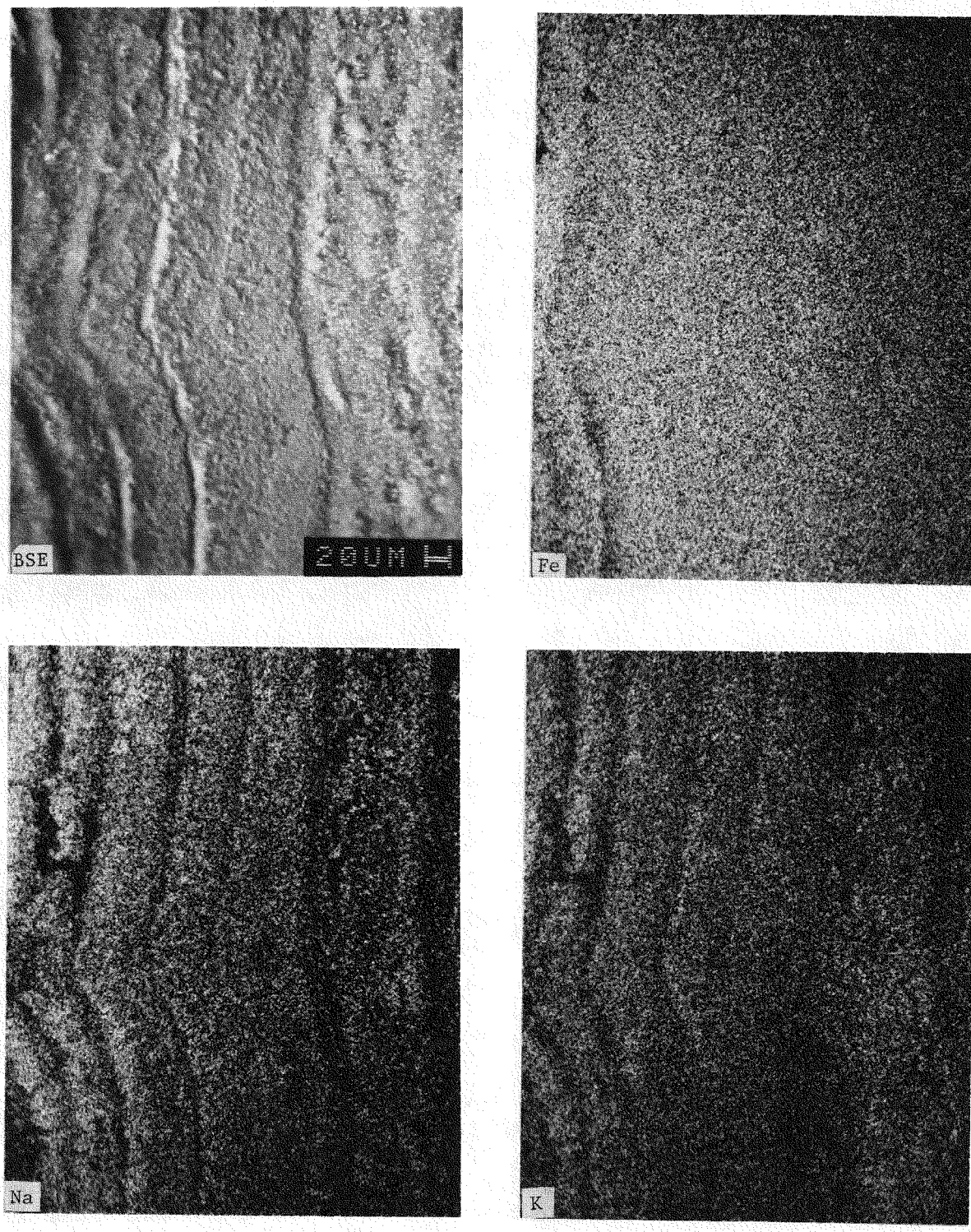

Figure 4-62. EMA area scans in deposit next to the Alloy 600 tube of Capsule AR-8

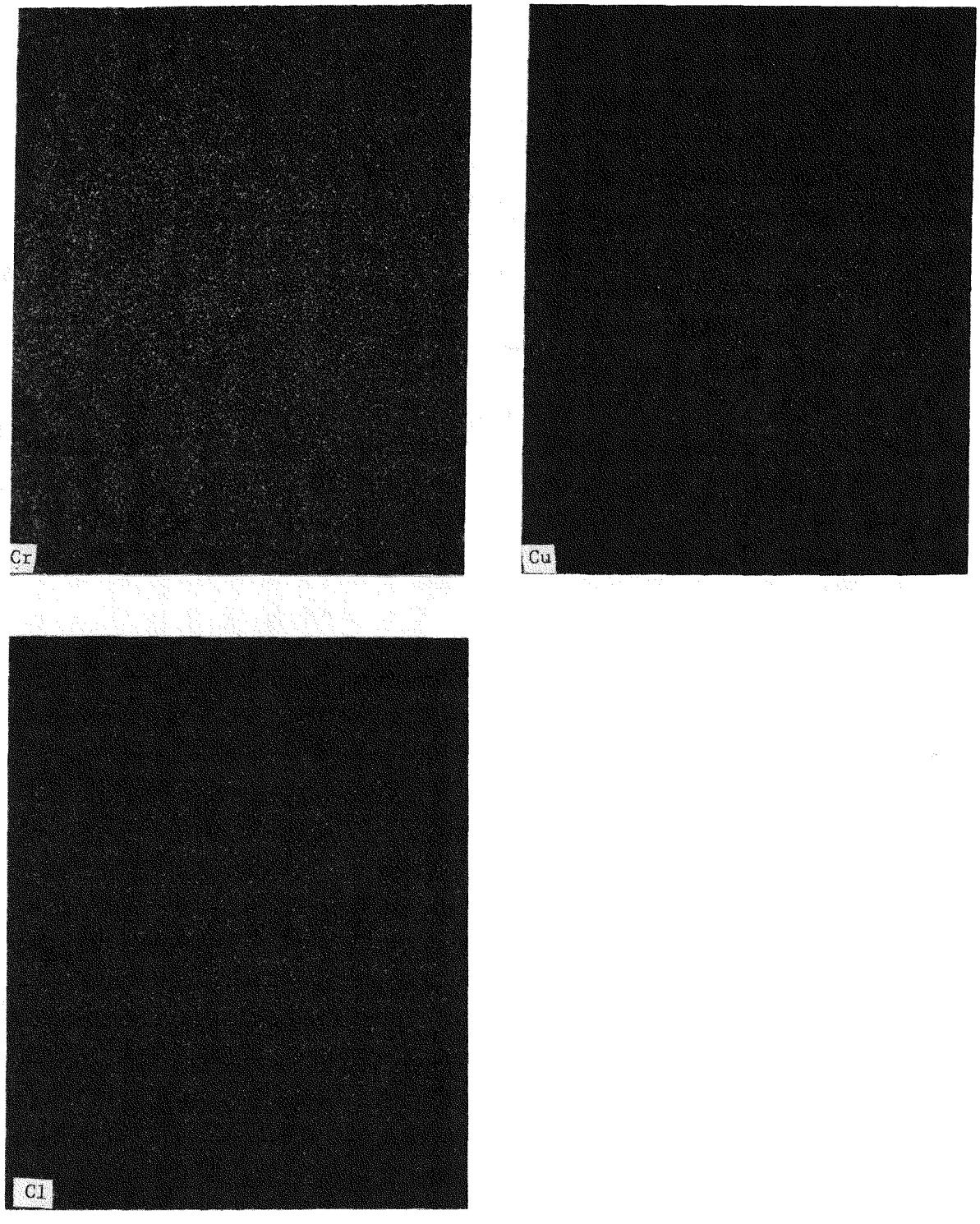

Figure 4-63. Continuation of EMA area scans next to the Alloy 600 tube of Capsule AR-8

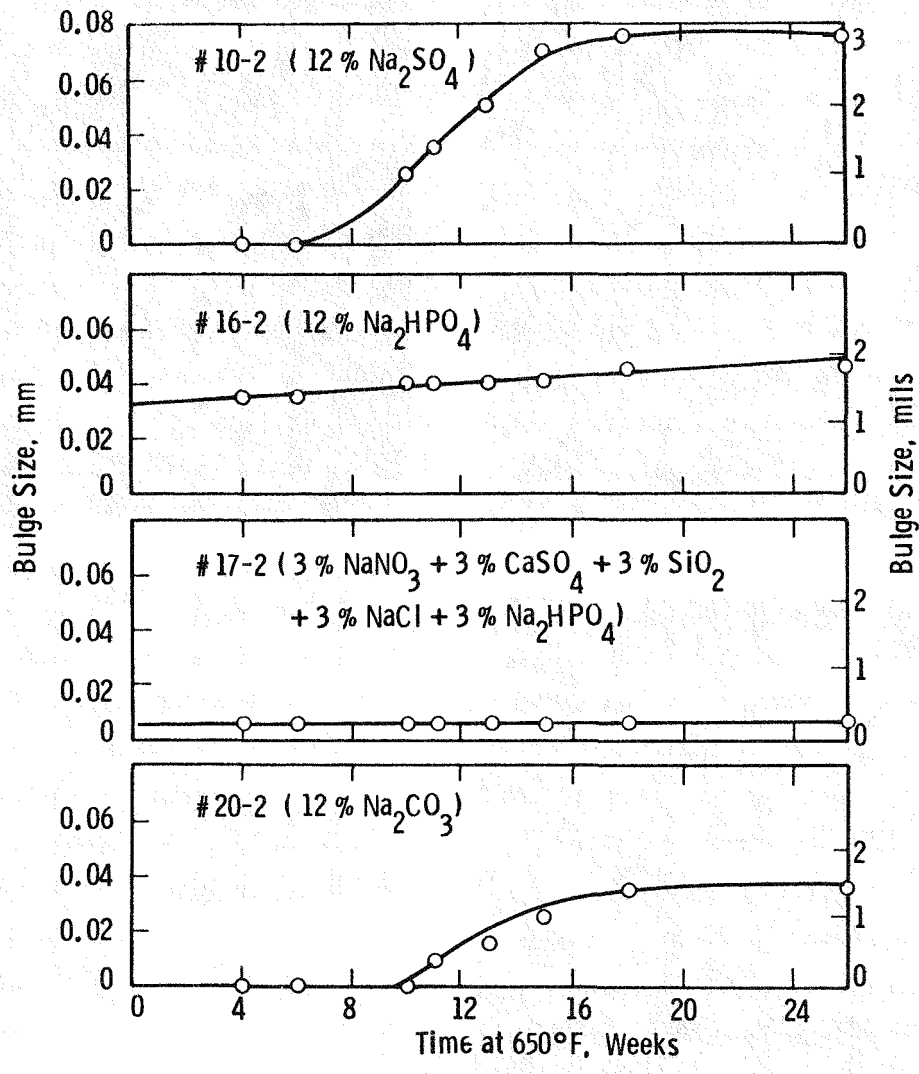

Figure 4-64. Bulging behavior of S183-2 capsules (40% NaOH + 10% KOH + indicated additives at 650°F)

REFERENCES

1. F. W. Pement, P. J. Kuchirka, and C. R. Wolfe. "Examination of Three Steam Generator Tubes from the Point Beach Unit 1 Nuclear Power Plant." EPRI report to be issued.

2. F. W. Pement. "Nuclear Steam Generator Tubes from RGE Ginna Station--A Detailed Metallographic and Microanalytical Evaluation." Topical Report prepared under EPRI Contract No. S138-2, January 12, 1981.

3. U. R. Evans. The Corrosion and Oxidation of Metals: Scientific Principles and Practical Applications. London: Edward Arnold (Publishers) Ltd., 1960, p. 660.

4. F. W. Pement, I. L. Wilson and R. G. Aspden. "Stress Corrosion Cracking Studies of High Nickel Austenitic Alloys in Several High Temperature Aqueous Solutions." Materials Protection and Performance, Vol. 19, No. 4, April 1980, pp. 43-49.

5. G. P. Airey. "Optimization of Metallurgical Variables to Improve the Stress Corrosion Resistance of Inconel 600." Palo Alto, Calif.: Electric Power Research Institute, Final Report on Contract RP1708-1; to be issued.

6. International Critical Tables of Numerical Data, Physics, Chemistry and Technology, III, McGraw-Hill, 1928, p. 370.

7. G. Economy and M. J. Wootten. "PWR Steam-Side Chemistry Follow Program." Palo Alto, Calif.: Electric Power Research Institute, August 1982, NP-2541, Final Report on Contract RP699-1.

8. E. C. Potter and G. M. W. Mann. Chemistry and Industry, 1964, p. 1768.

9. E. C. Potter and G. M. W. Mann. "Oxidation of Mild Steel in High Temperature Aqueous Solutions." In Proceedings of the 1st International Congress on Metallic Corrosion, 1961. London: Butterworths, 1962, p. 417.

10. E. C. Potter and G. M. W. Mann. British Corrosion Journal, Vol. 1, 1965, p. 26.

11. C. R. Wolfe et al. "Laboratory Studies Related to Steam Generator Tube Denting." Palo Alto, Calif.: Electric Power Research Insitute. Final Report on Contract S112-1; to be issued.

12. G. Economy and C. R. Wolfe. "Cause of Denting." Palo Alto, Calif.: Electric Power Research Institute. Final Report on Contract S157; to be issued.

Section 5

RECOMMENDATIONS

SCREENING TEST - TASK 300

In Task 300 tests, Cr_2O_3 additions to the reference environment (40 wt % NaOH + 10% KOH at 650°F) were found to increase the amount of IGA by almost an order of magnitude over that produced in the reference environment alone. Since Cr_2O_3 is a sludge constituent, other metal oxide sludge components should be evaluated to determine their effect on the amount of caustic induced IGA. Such tests may be beneficial in establishing new reference environment conditions for accelerating IGA in laboratory tests. An environment capable of producing large amounts of IGA in a short period of time would be valuable in screening chemical additives as inhibitors.

In this task nitrate additions to the caustic reference environment were shown to inhibit both SCC and IGA. Further screening tests are required to determine how this inhibition is effected. Further understanding is required not only to optimize nitrate useage but also to select other additives which may be able to produce the same effect.

In parallel with testing in caustic environments, screening tests in more mildly alkaline environments, such as sodium silicate and sodium carbonate, should be undertaken. These environments would be tested with and without other chemical additives which have also been hypothesized as species which may exist in tubesheet crevices. If IGA can be produced in the laboratory in these environments in significant quantities and on a reasonable time scale, then these mildly alkaline environments could replace strong caustic solutions as an IGA reference environment.

Two additional test devices (controlled superheat capsules and a four tube crevice simulator) could prove instrumental in selecting environments to be tested and in producing IGA and evaluating remedial actions, respectively. Controlled superheat capsule tests would provide a method for experimentally predicting the amount of water required to produce a solution resulting from various mixtures of solid

species (e.g., NaOH, SiO_2). This method would allow steam to equilibrate with the solid additives under a temperature gradient simulating the temperature gradient between the tubesheet crevice and a steam generator bulk environment. Such controlled superheat capsule tests would eliminate one variable, namely concentration, which has been arbitrarily selected in most screening tests to date. A multi-tube full length tubesheet crevice simulator capable of maintaining prototypical tubesheet and bulk water temperature conditions would be a valuable tool for further evaluating environments and conditions identified in screening tests as contributing to IGA. Such a system has the advantage of in situ generation of an environment under conditions approximating those of an operating steam generator.

MODEL BOILER TESTING - TASK 400

A considerable amount of Single Tube Model Boiler (STMB) testing has already been directed at defining the causes of Alloy 600 IGA/SCC. Reproducible through-wall stress corrosion crack rates and varying amounts of IGA have been produced in STMB's with 0.3 ppm Na_2CO_3/50 ppb N_2H_4 and Simulated Plant Sludge (SPS). These chemistry conditions preferentially cause SCC rather than extensive IGA. However in the process of conducting this testing, several chemistries have shown IGA producing tendencies which may lead to extensive IGA if slight modifications to the test conditions are made. In several tests it appeared that if the tube had not failed so quickly due to SCC, further exposure to the environment would have resulted in a more extensive network of IGA. Therefore the strategy of future STMB testing will be to use chemistries previously shown to have a propensity toward causing IGA but modified to mitigate SCC by reducing the aggressiveness of the environment. In an electrochemical sense this amounts to moving the electrochemical potential of Alloy 600 from an anodic regime where SCC occurs to a cathodic one where IGA dominates. This can be accomplished by adjusting the pH, thermal/hydraulic conditions, amount of oxidant, type of oxidant, concentration of carbonate or by adding other chemical species. The nature of these adjustments will be defined using electrochemical principals to ensure that Alloy 600 is at a cathodic potential in the test environment. This test logic is recommended for development of a STMB reference IGA test against which remedial actions can be evaluated.

The objective of Task 400 of the S183-2 program was to evaluate and select candidate inhibitors to prevent IGA. Model boiler test results with boric acid and S183-2 Task 300 results with capsule, mini-autoclave and electrochemical

studies with sodium nitrate indicate that these additives decrease the susceptibility of Alloy 600 to SCC and IGA. The Task 400 recommended inhibitors are therefore boric acid and sodium nitrate. Upon development of a reference STMB IGA test it is recommended that these additives be tested to determine their effectiveness against IGA in the reference environment.

Appendix A

MODEL BOILER SCANNING ELECTRON MICROSCOPE/ENERGY DISPERSIVE X-RAY ANALYSIS RESULTS

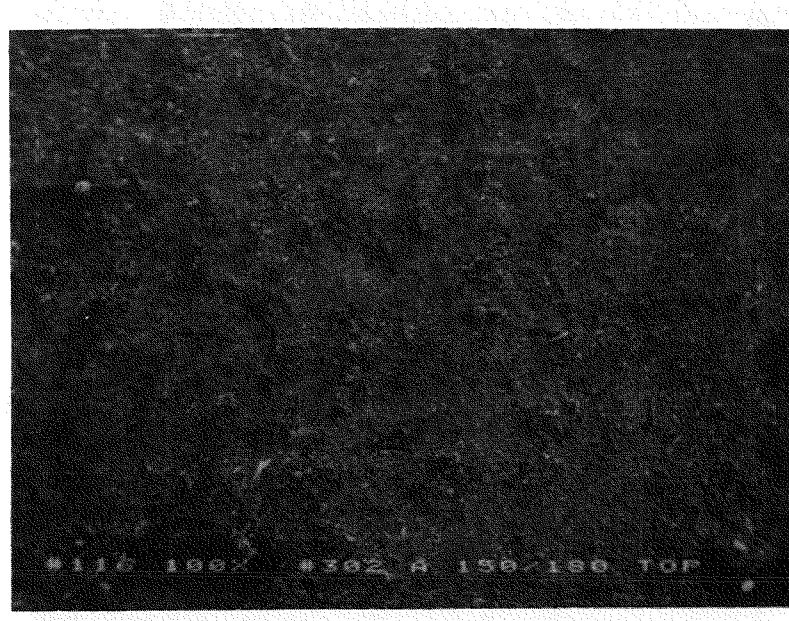

(A) 100X*- Plate 116

(B) 500X*- Plate 117

Figure A-1. Tube Area 1/4" Above Top of Sludge Cup Showing Thin Layer of Black Sludge Covering a Copper Deposit.

*Please note that the illustration(s) on this page has been reduced 10% in printing.

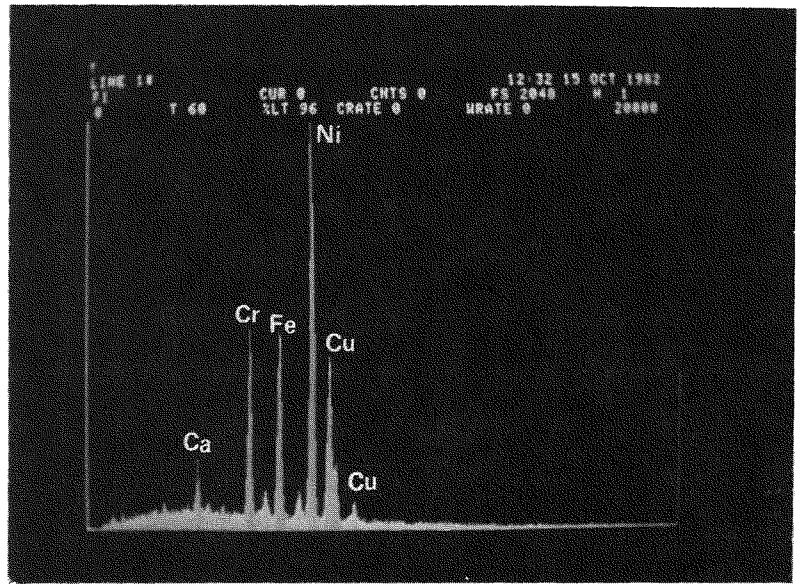

Electron Volts	Counts/Intensity	Element	Transition
3716	357	Ca	K_{α}
5436	947	Cr	K_{α}
5952	212	Cr	K_{β}
6416	966	Fe	K_{α}
7080	202	Fe	K_{β}
7492	2015	Ni	K_{α}
8052	822	Cu	K_{α}
8920	142	Cu	K_{β}

Figure A-2. EDAX of Area Shown in Plate 117 – Figure A-1

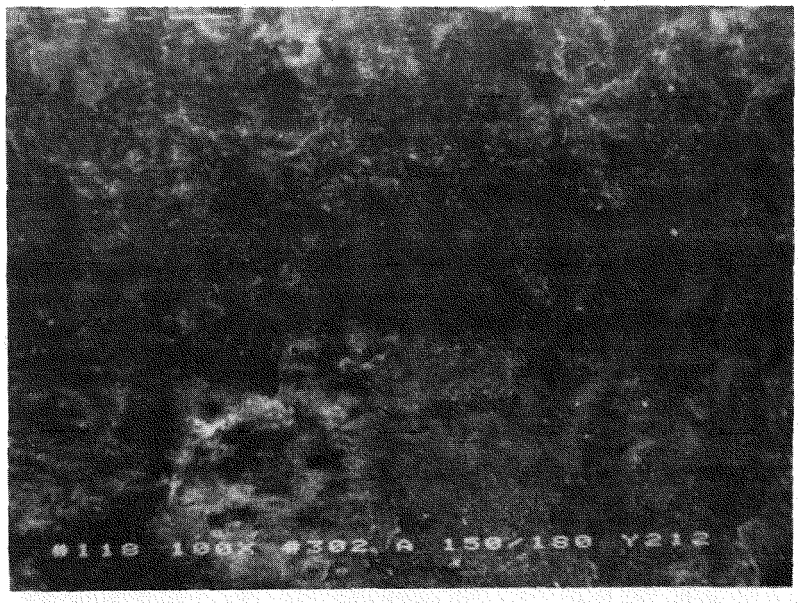

(A) 100X*Plate 118

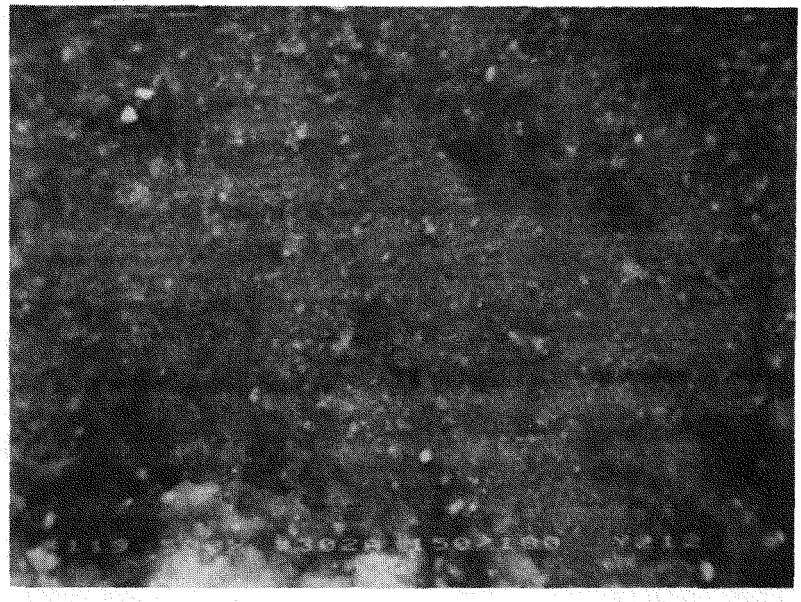

(B) 500X*Plate 119

Figure A-3. Tube Area 1/8" Above Top of Sludge Cup Showing Predominantly Black Deposit Mixed with Small Amount of White Material.

*Please note that the illustration(s) on this page has been reduced 10% in printing.

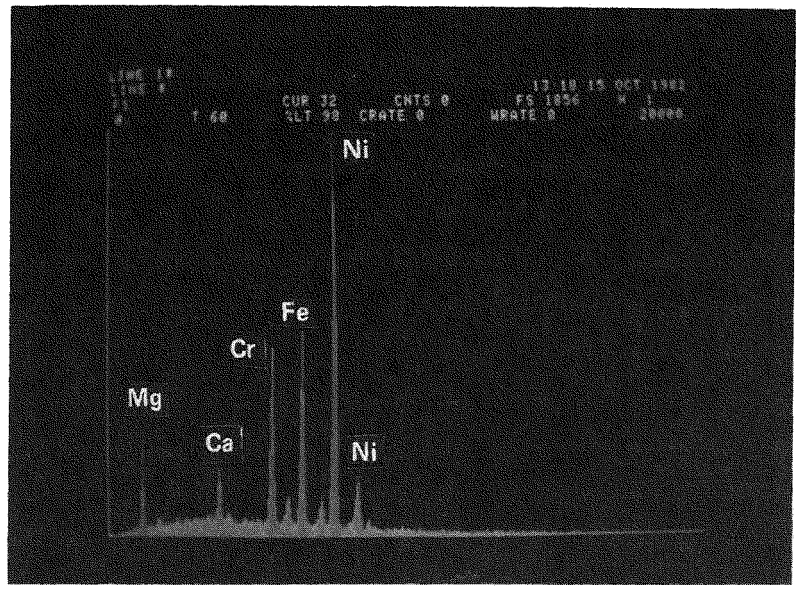

Electron Volts	Counts/Intensity	Element	Transition
1244	507	Mg	K_{α}
3696	283	Ca	K_{α}
5396	835	Cr	K_{α}
5936	184	Cr	K_{β}
6404	927	Fe	K_{α}
7052	200	Fe	K_{β}
7448	1712	Ni	K_{α}
8240	277	Ni	K_{β}

Figure A-4. EDAX of Area Shown in Plate 119 – Figure A-3

(A) 100X* Plate 120

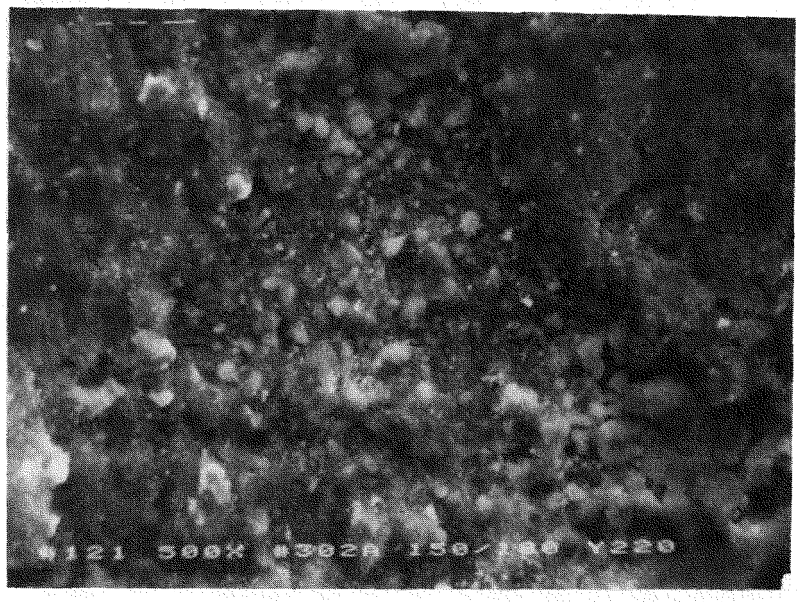

(B) 500X* Plate 121

Figure A-5. Tube Area 1/16" Above Top of Sludge Cup Showing a Thick White Deposit.

*Please note that the illustration(s) on this page has been reduced 10% in printing.

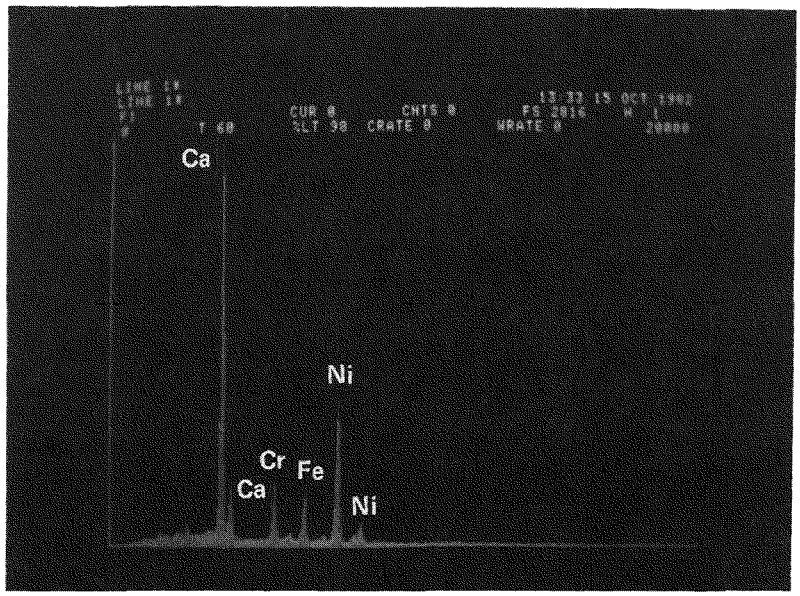

Electron Volts	Counts/Intensity	Element	Transition
3684	2777	Ca	K_α
4008	424	Ca	K_β
5412	438	Cr	K_α
5956	111	Cr	K_β
6388	444	Fe	K_α
7044	103	Fe	K_β
7460	976	Ni	K_α
8260	173	Ni	K_β

Figure A-6. EDAX of Area Shown in Plate 121 – Figure A-5

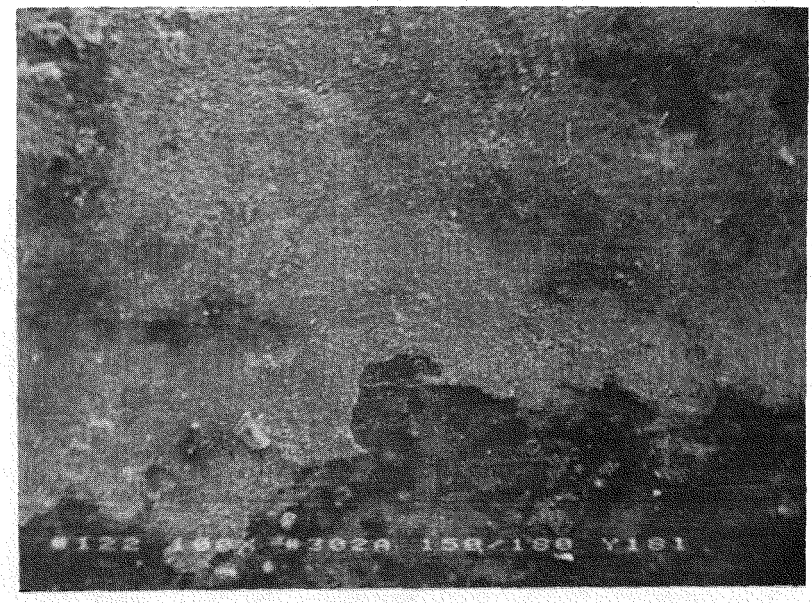

(A) 100X*Plate 122

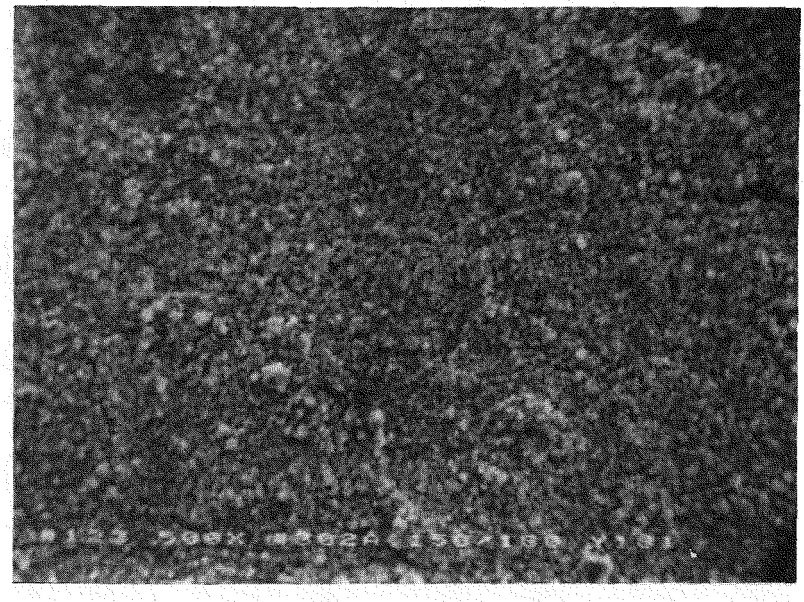

(B) 500X*Plate 123

Figure A-7. Tube Area at Top of Sludge Cup

*Please note that the illustration(s) on this page have been reduced 10% in printing.

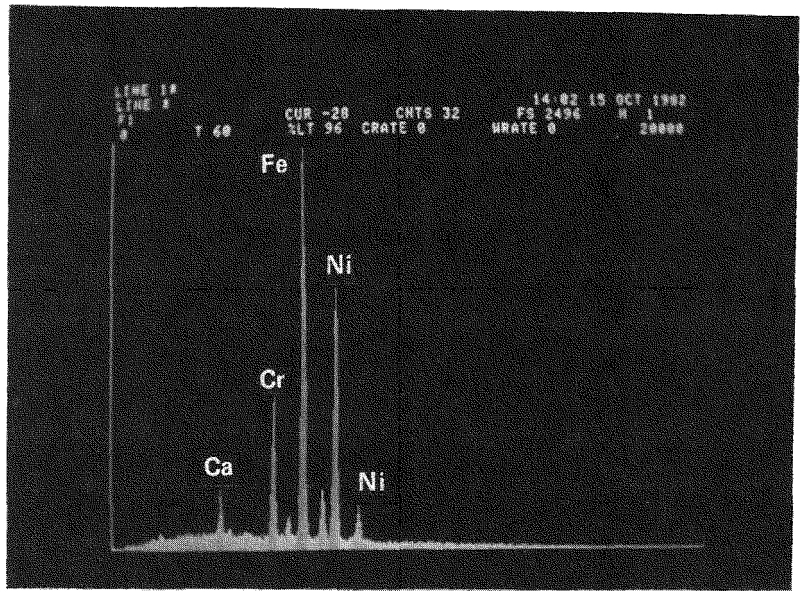

Electron Volts	Counts/Intensity	Element	Transition
3680	366	Ca	K_α
4020	136	Ca	K_β
5424	906	Cr	K_α
5928	212	Cr	K_β
6396	2517	Fe	K_α
7044	387	Fe	K_β
7476	1568	Ni	K_α
8232	253	Ni	K_β

Figure A-8. EDAX of Area Shown in Plate 123 – Figure A-7

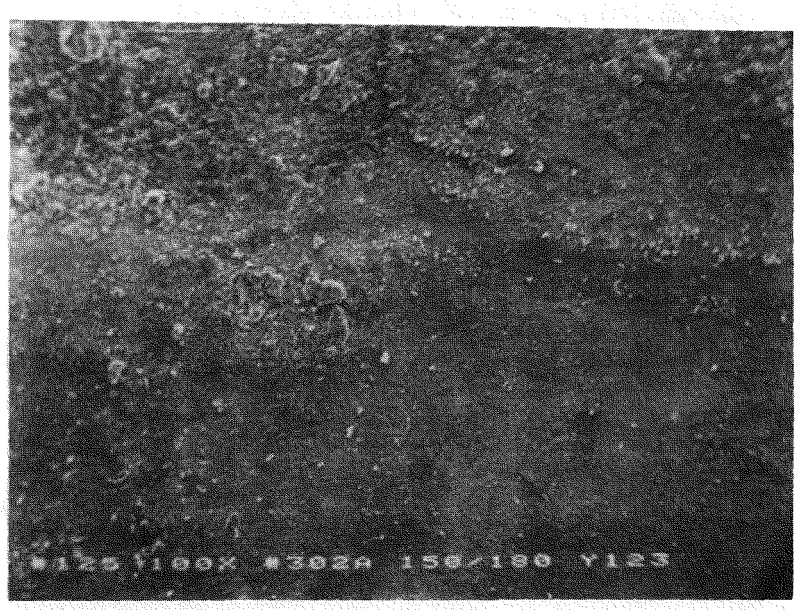

(A) 100X*Plate 125

(B) 500X*Plate 126

Figure A-9. Tube Area at Bottom of Sludge Cup.

*Please note that the illustration(s) on this page has been reduced 10% in printing.

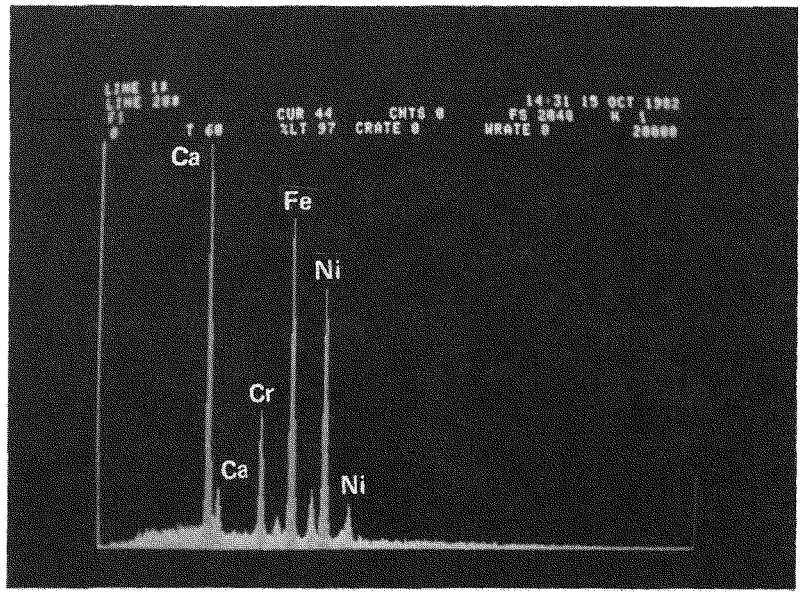

Electron Volts	Counts/Intensity	Element	Transition
3684	2100	Ca	K_α
4000	322	Ca	K_β
5400	695	Cr	K_α
5944	169	Cr	K_β
6408	1637	Fe	K_α
7032	294	Fe	K_β
7480	1258	Ni	K_α
8252	230	Ni	K_β

Figure A-10. EDAX of Area Shown in Plate 126 – Figure A-9

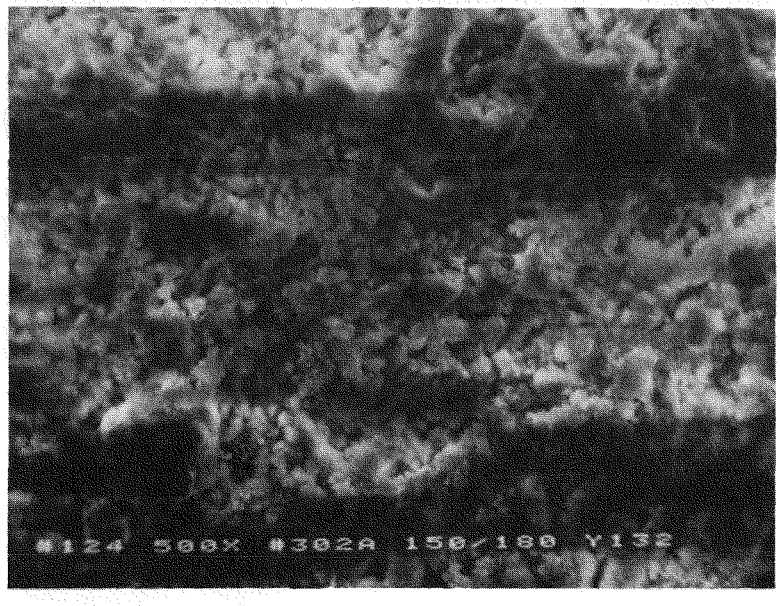

500X* Plate 124

Figure A-11. White Tube Deposit Just Below Bottom of Sludge Cup.

*Please note that the illustration(s) on this page has been reduced 10% in printing.

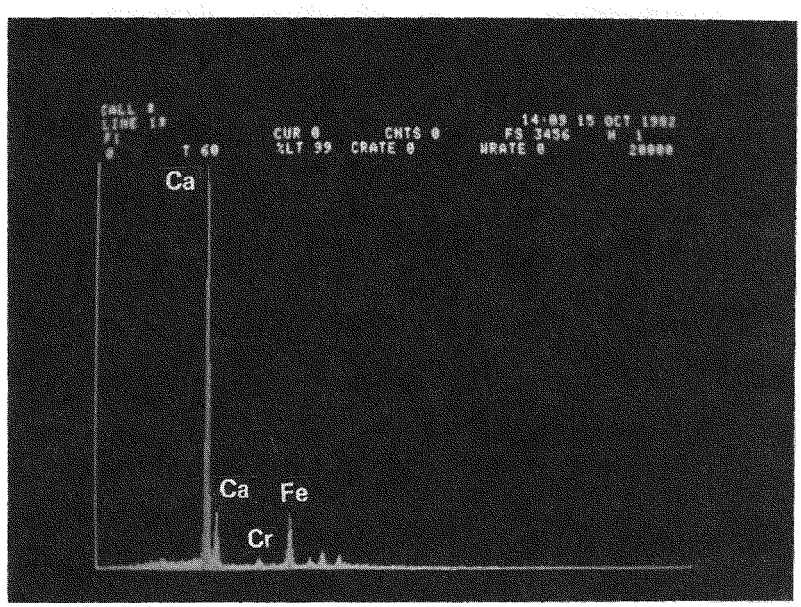

Electron Volts	Counts/Intensity	Element	Transition
3688	3523	Ca	K_{α}
4012	548	Ca	K_{β}
5404	105	Cr	K_{α}
6396	456	Fe	K_{α}
7052	108	Fe	K_{β}
7472	157	Ni	K_{α}
8032	111	Cu	K_{α}

Figure A-12. EDAX of Area Shown in Plate 124 – Figure A-11

(A) 100X* Plate 127

(B) 500X* Plate 128

Figure 4-13. Tube Area 1/4" Below Sludge Cup.

*Please note that the illustration(s) on this page has been reduced 10% in printing.

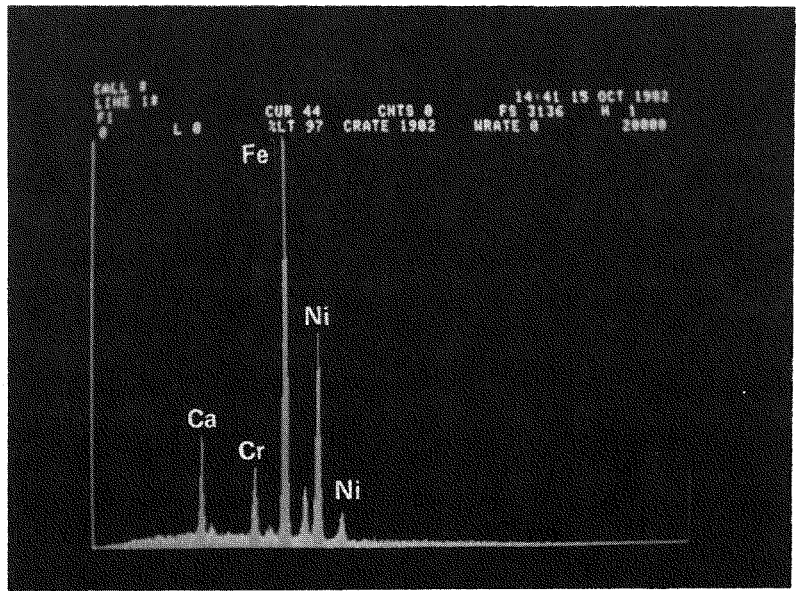

Electron Volts	Counts/Intensity	Element	Transition
3668	829	Ca	K_{α}
3938	201	Ca	K_{β}
5396	620	Cr	K_{α}
5924	174	Cr	K_{β}
6392	3236	Fe	K_{α}
7040	501	Fe	K_{β}
7472	1544	Ni	K_{α}
8296	250	Ni	K_{β}

Figure A-14. EDAX of Area Shown in Plate 128 – Figure A-13

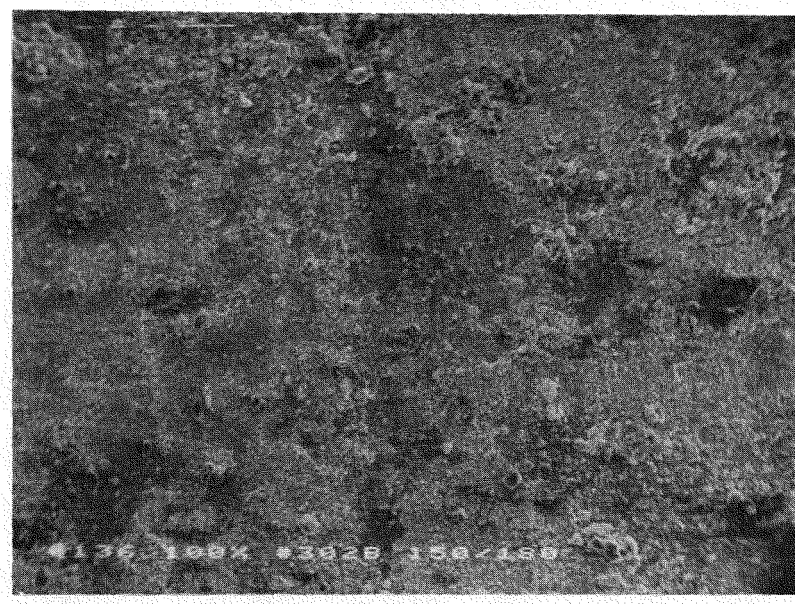

(A) 100X* Plate 136

(B) 500X* Plate 137

Figure A-15. Tube Area 1" Below Sludge Cup

*Please note that the illustration(s) on this page has been reduced 10% in printing.

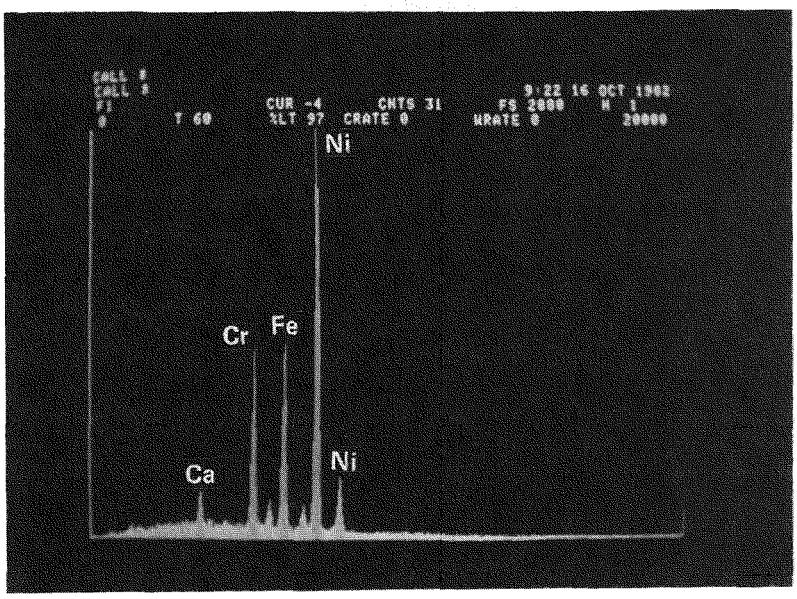

Electron Volts	Counts/Intensity	Element	Transition
1480	133	Al	K_α
1740	100	Si	K_α
3684	402	Ca	K_α
4012	131	Ca	K_β
5404	1306	Cr	K_α
5948	289	Cr	K_β
6408	1347	Fe	K_α
7028	258	Fe	K_β
7464	2834	Ni	K_α
8252	445	Ni	K_β

Figure A-16. EDAX of Area Shown in Plate 137 – Figure A-15

(A) 100X*Plate 138

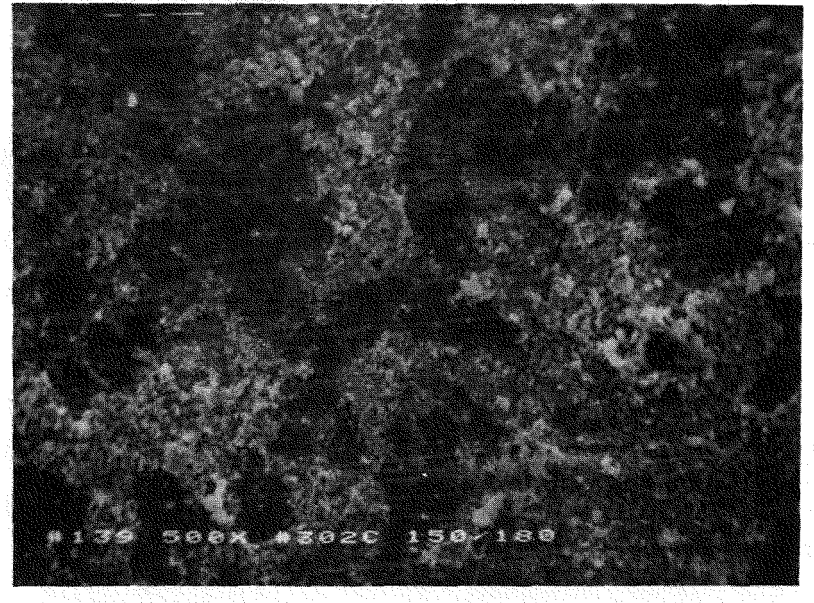

(B) 500X*Plate 139

Figure A-17. Tube Area 2" Below Sludge Cup.

*Please note that the illustration(s) on this page have been reduced 10% in printing.

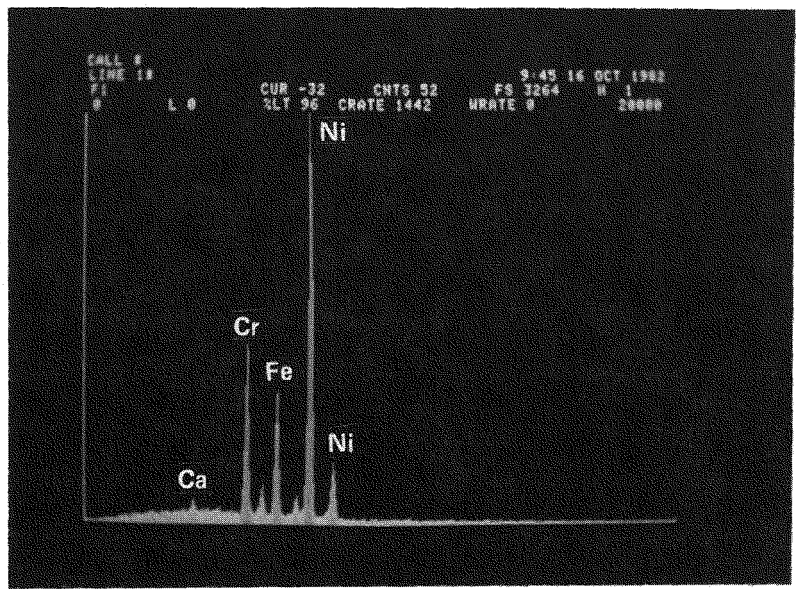

Electron Volts	Counts/Intensity	Element	Transition
3668	216	Ca	K_α
5416	1496	Cr	K_α
5944	319	Cr	K_β
6392	1153	Fe	K_α
7064	233	Fe	K_β
7448	3319	Ni	K_α
8232	516	Ni	K_β

Figure A-18. EDAX of Area Shown in Plate 139 — Figure A-17

(A) 100X*Plate 130

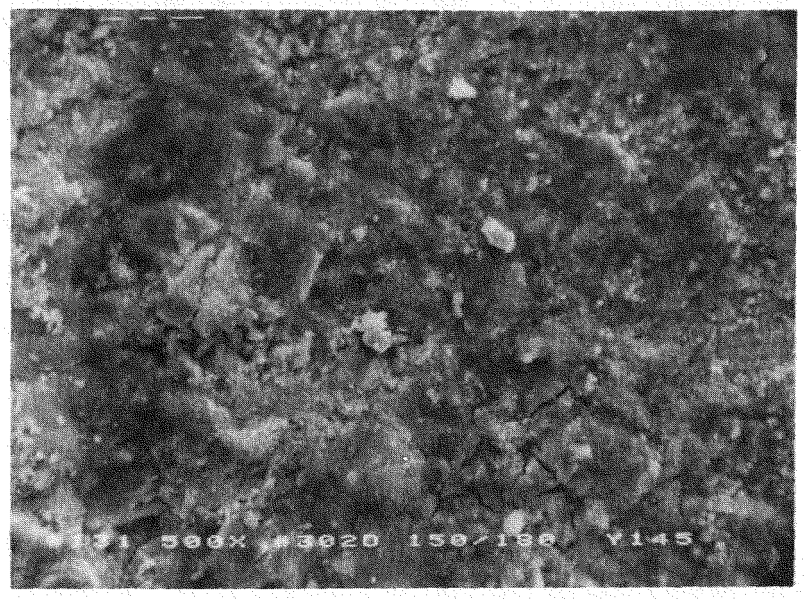

(B) 500X*Plate 131

Figure A-19. Tube Area At Beginning of Roll Transition Region

*Please note that the illustration(s) on this page has been reduced 10% in printing.

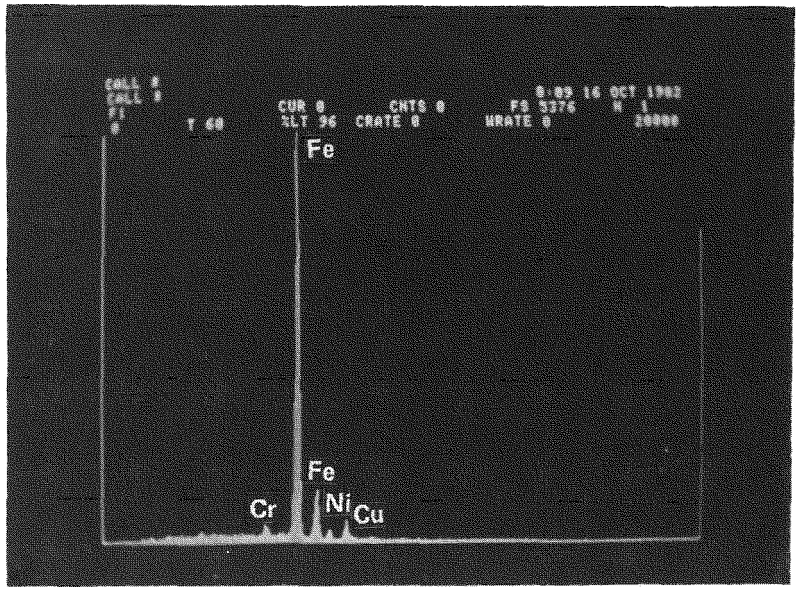

Electron Volts	Counts/Intensity	Element	Transition
5420	259	Cr	K_α
6412	5495	Fe	K_α
7068	742	Fe	K_β
7460	186	Ni	K_α
8056	304	Cu	K_α

Figure A-20. EDAX of Area Shown in Plate 131-Figure A-19

(A) 100X*Plate 132

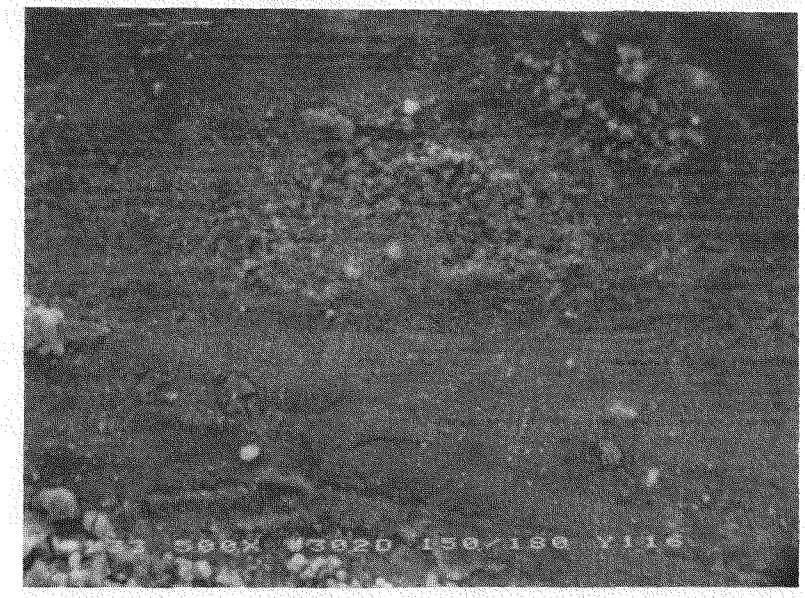

(B) 500X*Plate 133

Figure A-21. Tube Area in Middle of Roll Transition Region

*Please note that the illustration(s) on this page has been reduced 10% in printing.

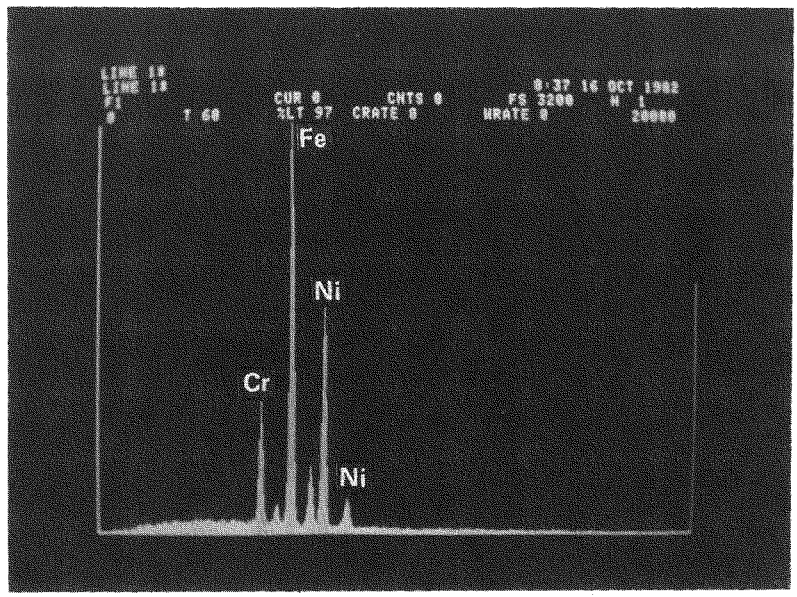

Electron Volts	Counts/Intensity	Element	Transition
5416	1087	Cr	K_{α}
5940	243	Cr	K_{β}
6396	3237	Fe	K_{α}
7032	541	Fe	K_{β}
7464	1708	Ni	K_{α}
8252	280	Ni	K_{β}

Figure A-22. EDAX of Area Shown in Plate 133 – Figure A-21

(A) 100X*Plate 134

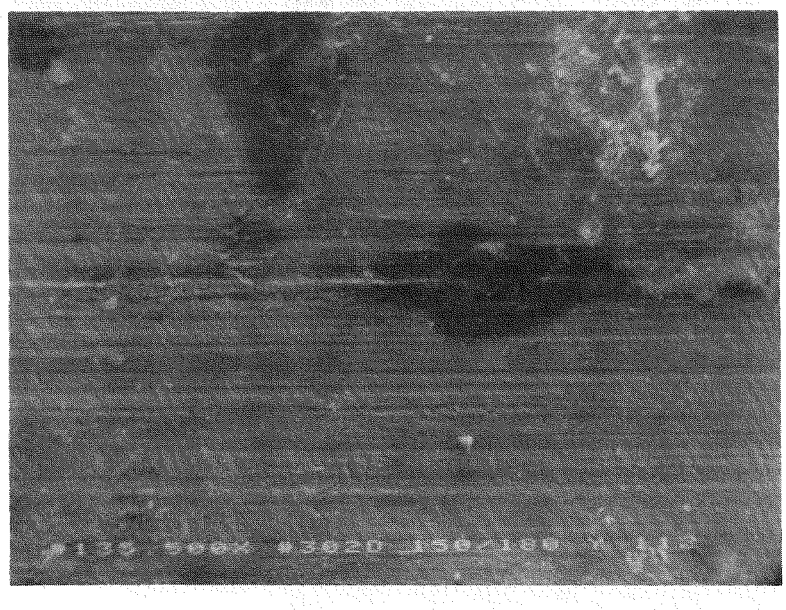

(B) 500X*Plate 135

Figure A-23. Tube Area at End of Roll Transition Region.

*Please note that the illustration(s) on this page has been reduced 10% in printing.

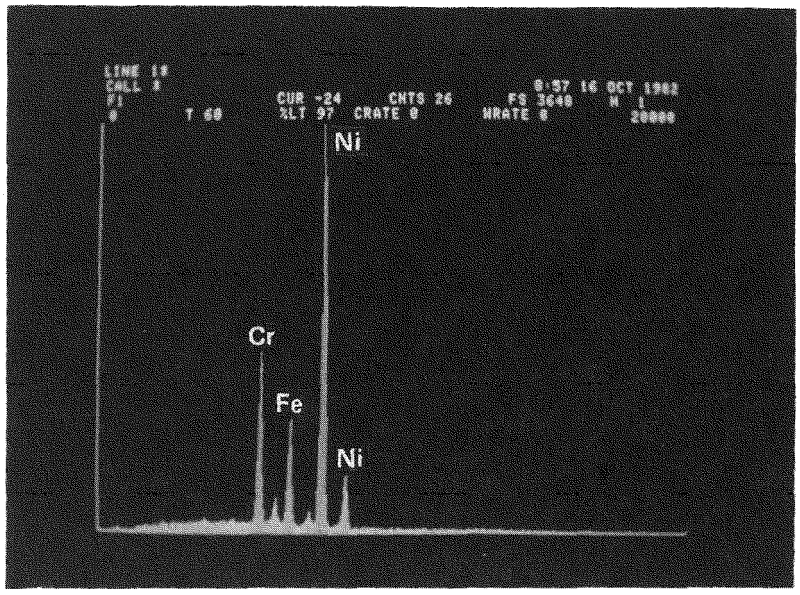

Electron Volts	Counts/Intensity	Element	Transition
5408	1622	Cr	K_α
5928	355	Cr	K_β
6392	1042	Fe	K_α
7032	204	Fe	K_β
7472	3631	Ni	K_α
8280	594	Ni	K_β

Figure A-24. EDAX of Area Shown in Plate 135 — Figure A-23

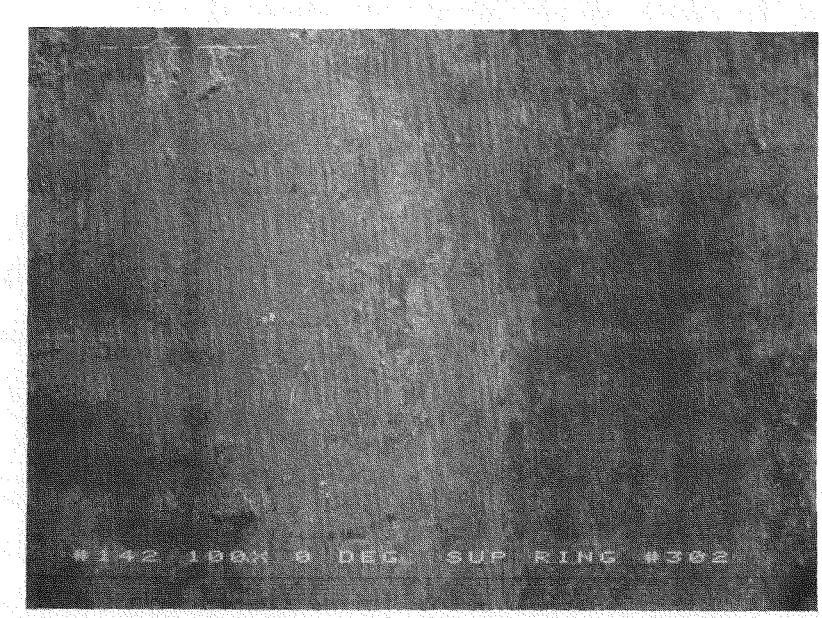

(A) 100X* Plate 142

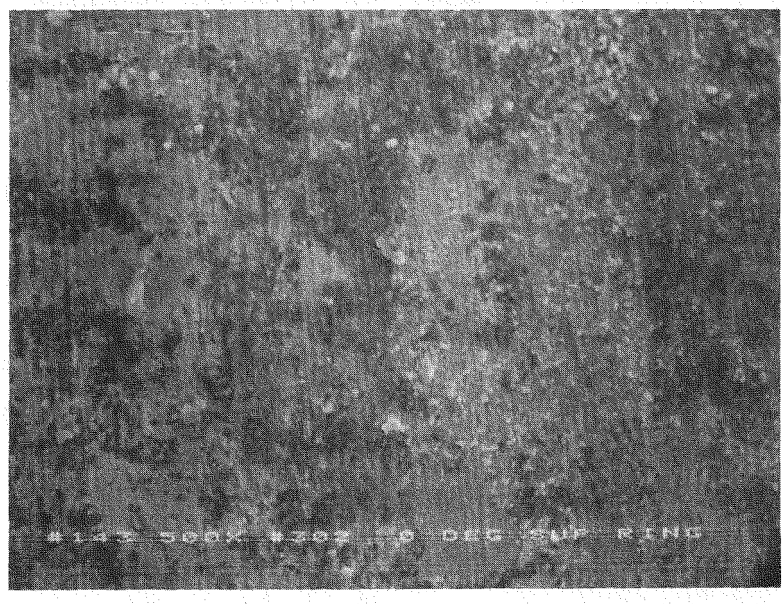

(B) 500X* Plate 143

Figure A-25. Tube Deposits Above Support Ring Crevice

*Please note that the illustration(s) on this page has been reduced 10% in printing.

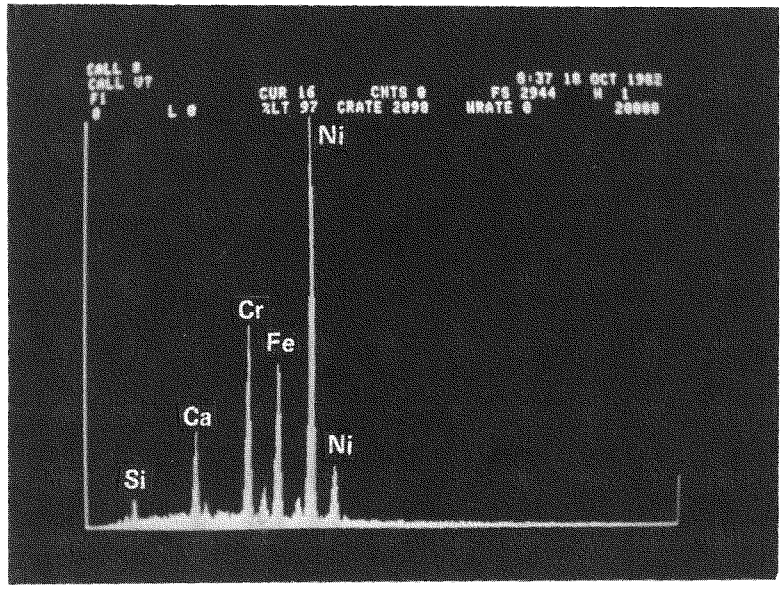

Electron Volts	Counts/Intensity	Element	Transition
1468	130	Al	K_α
1708	279	Si	K_α
3672	708	Ca	K_α
3988	202	Ca	K_β
5420	1455	Cr	K_α
5928	329	Cr	K_β
6380	1168	Fe	K_α
7052	218	Fe	K_β
7476	2807	Ni	K_α
8260	456	Ni	K_β

Figure A-26. EDAX of Area Shown in Plate 143 - Figure A-25

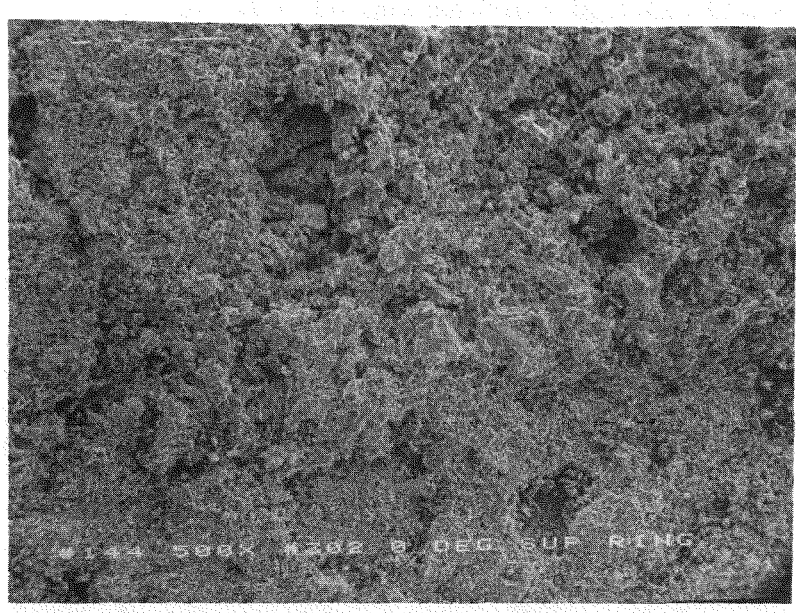

(A) 100X*Plate 144

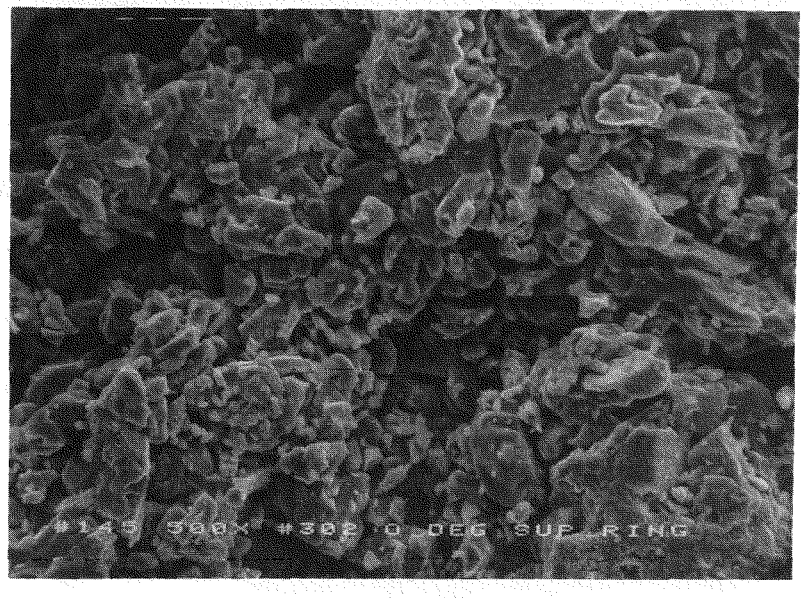

(B) 500X*Plate 145

Figure A-27. Crystalline Fe Oxide Deposits Beneath the Support Ring at 0°.

*Please note that the illustration(s) on this page has been reduced 10% in printing.

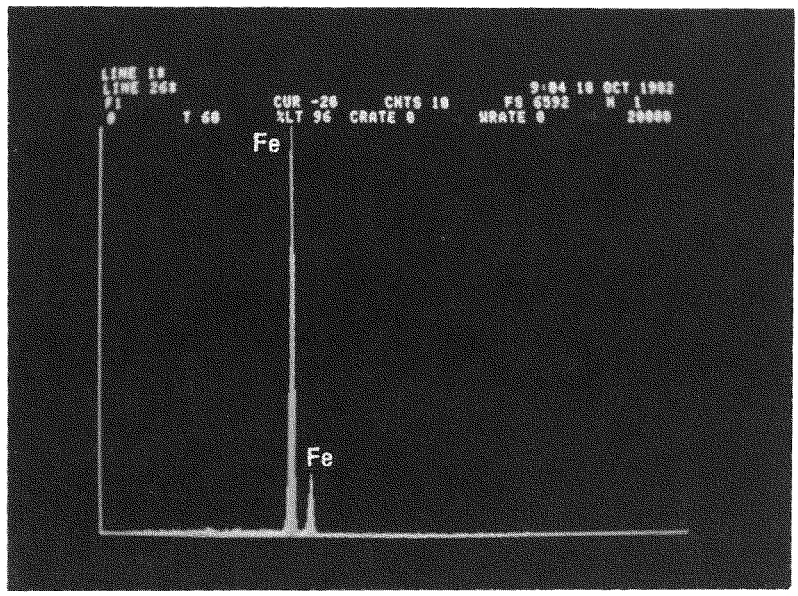

Electron Volts	Counts/Intensity	Element	Transition
6408	6733	Fe	K_{α}
7040	1020	Fe	K_{β}

Figure A-28. EDAX of Area Shown in Plate 145 - Figure A-27